Field Testing of Railroad Flatcar Bridges Volume II: Multiple Spans

Final Report
August 2007

Sponsored by
the Iowa Department of Transportation
and
the Iowa Highway Research Board (Project TR-498)

IOWA STATE UNIVERSITY

About the Bridge Engineering Center

The mission of the Bridge Engineering Center is to conduct research on bridge technologies to help bridge designers/owners design, build, and maintain long-lasting bridges.

Disclaimer Notice

The contents of this report reflect the views of the authors, who are responsible for the facts and the accuracy of the information presented herein. The opinions, findings and conclusions expressed in this publication are those of the authors and not necessarily those of the sponsors.

The sponsors assume no liability for the contents or use of the information contained in this document. This report does not constitute a standard, specification, or regulation.

The sponsors do not endorse products or manufacturers. Trademarks or manufacturers' names appear in this report only because they are considered essential to the objective of the document.

Nondiscrimination Statement

Iowa State University does not discriminate on the basis of race, color, age, religion, national origin, sexual orientation, gender identity, sex, marital status, disability, or status as a U.S. veteran. Inquiries can be directed to the Director of Equal Opportunity and Diversity, (515) 294-7612.

Technical Report Documentation Page

1. Report No. IHRB Project TR-498	2. Government Accession No.	3. Recipient's Catalog No.
4. Title and Subtitle Field Testing of Railroad Flatcar Bridges Volume II: Multiple Spans		5. Report Date August 2007
		6. Performing Organization Code
7. Author(s) Terry J. Wipf, F. Wayne Klaiber, Josh J. Massa, Brian Keierleber, and Jim Witt		8. Performing Organization Report No.
9. Performing Organization Name and Address Center for Transportation Research and Education Iowa State University 2711 South Loop Drive, Suite 4700 Ames, IA 50010-8664		10. Work Unit No. (TRAIS)
		11. Contract or Grant No.
12. Sponsoring Organization Name and Address Iowa Highway Research Board Iowa Department of Transportation 800 Lincoln Way Ames, IA 50010		13. Type of Report and Period Covered Final Report
		14. Sponsoring Agency Code

15. Supplementary Notes

Visit www.ctre.iastate.edu for color PDF files of this and other research reports.

16. Abstract

Based on the conclusions of TR-444, Demonstration Project Using Railroad Flat Car Bridges for Low Volume Road Bridges, additional research on the use of RRFC bridges was undertaken.

This portion of the investigation investigated:

- Different design and rating procedures
- Additional single span configurations plus multiple span configurations
- Different mechanisms for connecting adjacent RRFCs and the resulting lateral load distribution factors
- Sheet pile abutments
- Behavior RRFCs that had been strengthened so that they could be used on existing abutments.

A total of eight RRFC bridges were tested (five single span bridges, two two-span bridge,s and one three-span bridge).

Based on the results of this study a simplified design and rating procedure has been developed for the economical replacement bridge alternative. In Volume 1, the results from the testing of four single span RRFC bridges are presented, while in Volume 2,this volume, the results from the testing of the strengthened single span bridge plus the three multiple span bridges are presented.

17. Key Words		18. Distribution Statement	
bridge replacement—field testing—multiple spans—railroad flatcar bridges		No restrictions.	
19. Security Classification (of this report)	**20. Security Classification (of this page)**	**21. No. of Pages**	**22. Price**
Unclassified.	Unclassified.	157	NA

Form DOT F 1700.7 (8-72) **Reproduction of completed page authorized**

FIELD TESTING OF RAILROAD FLATCAR BRIDGES VOLUME II: MULTIPLE SPANS

Final Report
September 2007

Principal Investigator
Terry J. Wipf
Professor, Department of Civil, Construction, and Environmental Engineering
Iowa State University

Co-Principal Investigators
F. Wayne Klaiber
Professor, Department of Civil, Construction, and Environmental Engineering
Iowa State University

Brian Keierleber
Buchanan County Engineer
Independence, Iowa

Jim Witt
Winnebago County Engineer
Forest City, Iowa

Research Assistant
Josh J. Massa

Authors
Terry J. Wipf, F. Wayne Klaiber, and Josh J. Massa

Sponsored by
the Iowa Highway Research Board
(IHRB Project TR-498)

Preparation of this report was financed in part
through funds provided by the Iowa Department of Transportation
through its research management agreement with the
Center for Transportation Research and Education.

A report from
Center for Transportation Research and Education
Iowa State University
2711 South Loop Drive, Suite 4700
Ames, IA 50010-8664
Phone: 515-294-8103
Fax: 515-294-0467
www.ctre.iastate.edu

TABLE OF CONTENTS

LIST OF FIGURES

LIST OF TABLES

ACKNOWLEDGMENTS

The investigation presented in this final report was conducted by the Iowa State University Bridge Engineering Center under auspices of Center for Transportation Research and Education of Iowa State University. The research was sponsored by the Project Development Division of the Iowa Department of Transportation and Iowa Research Board under Research Project TR-498.

The authors wish to thank the various Iowa DOT engineers who helped with this project and provided their input and support. A special thanks is accorded to the following counties and their respective county engineers for their cooperation and assistance with the field tests: Buchanan County: Brian Keierleber, County Engineer; Winnebago County: Jim Witt, County Engineer; Winneshiek County: Lee Bjerke, County Engineer.

The input, advice, and assistance of the project Technical Advisory Committee: B. Keierleber, Buchanan County Engineer; D. Rolando, Floyd and Chickasaw County Engineer, is gratefully acknowledged.

Special thanks are extended to Doug Wood, Manager of the ISU Structural Engineering Laboratory and the numerous Civil Engineering graduate and undergraduate students for their assistance in various aspects of the project.

EXECUTIVE SUMMARY

Based on the conclusions of TR-444, Demonstration Project Using Railroad Flatcar Bridges for Low Volume Road Bridges, additional research on the use of RRFC bridges was proposed to increase the understanding of RRFC bridges and the range of applications for which RRFC bridges could be used. Different design alternatives, such as span lengths, span configurations (single vs. multiple), longitudinal connection type, and abutment attachment were investigated through the field testing and subsequent analysis of eight additional RRFC bridges.

In Volume 1, four single span RRFC bridges were investigated; two are located in Buchanan County, Iowa (BCB2 and BCB3), one is located in Delaware County, Iowa (DCB), and one is located in Winnebago County, Iowa (WCB2). BCB2 is constructed from two 56-ft V-deck RRFCs and has a cast-in-place reinforced concrete beam for connecting the adjacent cars. The bridge is 20'-7" wide and spans 54'-0". BCB3 is constructed from three 89-ft RRFCs that have been symmetrically trimmed to produce a bridge that has a center to center of abutments length of 66'-2" and is 26'-5 1/2" wide. The BCB3 longitudinal flatcar connection is comprised of 1 1/4" diameter bolts through the adjacent RRFC exterior girders spaced three feet on center. The DCB is constructed from two symmetrically trimmed 89-ft RRFCs. The bridge is 18'-4" wide and spans 66'-4" center to center of abutments. The DCB longitudinal connection is comprised of a 1/2 inch steel plate welded to both RRFCS at the deck level. The WCB2 bridge was constructed from three 89-ft RRFCs that had been symmetrically trimmed to produce a bridge that was 27'-0" wide and spanned 66'-4" center of abutment to center of abutment with 2'-1 3/4" overhangs at each end. The WCB2 longitudinal connection was almost identical to the connection developed for WCB1. Timber planking was again used on WCB2

In Volume 2, this volume, three multiple span RRFC bridges were investigated: two in Buchanan County, Iowa (BCB4 and BCB5) and one in Winnebago County, Iowa (WCB3) plus a single span RRFC bridge (WINNRRFC) in Winneshiek County that had steel plates (23"x5/8") welded to the bottom flanges of the main RRFC girders. BCB4 is constructed from two 89-ft RRFCs to produce a RRFC bridge that has a 40'-3" west span and a 39'-9" east span. There are also end overhangs of 4'-11" and 4'-1" at the west and east ends, respectively. The bridge is 18'-7" wide and has a reinforced concrete beam for the longitudinal connection between cars. BCB5 is constructed from two 89-ft RRFCs to produce a RRFC bridge that has a 42'-8" south span and a 43'-10" north span for a center to center abutments length of 86'-6". The longitudinal connection is a bolted connection similar to BCB3, except with 5/8 inch diameter bolts; the bridge is 17'-1" wide. WCB3 is constructed from three 89-ft RRFCs and is almost identical to WCB1. The major different is that WCB3 features sheet pile abutments. The two RRFCs in the WINNRRFC were strengthened so that the original abutments at the site could be used.

To further increase the ease in which a RRFC bridge can be implemented, a simplified design procedure was developed to aid in the design of future RRFC bridges. The simplified design procedure relates a single flexural moment for the entire bridge to a target girder live load moment based on a lateral distribution factor. This factor, which is dependent on the RRFC type, longitudinal connection, and span configuration, was developed for all the different bridge configurations that were tested as part of this investigation. This procedure follows a similar methodology developed in TR-444 and is presented in Volumes 1 and 2 for simple span and multiple span bridges, respectively.

As recommended in TR-444, a rating procedure was developed for use with RRFC bridges. Using the American Association of State Highway Transportation Officials (AASHTO) allowable stress rating methodology, a rating procedure was developed to provide engineers with a conventional rating procedure, which uses the factors developed for the simplified design procedure. The rating procedure is discussed in both Volumes 1 and 2, with an example of the procedure presented in Volume 1 Appendix D.

1.0 INTRODUCTION

1.1 Background

According to Better Roads Magazine 2006 bridge inventory, there are approximately 24,600 bridges in the State of Iowa, with 20,600, or 84%, on the secondary (county) road system. Of the bridges on the secondary road system in Iowa, 6,100, or 30%, are deficient, either structurally or functionally [1]. Iowa ranks first in the nation in the number of secondary roadway bridges and thirtieth in population [2], which greatly limits the ability of the state and local governments to fund projects with tax dollars. The large number of bridges in Iowa and low state population presents problems for maintenance and replacement.

At the request of Cerro Gordo County, the Bridge Engineering Center at Iowa State University investigated the feasibility of using railroad flatcar (RRFC) bridges as an economical bridge alternative for low volume roads. Beginning with a 1999 feasibility study [3] and 2003 demonstration project [4], research has been conducted by the Iowa State University Bridge Engineering Center to determine the feasibility of using RRFC bridges on low volume roads as well as techniques to evaluate the RRFC bridges in regard to structural integrity and compatibility with Iowa legal loads.

1.2 Railroad Flatcar Selection

A railroad flatcar may be decommissioned from use for several reasons including age, derailment, and economics. RRFCs that have been decommissioned due to age may present a concern about fatigue limiting the lifespan of the bridge. However, fatigue is assumed not to be a major concern because the RRFCs are being used in bridges on low volume roads. RRFCs that have been decommissioned due to derailment should be avoided for use in RRFC bridges as the flatcars may have significant damage that could influence the load carrying capability of the flatcar. RRFCs that have been decommissioned due to economic reasons, however, are ideal for RRFC bridges. As newer, lighter, more economically built and maintained flatcars are put into operation, older cars are replaced as maintenance costs exceed the value of the car [4]. This relative “good” condition of the RRFCs makes them ideal for use as RRFC bridges.

Prior to selection for use in a bridge, the structure of a RRFC should be examined to determine if the flatcar is in an acceptable condition for use in a bridge. Through investigating different RRFCs, several criteria have been developed to assist in the selection of RRFCs that are adequate for use in bridges. The selection criterion includes [4]:

- RRFC substructure: Ideal RRFC should have a redundant cross section (more than one longitudinal load path) and exterior girders that allow for easy connections between adjacent flatcars. RRFCs should also possess adequate strength and stiffness at bearing points. No structural members should be damaged or missing.
- Structural connections: RRFCs with welded connections are preferred over riveted connections. Welds should be examined for cracks and other signs of fatigue.
- Camber: For ease in constructing a longitudinal connection between adjacent cars, the camber of adjacent flatcars should be within ± 1 inch.

- Availability: Readily available RRFCs should be used to decrease the amount of design

needed for future RRFC bridges.

Two types of RRFCs have been used throughout the RRFC research conducted by the Iowa State University Bridge Engineering Center – a 56-ft v-deck flatcar and an 89-ft flatcar [4].

1.2.1 56-ft v-Deck RRFC

The first type of RRFC that has been used in the RRFC projects conducted by the Bridge Engineering Center is a 56-ft v-deck flatcar. This flatcar, shown in Figure 1.1, consists of W-shape interior and exterior girders with two different sized C-shaped channels for transverse members. The cross section of the 56-ft flatcar allows for load path redundancy, with load paths traveling through the interior main girder as well as the exterior girders. The v-deck configuration positions the interior girder approximately eight inches below the exterior girders [4].

1.2.2 89-ft RRFC

The second RRFC type that has been used in the RRFC projects conducted by the Bridge Engineering Center is an 89-ft flatcar. This flatcar, shown in Figure 1.2, consists of an interior box girder with C-shaped channels for exterior girders. Transverse members vary throughout the length of the flatcar, as seen in Figure 1.2j. L-shaped transverse members are positioned at the ends and middle of the major cross section. S-shaped transverse members are positioned between the L-shaped members. U-shaped transverse members are located in the minor cross-section area and transition regions of the RRFC [4].

1.2.3 Material Testing

As part of already completed research into the feasibility of RRFC bridges, tensile tests were conducted on steel coupons from both type of RRFCs to determine the elastic modulus and strength of the steels. The results for the 56-ft V-deck flatcar indicated a modulus of elasticity of 29,000 kips per square inch (ksi) and a yield strength of 40 ksi. The results for the 89-ft flatcar indicated similar results. Material testing has not been conducted on subsequent flatcars [4].

1.3 Previous Railroad Flatcar Bridges

Several RRFC bridges have been constructed and/or tested across the state of Iowa by county road departments in conjunction with ongoing research to determining the feasibility of RRFC bridges for low volume roads. In the 1999 feasibility study, an existing RRFC bridge in Tama County, Iowa was tested. In the 2003 demonstration project, two RRFC bridges – one in Buchanan County, Iowa and one in Winnebago County, Iowa – were designed, constructed, and tested by Iowa State University. Following the 2003 demonstration project, four more single span RRFC bridges have been tested – two in Buchanan County, one in Delaware County, and one in Winnebago County.

a. The 56-ft RRFC at the Erman Corporation

b. The v-deck

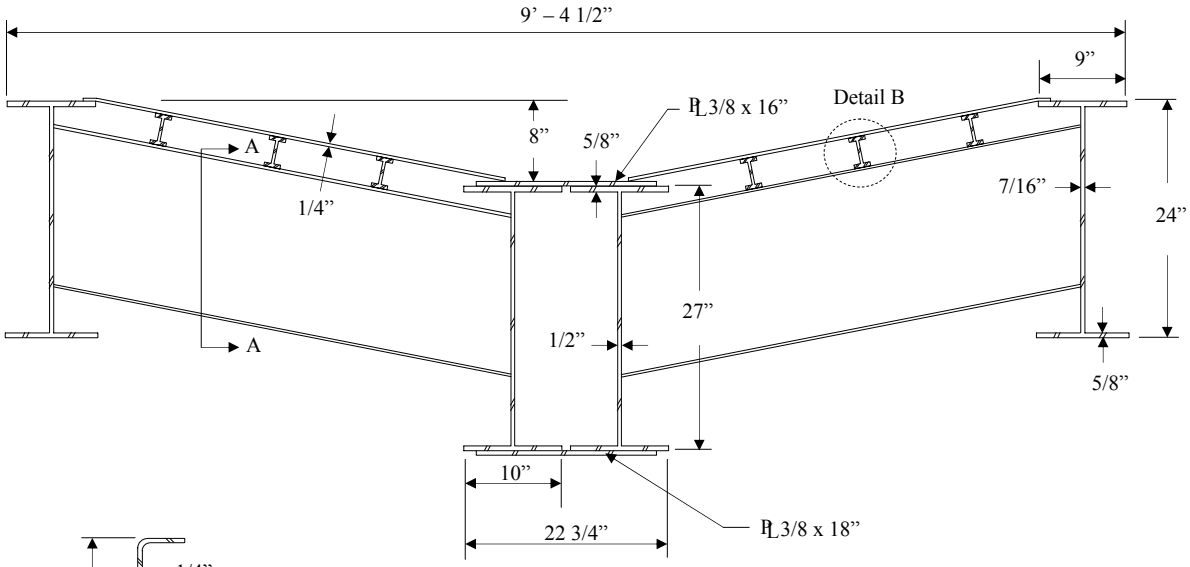

c. Cross-section at midspan

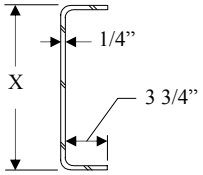

X = 12” for the Small Transverse Member.

X = 16 3/8” for the Large Transverse Member.

d. Section A - A

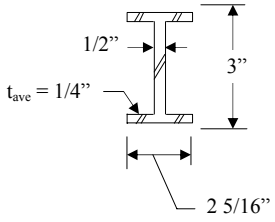

e. Detail B

Figure 1.1. 56-ft v-deck RRFC

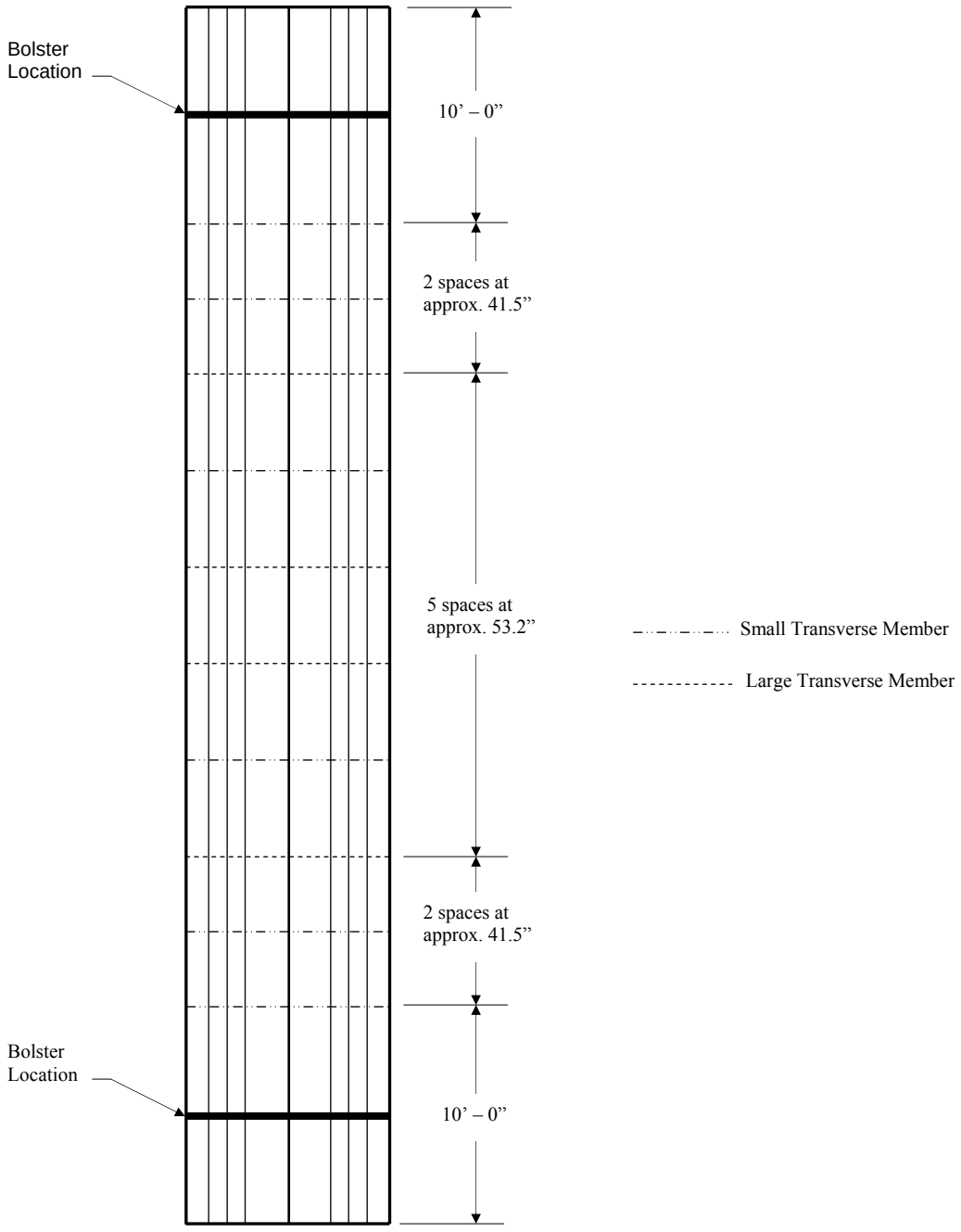

f. Locations of small and large transverse members

Figure 1.1. Continued

a. The 89-ft RRFC (Type A) at the Erman Corporation

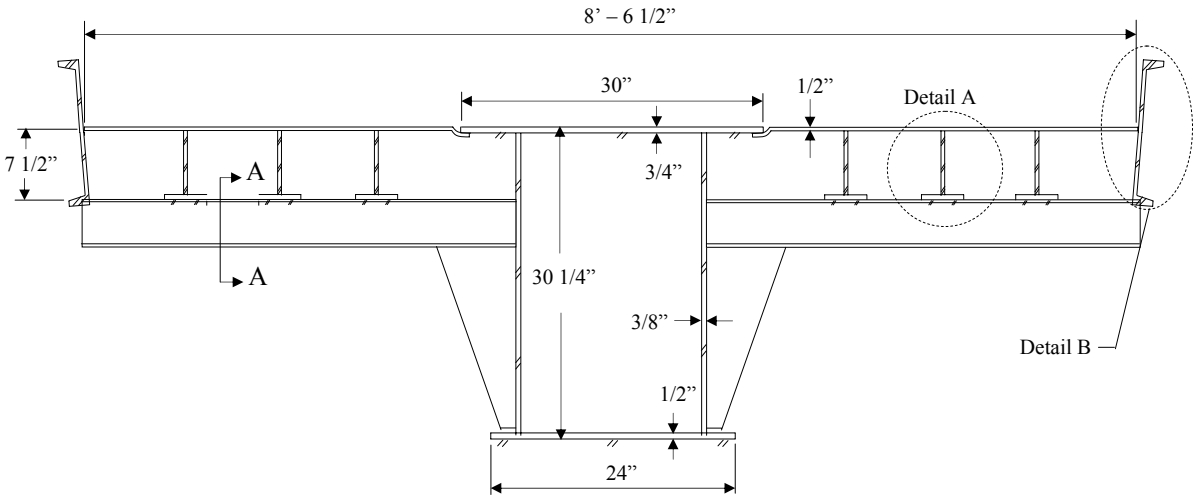

b. Cross-section with S-shape transverse member

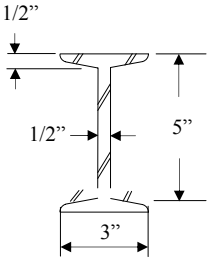

c. Section A – A (S-shape)

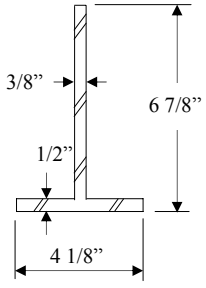

d. Detail A (Tee-shape)

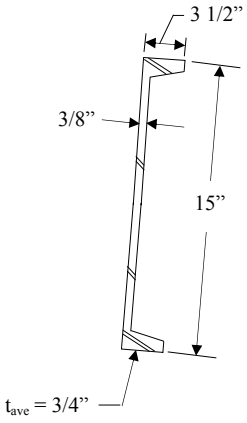

e. Detail B

Figure 1.2. 89-ft RRFC

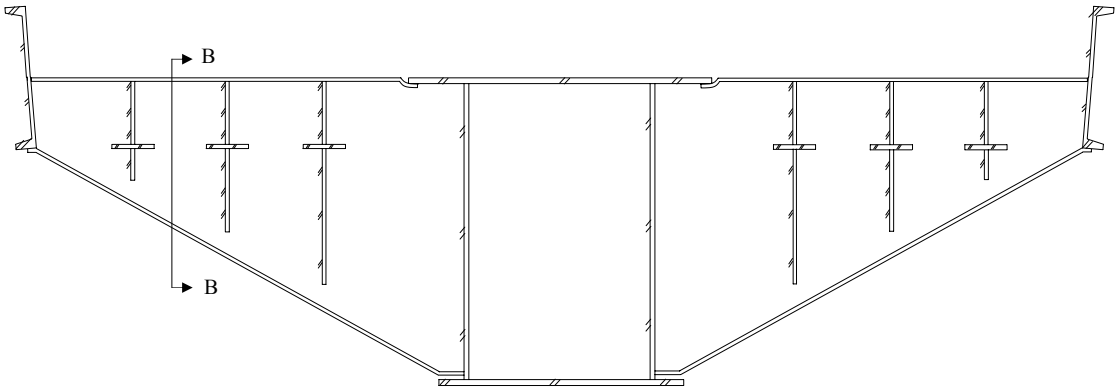

f. Cross-section with L-shaped transverse member

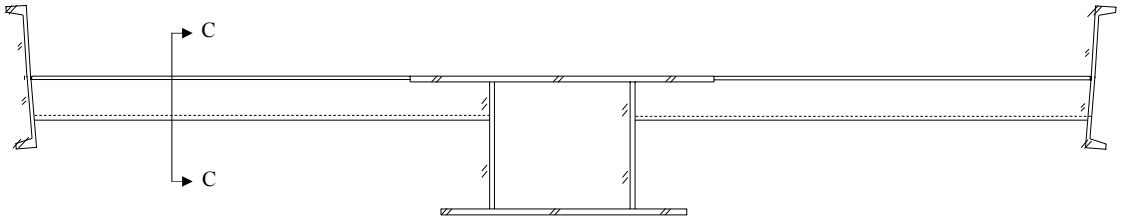

g. Cross-section with U-shaped transverse member

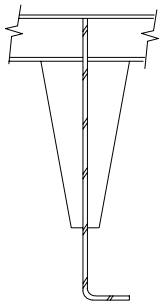

h. Section B – B (L-shape)

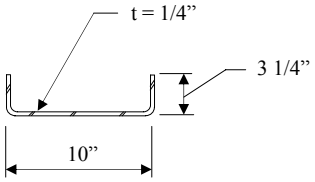

i. Section C – C (U-shape)

Figure 1.2. Continued

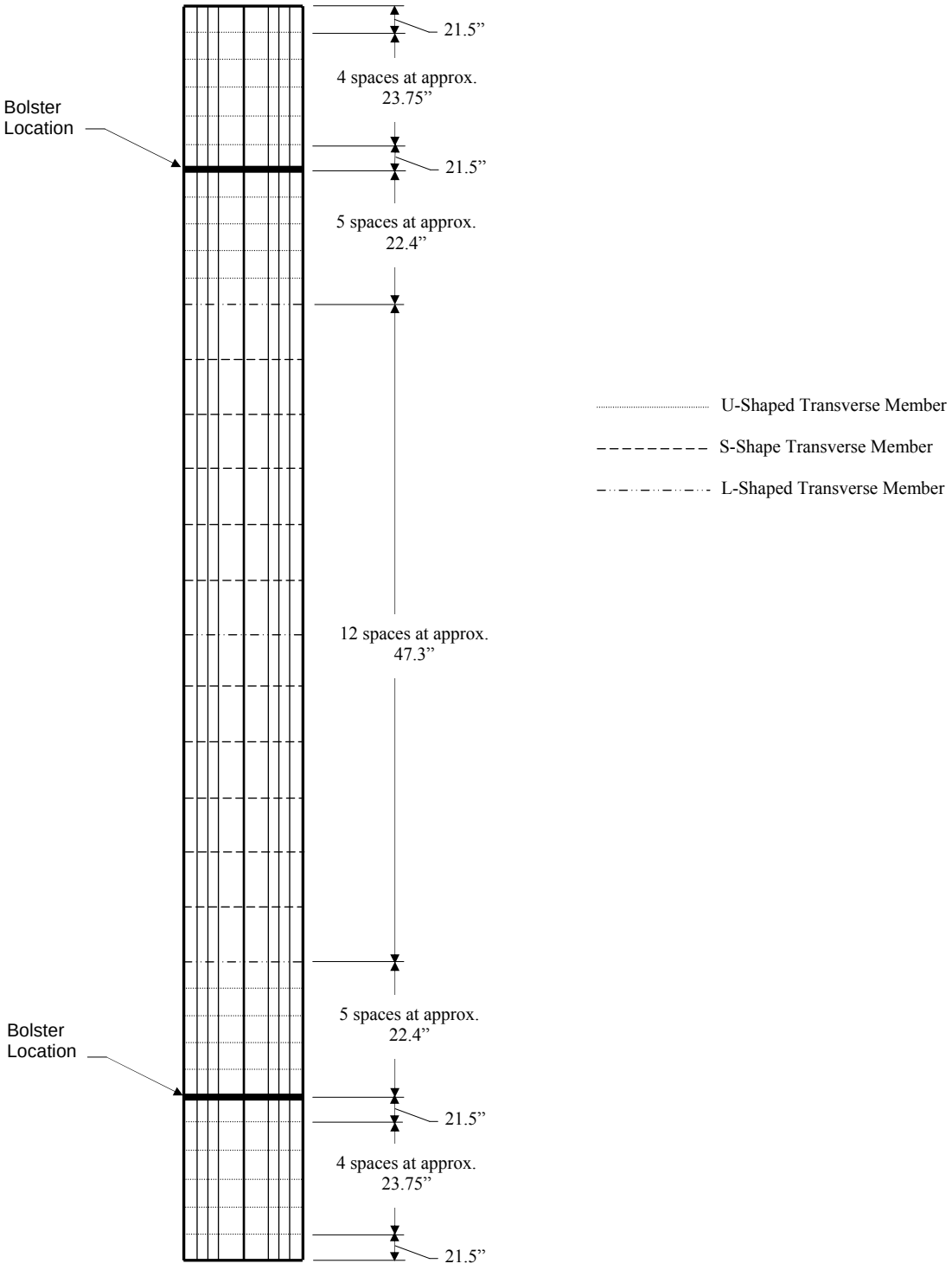

j. Transverse member locations

Figure 1.2. Continued

1.3.1 Tama County, Iowa Bridge [3]

As part of the 1999 Feasibility Study [3], a field load test was conducted on an existing RRFC bridge located two miles east of Chelsea, Iowa in Tama County.

1.3.1.1 Dimensions and Properties

The Tama County bridge consists of two RRFCs positioned side-by-side on timber abutments. The bridge spans 42 feet on a Class B rural gravel road. The RRFCs used for the Tama County bridge were each nine feet wide. Initially, there was no longitudinal connection between the two RRFCs, which had an eight inch gap between the adjacent flatcars. The bridge has metal grating over the entire RRFC surface for a deck with four inch by twelve inch timbers over the center twelve feet of the bridge to provide a driving surface.

Each flatcar has four main longitudinal members (two interior and two exterior) and six major transverse members. The exterior longitudinal members are constructed from a plate riveted to two angles to form built-up C sections with a depth ranging from 24 inches at midspan to twelve inches at the supports. The interior longitudinal members are constructed from a plate riveted to four angles to form built-up I - sections with a depth of 30 inches at midspan and twelve inches at the supports. The main transverse members are also built-up I shapes constructed in the same manner as the other sections.

The overall condition of the bridge is not good. Several of the major transverse members of each RRFC are severely deformed out-of-plane. Exterior and interior members of one flatcar also have significant out-of-plane deformation. A closer inspection of the RRFCs revealed that several rivets were either loose or missing completely. According to Tama County officials, the RRFCs were damaged prior to being installed at the bridge site. Support conditions at the abutments also varied for the two RRFCs. This caused some questioning of the redundancy in the bridge with respect to load paths.

1.3.1.2 Analysis

The Tama County Bridge was analyzed by conducting a field load test and by constructing an analytical model. The field load test was conducted by placing strain transducers and string potentiometers along the bridge and then driving a tandem axle dump truck of a known weight over the bridge. The field load test was conducted twice – once “as found” with no transverse connections between flatcars and once after connections had been added at the 1/4, 1/2, and 3/4 points along the span. Live load distribution was also analyzed using a grillage model of the bridge.

1.3.1.3 Results

Results from the field tests indicated that deflections were below the recommended live load deflection limit of span/800 as set forth by the American Association of State and Highway Transportation Officials (AASHTO) [5]. Stress levels were also below the allowed maximum values. Comparing the results from the different field load tests, the addition of the longitudinal connections did not produce results that varied significantly from the no connection field test, indicating that the presence of the connections did not impact the overall performance of the bridge. The results of the grillage model verified the field load test results. Even though the Tama County Bridge had several damaged members, the field tests and analytical model verified the ability of the bridge to support Iowa legal loads.

1.3.2 Buchanan County, Iowa Bridge 1 [4]

The RRFC bridge that was constructed in Buchanan County, Iowa (BCB1) as part of the demonstration project TR-444 [4] is located five miles southwest of Independence, Iowa. The previous bridge at the site was a two span bridge 16'-0" wide and 38'-5" in length constructed in 1878. The west span of the bridge was a pin-connected kingpost pony truss that spanned 24'-0". The 14'-5" east span of the bridge consisted of a timber stringer structure. Both spans of the bridge featured a timber deck. The bridge had a tandem-axle truck rating of ten tons.

1.3.2.1 Dimensions and Properties

Three 56-ft v-deck flatcars were selected for use in the BCB1. The resulting bridge is a single span bridge which is 59'-0" in length out-to-out of the abutments and has a width of 29'-0". The bridge was constructed on new concrete abutments supported by five HP 10x42 piles. On one end of the bridge, the RRFCs were built integrally with the abutment while the other end of the bridge features an expansion joint. A 14 1/2 inches wide by 24 inches deep reinforced concrete beam was cast between the RRFCs to provide a longitudinal connection between the adjacent flatcars. Threaded rods were also placed on 24 inch intervals through the reinforced concrete beam connection. Pea gravel was added to the v-section of the RRFC to facilitate drainage of the flatcars. A driving surface of asphalt millings was added along with a guardrail to finish the bridge.

1.3.2.2 Analysis

Three field load tests were conducted to determine the structural adequacy of the bridge. The first field load test was conducted before the flatcars were connected together. This test was conducted to verify the anticipated behavior of the individual flatcars. The second load test, which used combinations of one and two trucks, was conducted after the transverse connections were installed. The second test was conducted twice – once before the placement of the driving surface and once after. The final field load test was conducted after approximately one year of service. Only one truck was used in the third field load test.

A live load grillage analysis was also completed to verify the results of the field load tests. A simplified dead load analysis was completed by hand. Several assumptions were made about span lengths and support conditions to produce conservative dead load stresses.

1.3.2.3 Results

The 2003 AASHTO Standard Specification for Highway Bridges specifies an allowable flexural stress for compact steel sections not subjected to lateral-torsional buckling equal to 55 percent of the yield strength of the material [6]. Considering the 40 ksi yield strength determined during the coupon testing, the resulting allowable stress limit is approximately 22 ksi. All stresses in BCB1 were below this allowable limit. Vertical deflections were also below the recommended AASTHO limit of span/800 [5].

Strain and deflection results for the second load test were lower than the results from the first load test, indicating the adequacy of the transverse flatcar connections in providing lateral load transfer. Comparing results from before and after the placement of the driving surface indicated that the driving surface had minimal effects on load distribution. Results from the third field load test were similar to the results of the second load test, indicating no change in the performance of the bridge after one year of service.

1.3.3 Winnebago County, Iowa Bridge 1[4]

The RRFC bridge that was constructed in Winnebago County, Iowa (WCB1) as part of the demonstration project TR-444 [4] is located three miles east and three and an eighth miles south of Buffalo Center, Iowa on 40th Avenue across the North Fork Buffalo Creek. The existing bridge was a timber bridge with three equal spans of 18'-8" for a total length of 56'-0". The bridge had a timber deck with a width of 20'-8". A tandem-axle truck rating of seven tons was assigned to this bridge.

1.3.3.1 Dimensions and Properties

Three 89-ft flatcars were selected for use in WCB1. The resulting three span bridge has a main span of 66'-0" with two 10'-0" end spans for a total length of 86'-0" and a width of 26'-9". New steel capped piers and abutments supported by HP 10x42 piles were constructed to support the bridge. The RRFCs were welded to the south abutment to provide an integral connection. Expansion joints were constructed at the piers and north abutment. To provide a longitudinal connection between the RRFCs, the flatcars were positioned with no gap between the bottom flanges of the adjacent exterior girders and connected together with threaded rods. Concrete and longitudinal reinforcement was then added between the flatcars, forming a cast-in-place reinforced concrete beam that was approximately four and one half inches wide by seven inches deep. Steel plates were also added above and below the concrete beam to confine the concrete in the connection area. Timber planks were laid over the flatcars to aid in transverse load distribution. A gravel driving surface and a guardrail were added to complete the bridge.

1.3.3.2 Analysis

Three field load tests were conducted on WCB1. The first load test was conducted before the longitudinal connections were installed. The second load test was conducted immediately after the construction of the bridge. The third load test was conducted the following summer, or after approximately nine months of service. As was done with the BCB1, a live load grillage analysis and simplified dead load analysis were conducted to verify the field load test data.

1.3.3.3 Results

Due to the configuration of the 89-ft RRFC exterior girders, the exterior girders of adjacent flatcars needed to be trimmed to provide a level driving surface. Results from the field load test of WCB1 indicated nearly zero strain in the trimmed exterior girders. Therefore, trimming the exterior girders essentially eliminated the longitudinal redundancy of the RRFC. As with the BCB1, the longitudinal connection and transverse timber planking provided adequate transverse load distribution. Results from the grillage analysis were also in close agreement with the results from the three field load tests.

Coupon tests from the 89-ft flatcar indicated a proportional limit of approximately 40 ksi. The resulting allowable stress limit is therefore approximately 22 ksi. All stresses (live load and dead load) in WCB1 were below this limit. The maximum vertical deflections were also below the AASHTO recommended limit of span/800.

1.3.4 Buchanan County, Iowa Bridge 2 [7]

The second RRFC bridge tested by Bridge Engineering Center in Buchanan County, Iowa (BCB2) is five miles southeast of Quasqueton, Iowa on 280th Street over Dry Creek. The RRFC bridge was designed and

constructed by the Buchanan County Engineering Department based on the procedure used for the design and construction of BCB1.

1.3.4.1 Dimensions and Properties

Two 56-ft v-deck flatcars were used in BCB2. The resulting single span bridge has a center of abutment to center of abutment length of 54'-0" and a width of 20'-7". New concrete abutments that were nearly identical to those used for BCB1 were constructed. A slight change included an expansion joint at each abutment (verses one expansion and one integral as used in BCB1). A cast in place reinforced concrete beam, 24 inches deep and 30 ½ inches wide was used as a longitudinal connection between the two flatcars. Pea gravel was added to facilitate drainage of the v-sections. A gravel driving surface and guardrail were added to complete the bridge.

1.3.4.2 Analysis

Only one field load test was conducted on BCB2. The bridge was divided into three lanes and a test vehicle of known weight was driven across the bridge in each of the lanes at a slow speed, producing pseudo static field load test results (both strains and deflections). A simplified dead load analysis similar to the one conducted for BCB1 and WCB1 was also completed.

1.3.4.3 Results

Total stresses for BCB2 (stress results calculated from the measured strains due to the test vehicle and dead load stresses) were below the 22 ksi allowable limit established during the demonstration project. However, the test vehicle is not necessarily the largest vehicle that might utilize the bridge. Therefore, the stress levels generated by the test vehicle were extrapolated to those of a HS-20 designated truck (the most likely design vehicle for this type of bridge). Stress results were still below the allowable limits. Deflections from the test vehicle were also adjusted up to a HS-20 truck, with the projected deflections below the span/800 recommended limit. Although slightly different in configuration, both BCB1 and BCB2 produced similar results, indicating consistency in the performance of RRFC bridges.

1.3.5 Delaware County, Iowa Bridge [7]

The Delaware County, Iowa RRFC bridge (DCB) is located three miles northeast of Greely, Iowa near the intersection of 270th Avenue and Rainbow Road over Elk Creek. The RRFC bridge was designed by the Delaware County Engineering Department and was constructed by a private contractor.

1.3.5.1 Dimensions and Properties

Two 89-ft flatcars were selected for the DCB. A center of abutment to center of abutment span of 66'-4" was needed for DCB. In order to maintain the symmetry of the 89-ft flatcars, equal amounts were removed from each end to produce the desired span length. The DCB has a width of 18'-4". To form the longitudinal connection between the RRFCs, the flatcars were aligned transversely so that there was no longitudinal gap between the bottom flanges of the adjacent exterior girders. Threaded rods were then installed to connect the RRFCs together. For transverse continuity of the bridge deck, a steel plate was welded over the resulting gap on the bridge deck. A fabric liner was placed over the bridge to prevent the gravel driving surface from falling through the numerous small holes that were in the deck. A guardrail was added to finish the bridge.

1.3.5.2 Analysis

Testing of the DCB consisted of two tests – one pseudo static as was done with BCB2 and one dynamic. For the static test, the bridge was divided into three lanes and a test vehicle of known weight driven across the bridge in each lane. For the dynamic test, the test vehicle was driven across the bridge in Lane 2 (center of bridge) at two different speeds – 10 miles per hour (mph) and 15 mph.

As was done for previous RRFC bridges, a simplified dead load analysis was conducted. However, based on the results of the live load grillage analysis from WCB1, all dead load was applied to the interior girders of the bridge.

1.3.5.3 Results

As was done with BCB2, field test results were adjusted up for HS-20 loading. Deflections from the field load test were below the recommended limit of span/800. However, after extrapolating the deflections to a HS-20 loading, deflections exceeded the recommended limit by approximately 15%. Exceeding the recommended deflection limit was deemed acceptable by Delaware County because the DCB is on a low volume rural road.

Maximum stresses from the static field test exceeded the allowable limit of 22 ksi by approximately 12%. This exceedance increased to 27% when the HS-20 adjustment was applied. As tested, the gravel driving surface was ten inches in depth. Decreasing the amount of gravel to three inches decreases the stresses to below the 22 ksi limit. When comparing the results from the static load test, the longitudinal flatcar connection appeared to perform adequately in regards to lateral load distribution.

Maximum stresses from the dynamic field load exceeded the allowable limit by approximately 16%. By reducing the amount of gravel driving surface as previously discussed, the stresses decreased and are within the allowable limits. All deflections from the dynamic load test were within the AASHTO recommended limit.

1.3.6 Buchanan County, Iowa Bridge 3 [8]

The third Buchanan County, Iowa RRFC bridge tested by the Bridge Engineering Center (BCB3) is located one and one-half miles east of Quasqueton, Iowa on 270th Street. The existing bridge was a 20’-0” wide two-span timber bridge constructed in 1948. The bridge was constructed on timber abutments that were supported by timber piles. Timber planks with a gravel overlay constituted the driving surface.

1.3.6.1 Dimensions and Properties

Three 89-ft flatcars were selected for the BCB3. The flatcars were trimmed as was done for the DCB to produce a single span bridge with a center of abutment to center of abutment span of 66’-2” and a deck width of 20’-5 1/2”. The BCB3 abutments are a modification of the Iowa Department of Transportation standard stub abutment with zero skew [9] supported by HP 10x42 piles. To form the longitudinal flatcar connection, the flanges of adjacent exterior girders were trimmed and the flatcars connected by bolting through the webs. A gravel driving surface and guardrail were added to finish the bridge.

1.3.6.2 Analysis

Field load testing of BCB3 consisted of both static and dynamic testing. For the static testing, the bridge was divided into five lanes and the test vehicle driven across the bridge in each lane. For the dynamic testing, the test vehicle was driven across the bridge at five different speeds, starting at 10 mph and increasing in 5 mph increments up to 30 mph. A simplified dead load analysis was conducted for BCB3 as well. Dead load was applied to the longitudinal girders in proportion to the moment of inertia of the girders. A theoretical analysis using HS-20 designated loading was also completed to determine the maximum stresses in the bridge.

1.3.6.3 Results

As was done with the DCB and BCB2, field test results were extrapolated to represent loading from a HS-20 test vehicle. Deflections for the field test vehicle were below the AASHTO recommended values of span/800. However, after adjustment to a HS-20 loading, the deflections exceeded this limit by approximately 32%. Stresses for the test vehicle plus dead load were slightly below the allowable limit of 22 ksi. Results from the theoretical analysis using HS-20 loading confirmed that the stresses would exceed the 22 ksi limit by 15%. Results of the dynamic analysis indicated that the highest dynamic amplification occurred at 25 mph.

1.3.7 Winnebago County, Iowa Bridge 2 [8]

The second Winnebago County, Iowa RRFC bridge (WCB2) tested by the Bridge Engineering Center is located five and one-half miles west and one mile north of Lake Mills, Iowa on 460th Street. The existing bridge was a three span timber bridge with an overall length of 62’-0” center of abutment to center of abutment. The bridge was supported by a timber substructure. The deck was constructed from three inch by twelve inch creosoted timber planks [8].

1.3.7.1 Dimensions and Properties

Three 89-ft RRFCs were used in the WCB2 bridge. The bridge has a main span of 66’-4” center to center of abutments with 2’-1 3/4” overhangs on each end for a total out-to-out length of 70’-7 1/2”. The bridge is 27’-0” wide with a 26’-5” driving surface. A reinforced concrete beam similar to the one used for WBC1 was used to connect the adjacent flatcars longitudinally. Timber planks were added to the driving surface to enhance the load distribution. The north side of the bridge has three inch by twelve inch timber planks that butted against each other, where as four inch x twelve inch tongue-and-groove timber planks were used on the south side of the bridge.

1.3.7.2 Analysis

Field testing of WCB2 included both static and dynamic load tests. For the static load test, the bridge was divided into four lanes with the test vehicle driven across the bridge in each lane. A dynamic load test was also conducted at four speeds (10, 15, 20, and 25 mph).

A simplified dead load analysis was conducted assuming that the bridge was simply supported at the abutment locations. Due to the different plank configurations, the dead load on each side of the bridge was uniformly distributed over only half of the bridge in the transverse direction with the change occurring where the timber planks changed. The dead load was assumed to be distributed evenly in the

longitudinal direction. Ratios of the moment of inertia for the various members were used to distribute the dead load from each side of the bridge to the interior and exterior girders. A theoretical analysis using HS-20 loading was also conducted to determine the maximum stresses in the RRFC.

1.3.7.3 Results

Deflections from the test vehicle were below the AASHTO recommended limit of span/800. However, after the deflections were adjusted for a HS-20 vehicle, deflections exceeded the recommended limit by approximately 27%. Stress values for the test vehicle were below the allowable limitation of 22 ksi. However, as was the case with deflections, stresses exceeded the allowable limit after the field test results were adjusted up for HS-20 loading.

Since the bridge had two different mechanisms for lateral load distribution, a comparison of the different plank configurations was also investigated. As would be expected, the tongue-and-grove planks provided better transverse load distribution. This was evidenced in the lower strains and deflections on the south side of bridge which had the tongue-and-groove plank connections. Results from the dynamic field load test indicated that the largest dynamic amplification occurred when the test vehicle crossed the bridge at 10 mph.

1.4 Objective and Scope of Project

Based on the recommendations for further study in the 2003 ISU RRFC demonstration project (TR-444) [4], a research project to continue investigating the behavior of various RRFC bridges was initiated. The primary objectives of this additional research were to:

- Investigate variables in bridge construction to improve the performance, cost, and constructability of RRFC bridges
- Design, construct, and test three RRFC multiple span bridges implementing variables from the previous objective
- Refine the design methodology presented in the demonstration project, TR-444 for multiple span RRFC bridges
- Develop a load rating process for multiple span RRFC bridges

To achieve the aforementioned objectives, the following tasks were completed:

- Data collection and analysis through field testing of three multiple span RRFC bridges with varying span lengths, widths, longitudinal connections, and abutment types.
- Analysis and design of construction variables including the use of sheet pile wall abutments

2.0 BUCHANAN COUNTY, IOWA BRIDGE 4 ON 250TH STREET

2.1 Background

The fourth RRFC bridge in Buchanan County, Iowa (BCB4) tested by the Bridge Engineering Center is located three miles northwest of Quasqueton, Iowa on 250th Street over Pine Creek (Figure 2.1). The previous bridge at this location was a single span high truss bridge constructed in 1905 with a length of 82'-0", a width of 15'-8", and a minimum clearance of 12'-0".

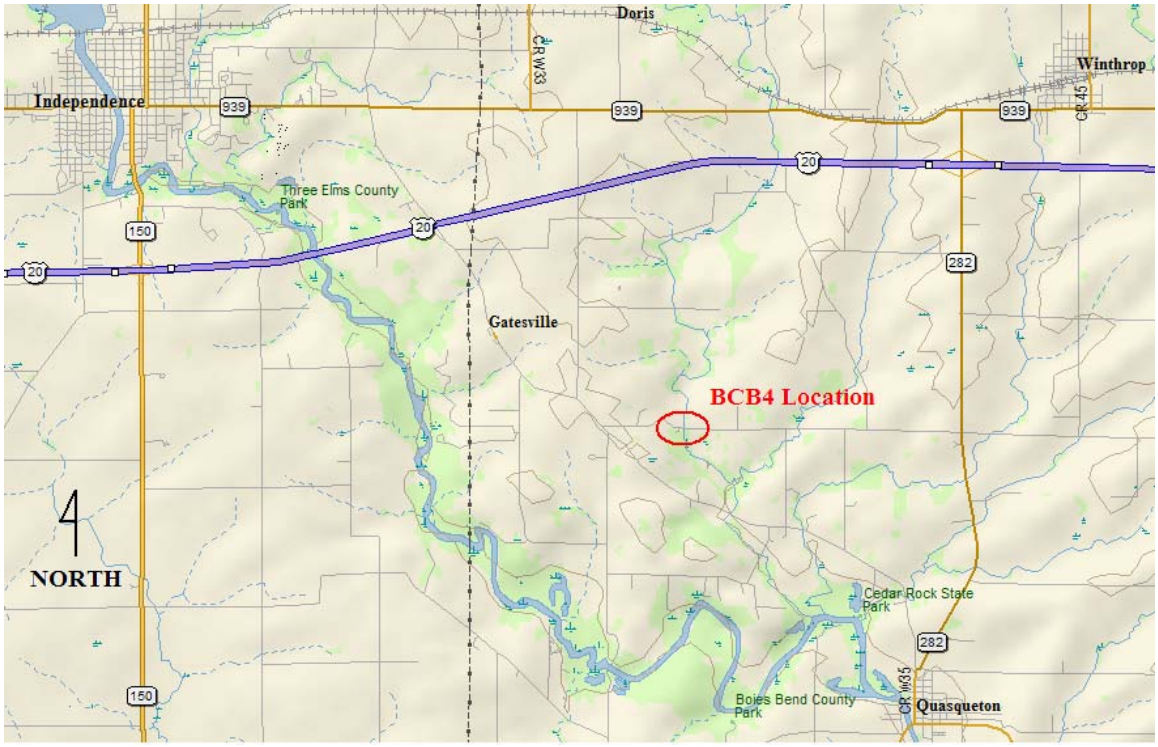

Figure 2.1. Location of Buchanan County RRFC Bridge 4 (BCB4) [10]

2.2 BCB4 Design and Construction

Buchanan County Bridge 4 (BCB4) is the first multiple span RRFC bridge designed, constructed, and tested in Buchanan County. This bridge was designed by the Buchanan County Engineer's office using guidelines and construction techniques developed from previous RRFC bridge projects.

Two 89-ft RRFCs were used in the construction of BCB4. The existing bridge single span was significantly longer than the maximum single span length (66 feet) that could be accommodated using RRFCs. Therefore, a new pier was constructed slightly offset from the middle of the span to compliment the existing abutments. The pier is supported by five HP 10x42 piles driven to refusal (approximately 30 feet). Although the existing bridge abutments were used for BCB4, a slight modification was needed. The seat of the abutments needed be raised approximately fourteen inches to facilitate the use of the RRFCs in conjunction with the new pier support. An idealized layout of the bridge with the 1/4 span locations dimensioned is shown in Figure 2.2.

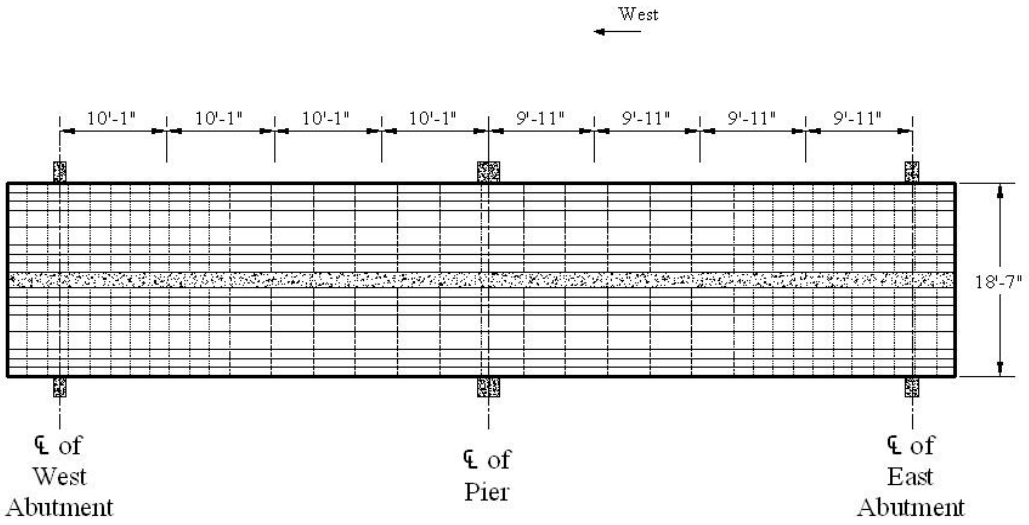

a. Idealized Plan View

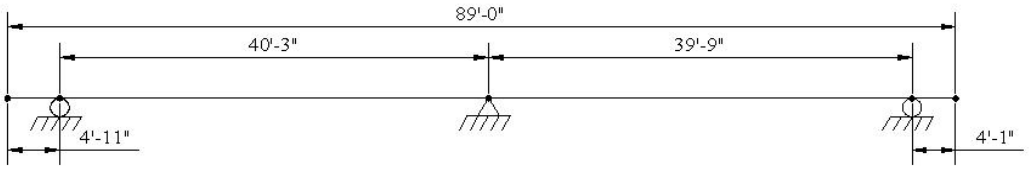

b. Idealized Profile View

Figure 2.2. Idealized layout of BCB4

There is no structural connection between the bridge and the concrete supports – the flatcars simply rest on the supports. At the abutments and piers, the interior girders of the bridge are supported by bearing plates. At these same locations, the exterior girders are supported by a stack of W-sections confined by inverted channels as shown in Figure 2.3.

Due to the geometry of the exterior girders of the 89-ft RRFC, the top portion of the exterior girder of the adjacent flatcars needed to be removed to provide a flush driving surface. After the top of the exterior girder was removed, the longitudinal flatcar connection (LFC) between the flatcars could be constructed. Similar to the LFC connection used in BCB1 and BCB2, this connection consists of a reinforced concrete beam twelve inches deep by eighteen inches wide and transverse 5/8 inch diameter threaded rods through the webs of the adjacent RRFC exterior girders as well as the reinforced concrete beam.

After the flatcars were placed and the longitudinal connection constructed, a layer of non-woven geo-textile fabric was laid over the top surface of the RRFCs to prevent the gravel driving surface from falling though small holes that were in the deck of the RRFC. Approximately four inches of gravel was then added for the driving surface of the bridge after which a guardrail was attached. The finished bridge is shown in Figure 2.4.

Figure 2.3. Miscellaneous I-shapes used as exterior girder support

Figure 2.4. Completed Buchanan County RRFC Bridge 4 (BCB4)

2.3 BCB4 Field Testing

To determine the behavior of BCB4, field load tests were conducted using Buchanan County Secondary Road Department tandem-axle trucks loaded with gravel. Two trucks were used for the load tests – one as the primary test vehicle and one as an auxiliary vehicle. The dimensions and weights of the trucks used are shown in Figure 2.5.

2.3.1 BCB4 Instrumentation

To determine the structural behavior of BCB4 during the field load tests, BDI strain transducers and string potentiometers were attached to the bridge. A data acquisition system was then connected to the instrumentation to obtain a continuous data record of the structural behavior of the bridge. As the

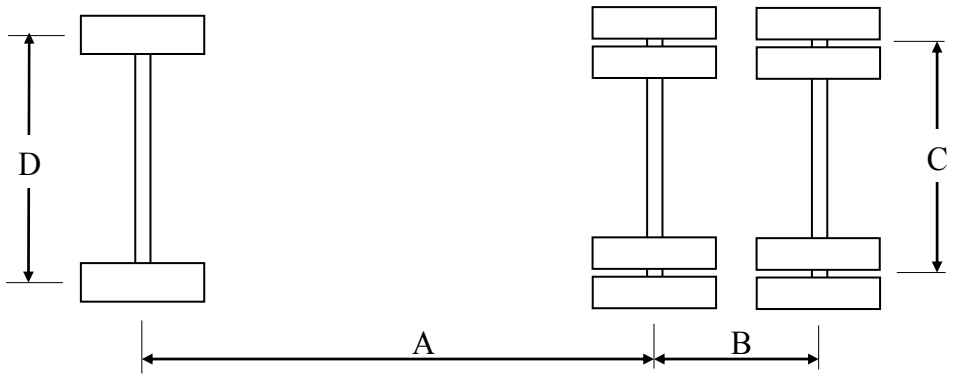

a. Top view

b. Side view

Truck	Dimensions (inches)				Load (lbs)		
	A	B	C	D	F	T	Gross
Primary	165	53	72	85	16,930	37,230	54,160
Auxiliary	167	53	72	84	17,020	37,440	54,460

tandem axle of the test truck crossed predetermined reference points on the bridge, a feature of the data acquisition system was used to "mark" the data for use in the analysis process. The reference points for BCB4 were the center of bearing for each support (both abutments and pier) as well as the 1/4, 1/2, and 3/4 span locations of each span for a total of nine reference sections.

Figure 2.5. Weights and dimensions of BCB4 test vehicles

The instrumentation plan for BCB4 is presented in Figure 2.6. As shown in Figure 2.6, 36 BDIs were placed at ten different cross sections along the bridge; sixteen string potentiometers were located on four cross sections along the bridge, as also shown in the figure.

A preliminary analysis indicated possible high strains at the shallow end of the tapered transition section (identified in Figure 2.7) of the RRFC profile (Detail A and I in Figure 2.6b and Figure 2.6j, respectively). Although the maximum moment does not occur at these locations, the section is significantly shallower, which results in a smaller moment of inertia and thus larger magnitudes of strain.

The pier location was also investigated for the possibility of large strains. BCB4 was instrumented with ten BDIs on the east side of the pier (Detail E in Figure 2.6f). At this location, BDIs were placed on the exterior girders of the bridge as well as on the RRFC exterior girders at the longitudinal flatcar connection. BDIs were also placed near the top of the main girder to measure the tensile strains. A BDI was also placed on the bottom flange of the south interior girder. The purpose of this transducer was two fold. First, it was used to measure the compressive strains occurring at the pier. Secondly, using the tensile strain from the companion transducer on the top of the interior girder at this location, the location of the experimental neutral axis at this location could be determined. Two BDIs were also placed on the bottom side of the deck in this cross section to investigate the contribution of the RRFC deck in resisting the negative moment. On the west side of the pier (Detail D in Figure2.6e), BDIs were placed near the top of the interior girders only. A BDI was also placed on the south guardrail (3 ft from the pier centerline) to determine the amount of load resisted by the guardrail.

At the east midspan (Detail G in Figure 2.6h), BDIs were placed on the bottom flanges of both interior girders to measure tensile strains. One BDI was also placed near the top of the south interior girder at this location so that the experimental neutral axis location could be determined. BDIs were also placed on the exterior girders of the bridge as well as the flatcar exterior girders that comprise the longitudinal connection. As was done in Detail E (Figure 2.6f), a BDI was also placed on the south guardrail.

Deflection instrumentation was placed mainly at the two midspan locations. At the east midspan, string potentiometers were placed below all the main girders (interior and exterior) as well as the exterior girders that comprise the longitudinal flatcar connection. String potentiometers were also placed at the 1/4 span and 3/4 span locations in the east span of the bridge. At these locations, one potentiometer was placed below each interior main girder and below the longitudinal connection. At the west midspan, string potentiometers were placed below the bottom of the interior girders and below the flatcar exterior girders comprising the longitudinal connection.

2.3.2 BCB4 Field Load Test

The BCB4 field test consisted of three different load tests. First, two trucks, one on each span, were transversely centered on the bridge to produce a large negative moment at the pier location (Figure 2.8). Two positions were investigated for the maximum negative moment. First, the trucks were positioned with the rear tandem axle centered at a location identified in a preliminary analysis as the truck position

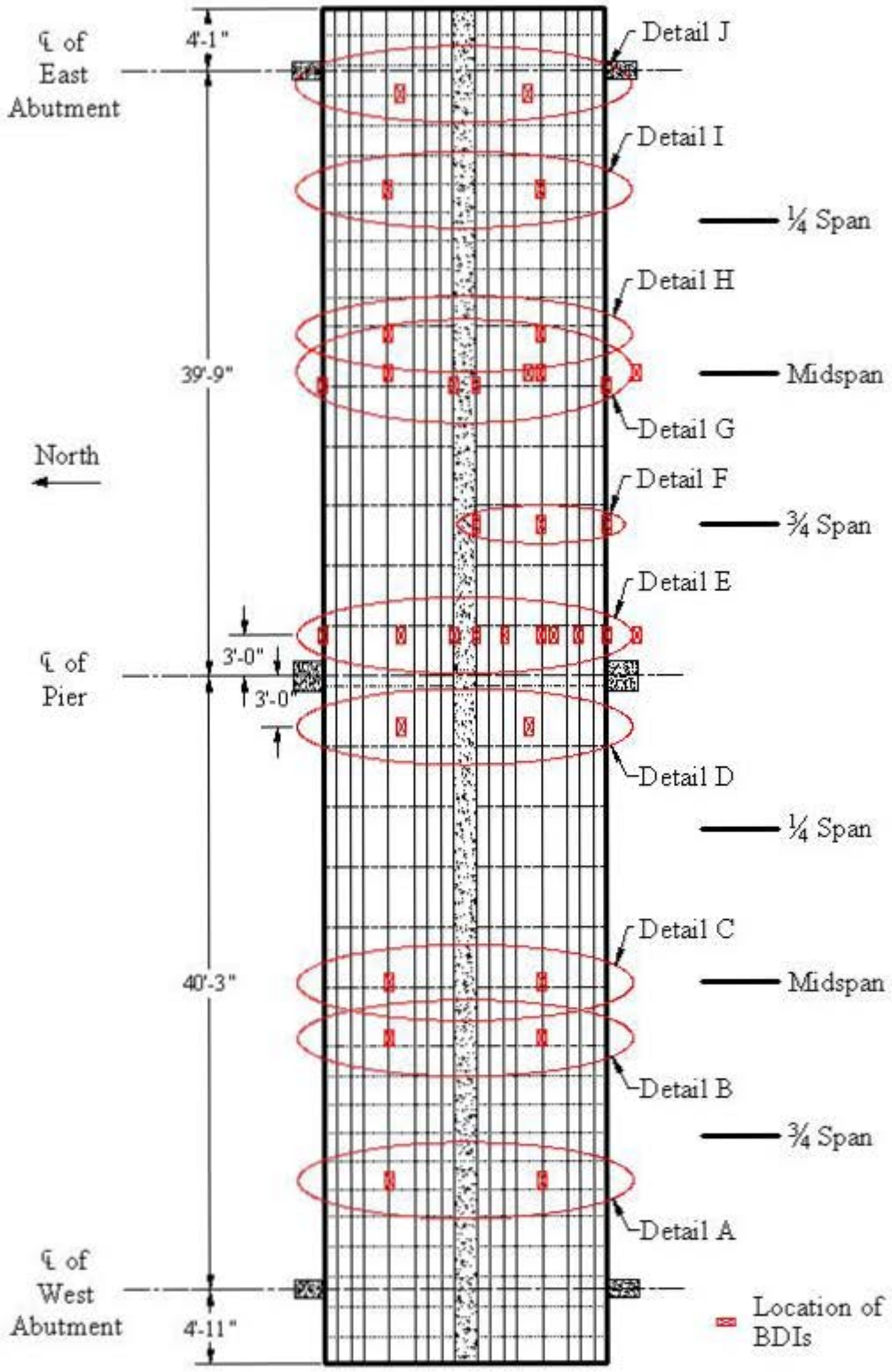

a. Strain Instrumentation

Figure 2.6. BCB4 instrumentation plan

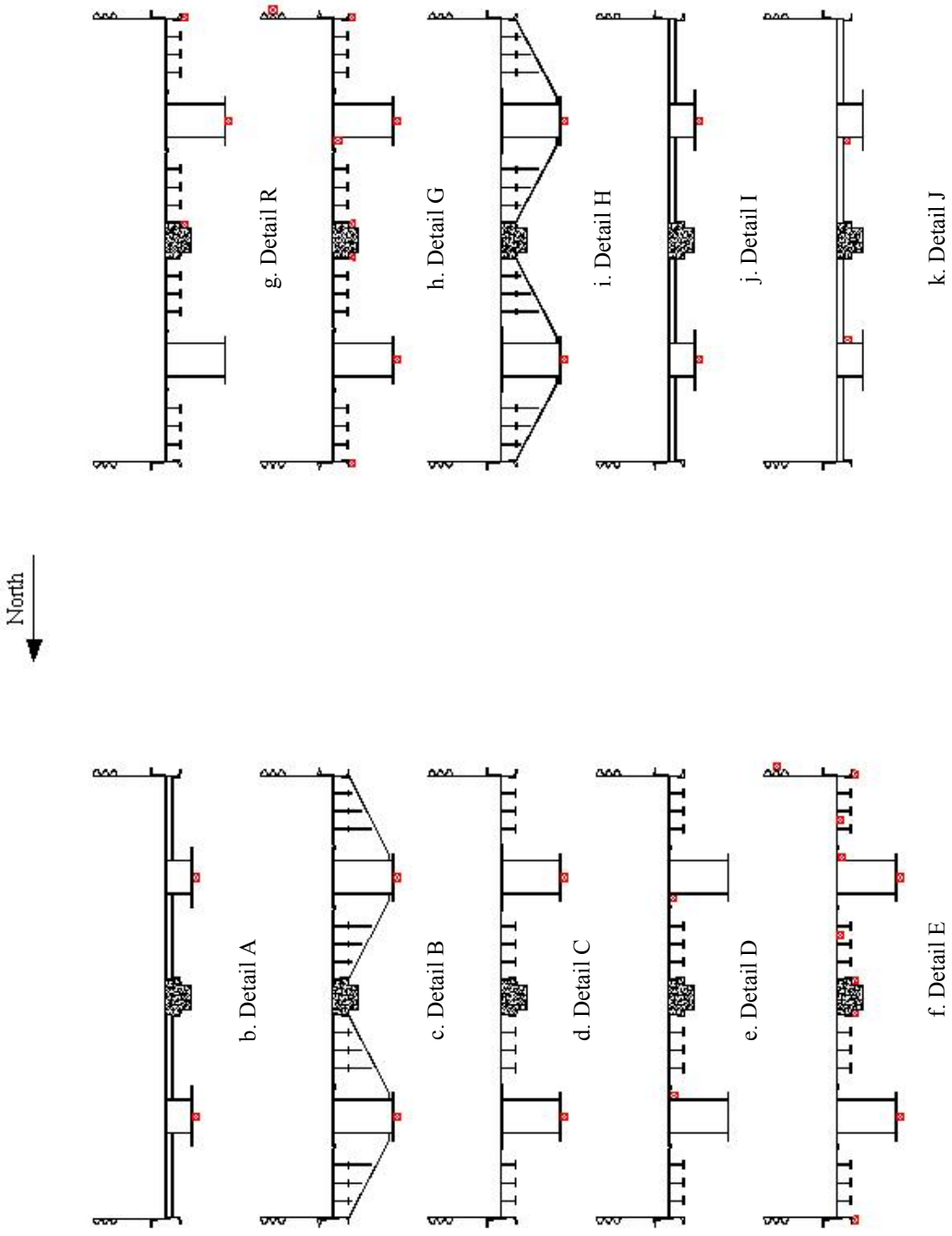

Figure 2.6. Continued

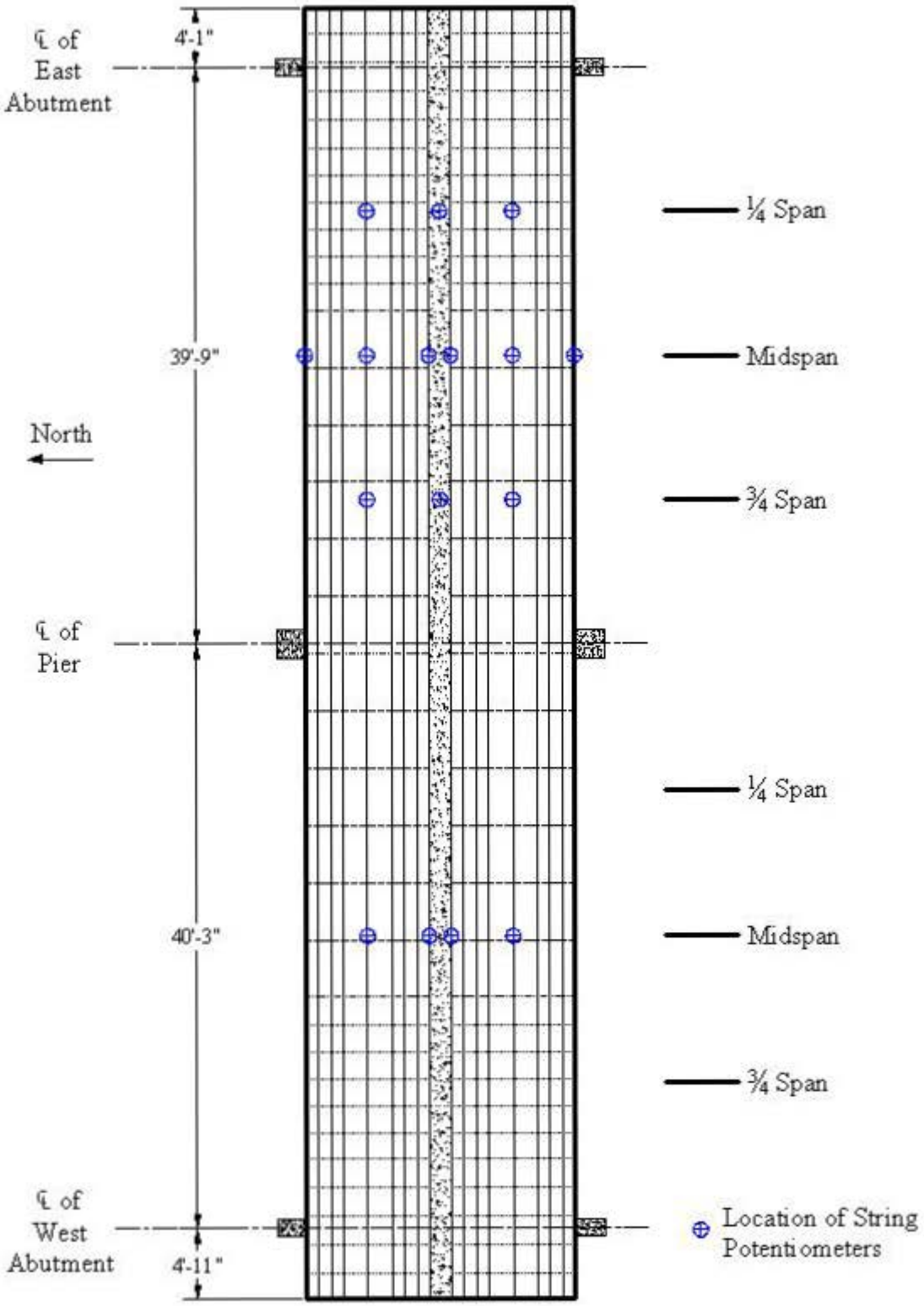

l. Deflection Instrumentation

Figure 2.6. Continued

Figure 2.7. Tapered transition section of RRFC profile

a. Front view of two-truck load test

b. Side view of two-truck load test

Figure 2.8. BCB4 two-truck load test

which producing the maximum negative moment. The trucks were then moved ahead to position the trucks with their tandem axle centered at the midspan location of each of the two spans.

Next, a pseudo-static test was conducted with the primary test vehicle crossing the bridge at an idle in one of the three lanes as shown in Figures 2.9 and 2.10. The interior lane (Lane 2) placed the truck transversely in the center of the bridge. The other two lanes (Lanes 1 and 3) placed the truck with the outer wheel line of the truck approximately two feet from the north and south edge of the bridge, respectively. Finally, a dynamic load test was conducted by having the test vehicle cross the bridge in the center lane (Lane 2) at approximately 30 mph. Each load test was conducted twice to investigate the repeatability in the behavior of the bridge and the recorded data.

a. Test Vehicle in Lane 2 (Middle Lane)

b. Test Vehicle in Lane 1 (North Lane)

c. Test Vehicle in Lane 3 (South Lane)

Figure 2.9. BCB4 pseudo-static load test

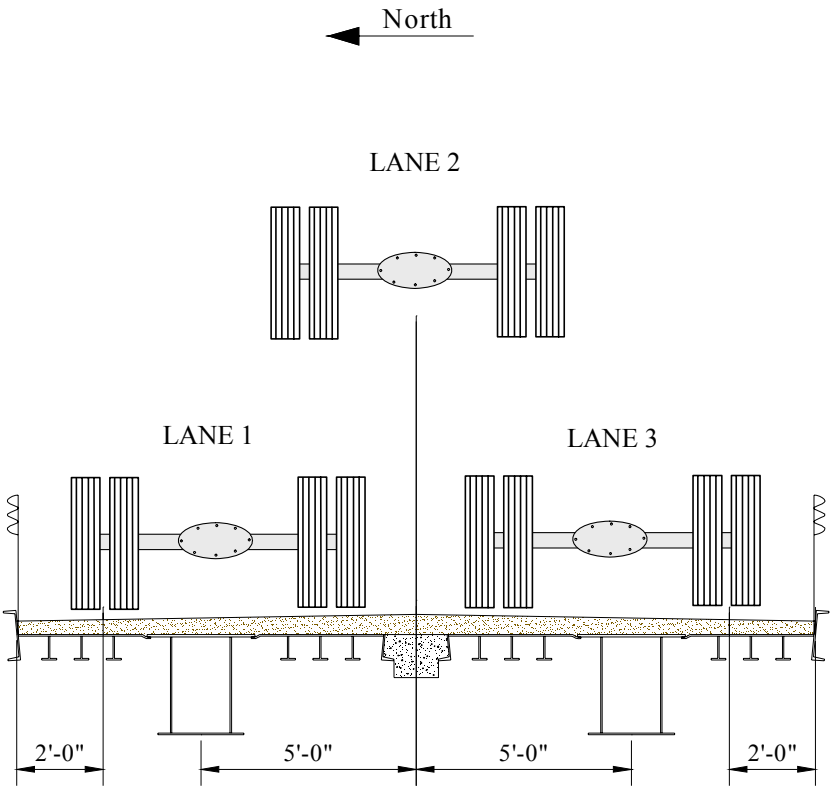

Figure 2.10. BCB4 lane configuration for load tests

2.4 BCB4 Dead Load Analysis

The total stresses occurring in BCB4 is the resultant of the live load stresses caused by the test vehicle and the stresses caused by the dead load on the bridge. To determine the total stresses in the bridge, a dead load analysis was completed. As was done in the analysis of previous RRFC bridges, several assumptions were made to simplify the dead load analysis. Based on the results of a grillage analysis conducted on the 89-ft flatcar as part of TR-444, it was assumed that the entire dead load is resisted by the main girders [4]. Also, as was done with previous RRFC bridges, the connected flatcars were assumed to form a rigid cross section. This allows for any additional dead load to be considered uniformly distributed on the bridge.

The dead load for BCB4 is comprised of mainly the driving surface and the weight of the flatcars. Based on previous reports, the RRFC was assumed to weigh 42,000 lbs or approximately 472 lbs/ft. The BCB4 driving surface is comprised of gravel with an approximate depth of 4 1/4 inches. A unit weight of 120 pound/ft^3 was assumed for the gravel. The longitudinal connection and the guardrail (100 lbs/ft) also added to the dead load. Adding the three dead loads, the total dead load per car for BCB4 is approximately 1,040 lbs/ft.

To determine the dead load stresses, an idealized model of the bridge was constructed in a structural analysis program. The model was then subjected to a uniform dead load of 1,040 lbs/ft to determine the resulting moments. At the critical sections – tapered transition, midspans, and the pier – the dead load moment was divided by the section modulus of the main girder of the bridge. The section modulus of the main girder was found by determining the neutral axis depth based on the entire approximate bridge cross section at the locations of interest. The moment of inertia for the main girder was then determined with respect to this neutral axis (instead of the neutral axis for the main girder only). This approach was used to better represent the actual behavior of the bridge. The resulting section modulus was also more conservative. For BCB4, the section modulus was calculated to be approximately 460 in^3. A modulus of elasticity of 29,000 ksi (See Section 1.2.3) was used to convert the dead load stresses to strains. The resulting dead load strains/stresses are shown in Table 2.1 ("+" indicates tension and "-" indicates compressive). Unless noted otherwise, the dead load strains/stresses reported are bottom flange values.

Table 2.1. BCB4 dead load strains (stresses) at critical locations

	WEST SPAN		EAST SPAN	
Location	Dead Load Microstrain	Dead Load Stress (ksi)	Dead Load Microstrain	Dead Load Stress (ksi)
Shallow End of Taper	+ 184	+ 5.3	+ 197	+ 5.7
Midspan	+ 82	+ 2.4	+ 78	+ 2.2
Pier - Top Flange	+ 55	+ 1.6	+ 55	+ 1.6
Pier - Bottom Flange	- 206	- 6.0	- 206	- 6.0

2.5 BCB4 Field Load Test Results

After completion of the field load tests, the results were analyzed to determine the structural behavior of BCB4. To determine the total stress occurring in BCB4, the live load strain values were converted to stresses using an elastic modulus of 29,000 ksi (See Section 1.2.3). The live load stresses were then added to the dead load stress, as appropriate, to determine the total stresses.

The 2003 AASHTO *Standard Specification for Highway Bridges* specifies an allowable flexural stress for compact steel sections not subjected to lateral-torsional buckling equal to 55 percent of the yield strength [6]. Coupon testing was conducted on the 89-ft RRFC during TR-444, with the results indicating a yield strength of 40 ksi. However, since no material testing has been conducted on subsequent RRFCs, a conservative yield stress of 36 ksi is assumed. Using the AASHTO limitation and a 36 ksi yield strength, the maximum allowable stress for BCB4 is 19.8 ksi (683 microstrain).

Although all of the test results were analyzed after completion of the field load tests, only the maximum results for the critical sections - tapered transition section (Figures 2.6b and 2.6j), midspans (Figures 2.6d and 2.6i), and at the pier (Figures 2.6e and Figure 2.6f) – will be discussed, as the results at these sections control the performance of the bridge. The strain results at other locations were of smaller magnitude and thus not of interest.

2.5.1 Static Test Results

After reviewing the field load test results, the largest live load strains due to a single vehicle occurred near the shallow end of the tapered transition section of the RRFC. The largest live load strain measured at this location was 170 microstrain (4.9 ksi), occurring in the east span of the bridge. The dead load stress at this same location was calculated to be 197 microstrain (5.7 ksi). Adding the dead load strains to the field test results, the total strain occurring at the shallow end of the tapered transition section is 367 microstrain (10.6 ksi), or 54% of the 19.8 ksi (683 microstrain) allowable limit.

Previous RRFC bridges tested by Iowa State University consisted of single span bridges with the exception of WCB1 which had short end spans, thus BCB4 was the first RRFC bridge that had significant negative bending moments. For this reason, there was particular interest in the strains, both live load and dead load, occurring at the pier.

At the pier location, the strain instrumentation was placed approximately two feet from the face of the pier (three feet from the pier centerline) to minimize local strain effects occurring due to the support condition at the pier. An adjustment factor was then used to correct the load test data to the pier location. To determine this adjustment factor, the bridge was analyzed in a structural analysis program to determine the theoretical moment envelope for the test vehicle. A moment ratio (i.e. the adjustment factor) was then determined by comparing the moment at the pier centerline and at the location two feet from the face of the pier. The adjustment factor for BCB4 was calculated to be 1.08.

Due to the geometry of the RRFC cross section, the BDIs at the pier could not be placed at the maximum tensile location (i.e. the top of the cross section). To adjust the tensile live load strains, the strain profile of the bridge was determined using the neutral axis location. The live load strains were then extrapolated to the top of the strain profile, assuming a linear distribution.

At the pier, after adjustment for gage location in the strain profile (distance from neutral axis) and proximity to the pier, the maximum live load tensile strain was 86 microstrain (2.5 ksi). After including the dead load strain of 55 microstrain (1.6 ksi), the maximum total tensile strain at the pier of BCB4 was 141 microstrain (4.1 ksi). The maximum compressive live load strain at the pier was -107 microstrain (-3.1 ksi). After adding the dead load strain of -206 microstrain (-6.0 ksi) to the live load strain, the maximum total compressive strain at the pier was -313 microstrain (-9.1 ksi), or approximately 46% of the allowable limit of -19.8 ksi (-683 microstrain).

For a continuously bridge structure, the midspan strains/deflections are not the largest in the span due to the continuity over the intermediate supports. However, the instrumentation was placed at the midspan for the BCB4 field load tests to measure the approximate maximums as the difference between the midspan values and the maximum values is usually minimal.

The strains and deflections measured for each midspan location are presented in Figure 2.11 – 2.13 for each of the three test lanes. Dashed lines have been added to provide a hypothetical linear trend line between the data points. As can be seen in the figures, the maximum deflection and strains occur in the flatcar on which the test vehicle is positioned. . The transverse distribution of the live load can be seen by the distribution in strain (or deflection) to the unloaded portion of the bridge

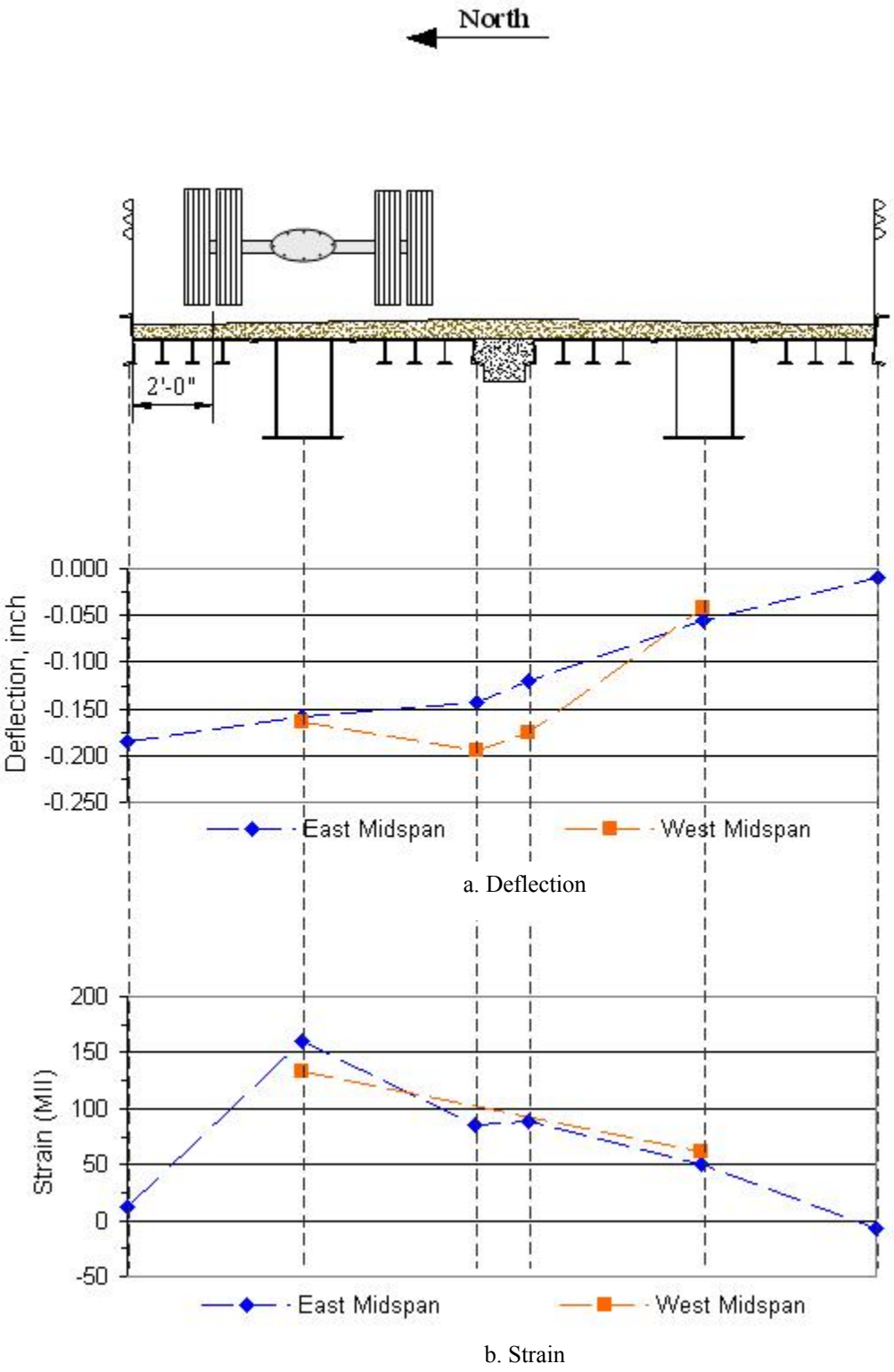

Figure 2.11. BCB4 Lane 1 midspan live load deflections and strains

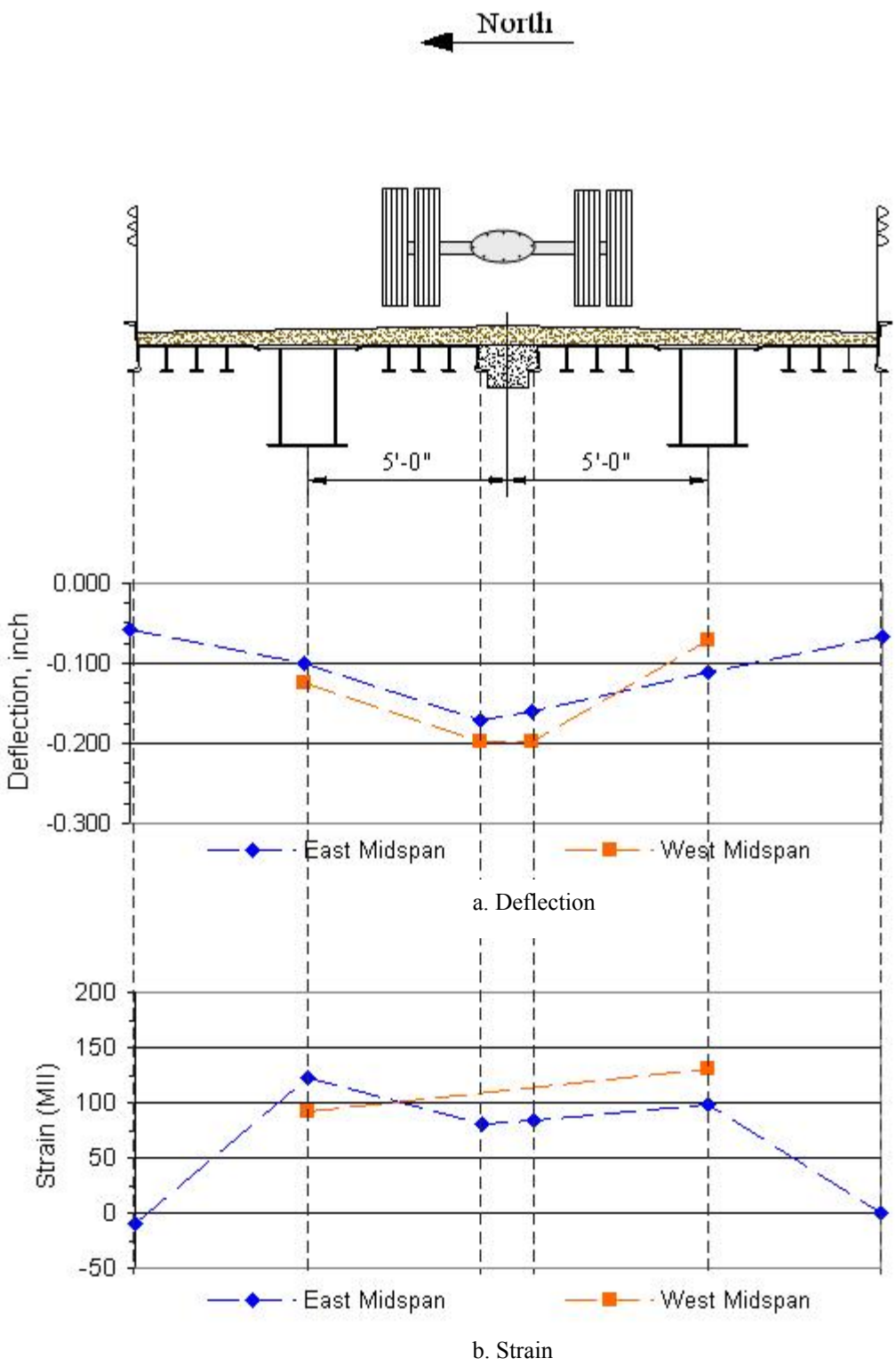

a. Deflection

b. Strain

Figure 2.12. BCB4 Lane 2 midspan live load deflections and strains

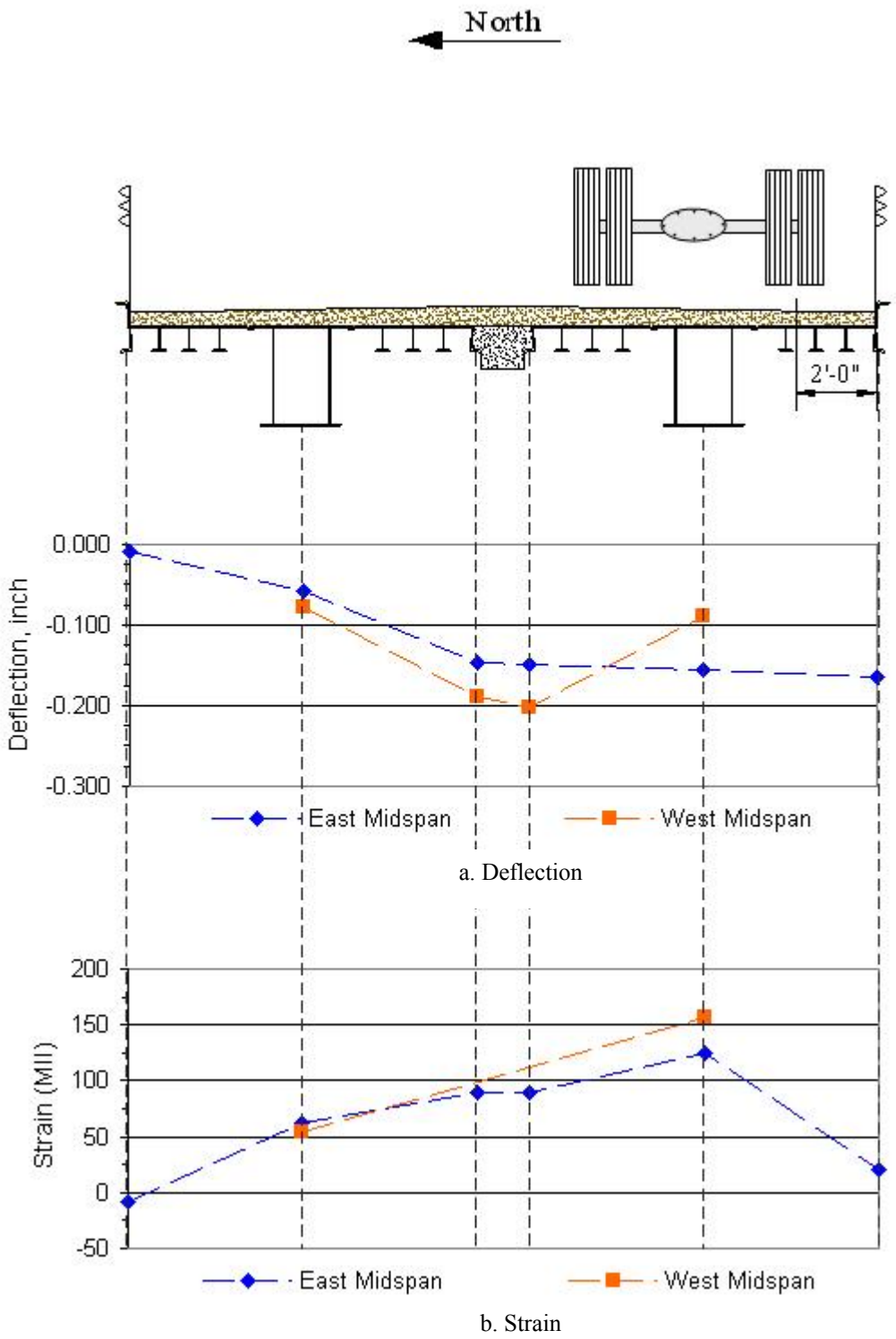

Figure 2.13. BCB4 Lane 3 Midspan live load deflections and strains

cross section. The maximum midspan strain that occurred as a result of the load test was 160 microstrain (4.6 ksi). Adding the dead load strain (stress) value of 78 microstrain (2.2 ksi) increases the total maximum strain (stress) occurring at the east midspan to 238 microstrain (6.8 ksi), approximately 35% of the allowable 19.8 ksi (683 microstrain) limitation.

After comparing the results presented in Figure 2.12 and 2.14, a discrepancy was discovered in the deflections recorded at the west midspan during the BCB4 field load test. This discrepancy is most evident in Figure 2.14, which has the test vehicle positioned directly over the instrumentation recording the questionable data. At this point, the string potentiometer below main girder of the south RRFC does not agree with corresponding strain data – the strain increases, but the deflection decreases from the other lane positions. After review of the BCB5 data, a similar discrepancy in the deflection data was discovered. Considering the BCB4 discrepancy, in addition to the similar disagreement with the BCB5 data, an instrumentation problem is believed to be the likely cause of the inconsistent behavior even though no apparent problem was found with the suspected transducers after they were reviewed by the laboratory manager. The BCB5 discrepancy is discussed in further detail in Section 3.5.1.

The maximum midspan live load deflection for the test vehicle was 0.202 inches, which occurred in the west span of the bridge. The AASHTO *LRFD Bridge Design Specification* recommends a maximum allowable live load deflection of span/800 for legal truck loads [5]. Using this approach, the maximum allowable live load deflection for the west span of BCB4 is 0.596 inches.

As was done in the testing of previous RRFC bridges, an adjustment factor was used to increase the results from the test vehicle to that of an HS-20 truck, the likely design vehicle for the bridge. To determine the adjustment factor, the test vehicle loading and an HS-20 loading were each positioned with the load center of gravity at the midspan location of each span. The respective maximum moment values were then compared (maximum moment for test vehicle loading vs. maximum moment for HS-20 loading) to produce the adjustment factor, which was calculated to be 1.168 for BCB4 (See Appendix E of TR-498 Volume 1 for an example [11]). Using this value, the projected maximum total strain for an HS-20 test vehicle on BCB4 becomes 396 microstrain (11.5 ksi) at the shallow end of the tapered transition section of the east span. This magnitude is still below the allowable value of 19.8 ksi (683 MS). Using the same approach, the maximum live load deflection becomes 0.236 inches, still within the AASTHO guidelines.

The moment fraction, which is the portion of the total transverse live load moment due to the applied load carried by an individual girder or flatcar in this situation, was also determined for BCB4. To determine the moment fraction, the area under the deflection (or strain) curve was determined. The area under the loaded RRFC was then compared to the entire area to determine the moment fraction. For BCB4, the experimental moment fraction was approximately 2/3, similar to the values reported in previous investigations.

To further investigate the strains occurring over the pier, an auxiliary vehicle was used in combination with the test vehicle as discussed in Section 2.3.2. At the pier, after adjustment for gage location in the strain profile (distance from neutral axis) and proximity to the pier, the maximum live load tensile strain was 138 microstrain (4.0 ksi). After adding the dead load strain of 55 microstrain (1.6 ksi), the maximum total tensile strain at the pier of BCB4 due to two trucks was 193 microstrain (5.6 ksi). The maximum compressive live load strain at the pier was -164 microstrain (-3.1 ksi). After adding the dead load strain of -206 microstrain (-6.0 ksi), the maximum total compressive strain at the

pier was -370 microstrain (-10.7 ksi), or approximately 54% of the allowable limit of -19.8 ksi (-683 microstrain).

2.5.2 Dynamic Test Results

As stated earlier, a dynamic load test was conducted by driving the test vehicle across the bridge in the center lane (Lane 2) at approximately 30 mph. From this field load test, the structural dynamic properties of the bridge were approximated, as well as the dynamic amplification due to the moving load.

The free vibration oscillations of the bridge were used to approximate the frequency, period, and damping occurring in the bridge superstructure. By observing the oscillations per time, the frequency of BCB4 was approximated as 7.75 hertz which resulted in a natural period of 0.13 seconds. The damping ratio, using a simple logarithmic decrement, was calculated to be approximately 1 %. Table 2.2 summarizes the dynamic properties of BCB4.

Table 2.2. BCB4 dynamic properties

Location	Frequency (Hz)	Logarithmic Decrement (δ)*	Damping Ratio (ζ)*
East Span North Girder	7.75	0.064	0.010
East Span South Girder	7.75	0.065	0.010
West Span North Girder	7.75	0.065	0.010
West Span South Girder	7.75	0.046	0.007

* Logarithmic Decrement and Damping Ratio determined over 20 cycles

The dynamic amplification was calculated by comparing the maximum strains for the main girders in each span. The dynamic amplification for BCB4 was calculated to be approximately 20%. The dynamic amplification for the south girder at the east midspan location is shown in Figure 2.14.

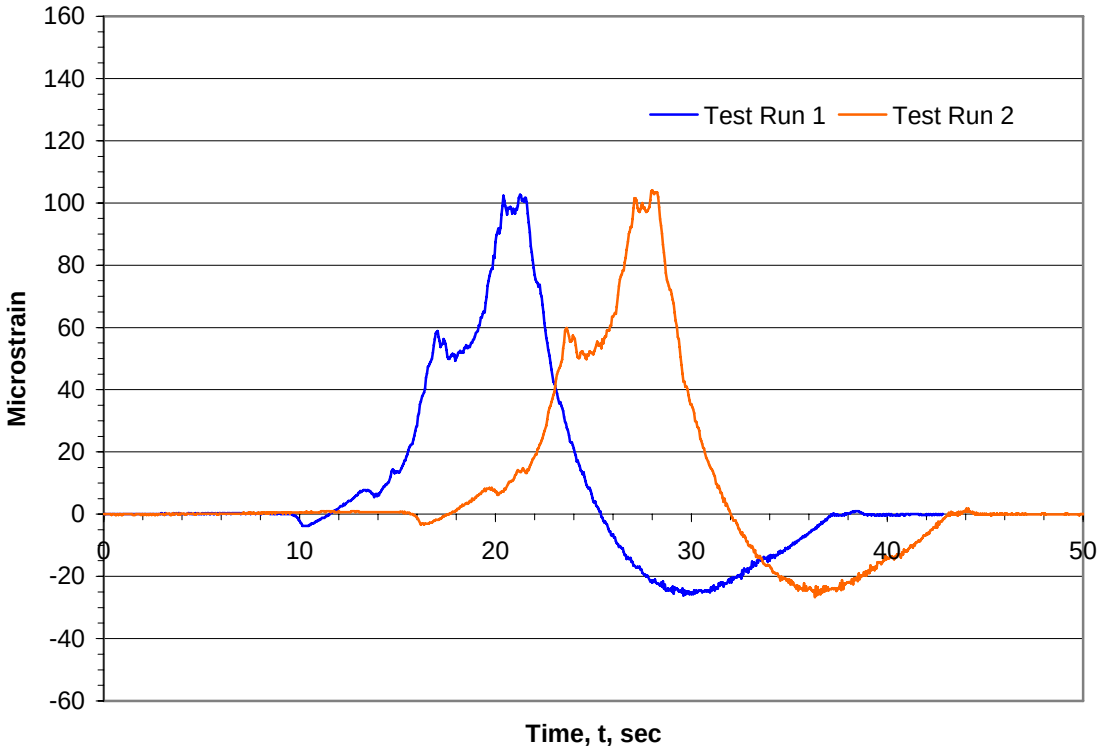

a. BCB4 South Girder Static Strain at East Midspan

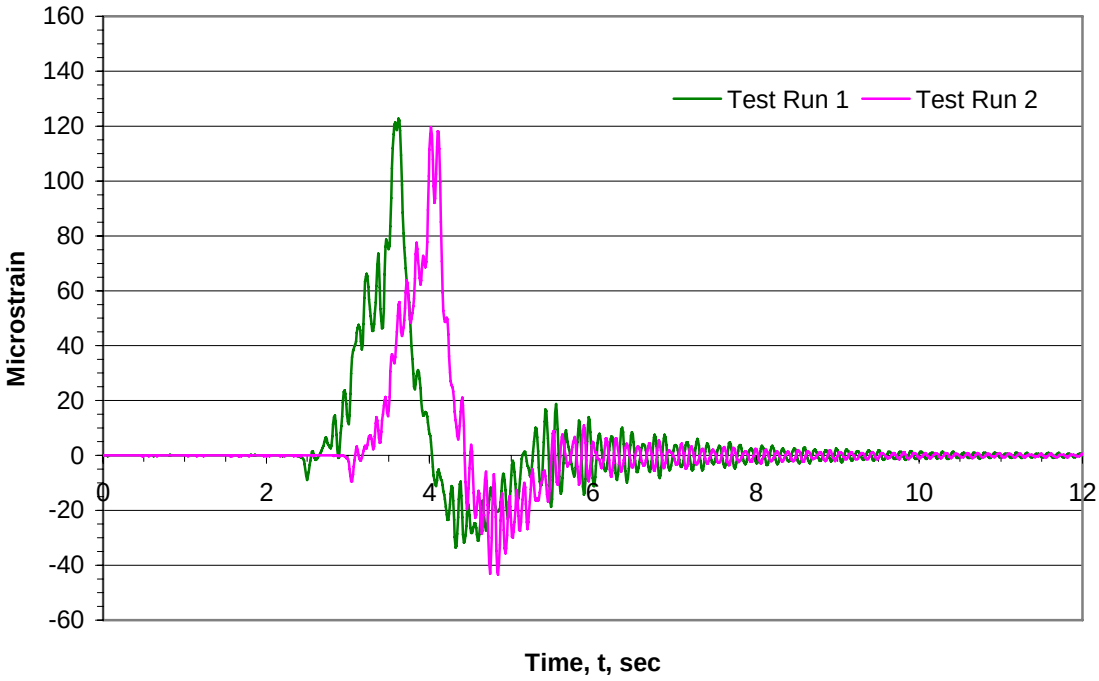

b. BCB4 South Girder Dynamic Strain at East Midspan

Figure 2.14. BCB4 dynamic amplification of strains

3.0 BUCHANAN COUNTY, IOWA BRIDGE 5 ON YORK AVENUE

3.1 Background

The fifth RRFC bridge in Buchanan County, Iowa (BCB5) tested by the Bridge Engineering Center is located one mile southeast of Monti, Iowa on York Avenue over Buffalo Creek (Figure 3.1). The previous bridge at the BCB5 site was an 88-ft long high truss bridge constructed in the early 20th Century. The original bridge had collapsed a few years prior to the construction of BCB5.

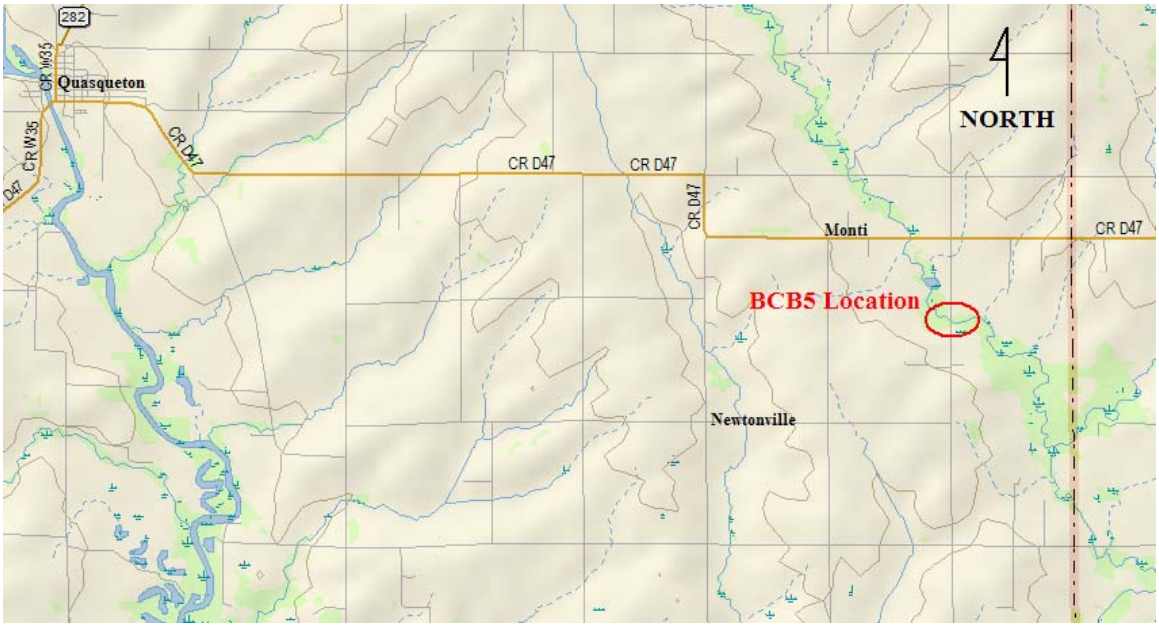

Figure 3.1. Location of Buchanan County RRFC Bridge 5 (BCB5) [10]

3.2 BCB5 Design and Construction

Buchanan County Bridge 5 (BCB5) is the fifth RRFC bridge constructed and tested in Buchanan County. This multiple span RRFC bridge – the second such configuration in the county – was designed by the Buchanan County Engineer's office using information and techniques developed in previous RRFC bridge projects.

Two 89-ft flatcars were used in the construction of BCB5. The existing bridge span at the BCB5 site was significantly longer than the maximum single span length (66 feet) that could be constructed using RRFCs. Therefore, a new pier, supported by HP 10x42 piles driven to refusal, was constructed slightly offset from the middle of the span to compliment the existing abutments. An idealized layout of BCB5 with the 1/4 span locations dimensioned is shown in Figure 3.2.

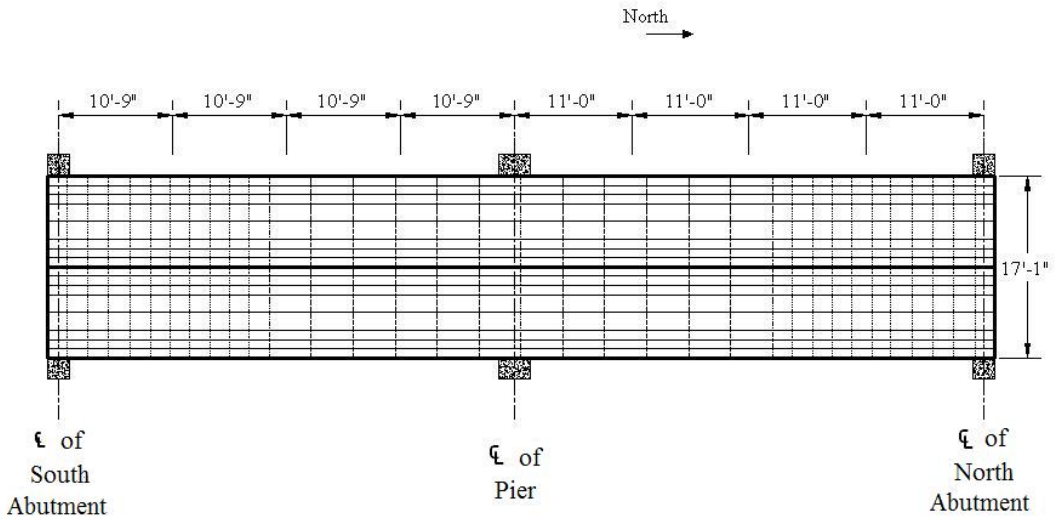

a. Idealized Plan View

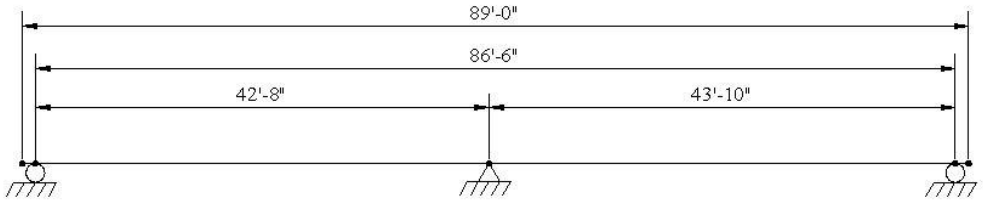

b. Idealized Profile View

Figure 3.2. Idealized layout of BCB5

At the BCB5 site, there is a concern of the bridge lifting off the supports during large hydrological events. Therefore, unlike BCB4, it was necessary to provide attachment between the bridge superstructure and substructure. To provide this attachment, clip angles were installed to tie the main girders of the bridge to the supports (Figure 3.3). At the pier, the interior girders are supported on approximately one inch thick neoprene bearing pads while the exterior girders are supported by a single W-section (Figure 3.4). At the abutments, the flatcars rested directly on the concrete, with steel shims as necessary to level the cars.

Due to the geometry of the exterior girders of the 89-ft RRFC, the top portion of the girder of the adjacent flatcars needed to be removed to provide a flush driving surface. The longitudinal connection between the flatcars required that the remaining bottom flange of the adjacent exterior girders also be removed. Four inch long 5/8 inch diameter threaded bolts spaced approximately 36 inches on center were then used to connect the webs of the adjacent flatcars (Figure 3.5). This connection is the same longitudinal connection that was used in BCB3.

Figure 3.3. Clip angle to attach RRFC to abutment

a. 1-inch Neoprene Bearing Pad under Interior Girder at Pier

b. I-shaped Support at Exterior Girder

Figure 3.4. BCB5 pier support conditions

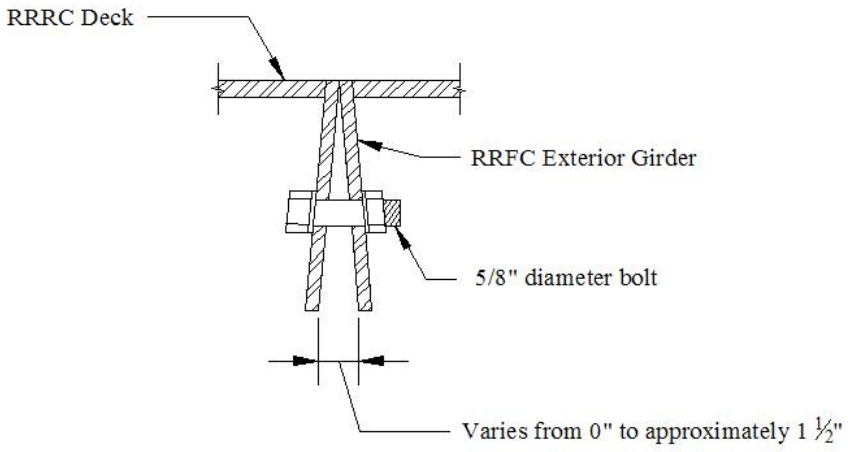

Figure 3.5. BCB5 longitudinal connection detail

After the flatcars were placed and the longitudinal connection completed, approximately four inches of gravel was added as the driving surface of the bridge. Finally, a guardrail was attached to the finish the bridge as shown in Figure 3.6.

Figure 3.6. Completed Buchanan County RRFC Bridge 5 (BCB5)

3.3 BCB5 Field Testing

To determine the behavior of BCB5, a field load test was conducted using Buchanan County Secondary Road Department tandem-axle trucks loaded with gravel. Two trucks were used in the load tests – one as the primary test vehicle and one as an auxiliary vehicle that was used in only one of the load tests. The dimensions and weights of the trucks used are shown in Figure 3.7.

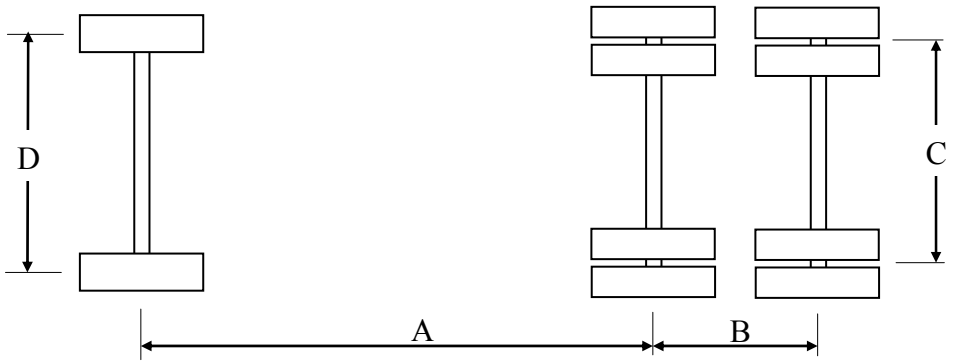

a. Top view

b. Side view

Truck	Dimensions (inches)				Load (lbs)		
	A	B	C	D	F	T	Gross
Primary	165	53	72	85	16,910	37,190	54,100
Auxiliary	167	53	72	84	17,030	37,420	54,500

Figure 3.7. Weights and dimensions of BCB5 test vehicles

3.3.1 BCB5 Instrumentation

To determine the structural behavior of BCB5 during the field load tests, BDI strain transducers and string potentiometers were attached to the bridge. A data acquisition system was then connected to the instrumentation for recording a continuous data record of the structural behavior of the bridge during the load test. As the tandem axle of the test truck crossed predetermined reference sections on the bridge, a feature of the data acquisition system was used to "mark" the data for use in the analysis process. The reference sections for BCB5 were the center of bearing for each support (both abutments and pier) as well as the 1/4, 1/2, and 3/4 span locations of each span for a total of nine reference sections.

The instrumentation plan for BCB5 is shown in Figure 3.8. As shown in Figure 3.8, 32 BDIs were placed at eight different cross sections along the bridge; fifteen string potentiometers were located on four cross sections along the bridge, as also shown in the figure. A preliminary analysis of BCB4 indicated possible large strains at the shallow end of the tapered transition section of RRFC profile. Since the configuration of BCB4 is very similar to that of BCB5, this same region was investigated for BCB5 as well (Details B and H in Figure 3.8c and Figure 3.8i, respectively). Although the maximum moment does not occur at these locations, the sections are significantly shallower, which results in a smaller moment of inertia and thus larger magnitudes of strains.

The pier location was also investigated for the possibility of large magnitude strains. BCB5 was instrumented with ten BDIs on the south side of the pier (Detail E in Figure 3.8f). At this location, BDIs were placed on the exterior girders of the bridge as well as on the flatcar exterior girders that comprise the longitudinal flatcar connection. BDIs were also placed on the main girder near the deck to measure the tensile strains. A BDI was also placed on the bottom flange of the east interior girder. The purpose of this transducer was two fold. First, it was used to measure the compressive strains at the pier. Secondly, using the tensile strains from the companion transducer on the top of the interior girder at this location, an approximation of the experimental neutral axis location could be made. Two BDIs were also placed on the bottom side of the deck in this cross-section to investigate the contribution of the deck in resisting the negative moment. On the north side of the pier (Detail F in Figure 3.8g), BDIs were placed near the top of the interior girders only. A BDI was also placed on the east guardrail on the south side of the pier, approximately three feet from the pier centerline to determine the amount of load resisted by the guardrail in the negative moment region.

At the south midspan (Detail C in Figure 3.8d), BDIs were placed on the bottom flanges of both interior girders to measure tensile strains. One BDI was also placed near the top of the east interior girder to measure the compressive strains so that an approximate location of the experimental neutral axis could be determined. BDIs were also placed on the exterior girders of the bridge as well as the flatcar exterior girders that comprise the longitudinal connection. As was done in Detail E (Figure 3.8f), a BDI was also placed on the guardrail.

Deflection instrumentation was placed mainly at the midspan locations. At the south midspan, string potentiometers were placed below all of the main girders (interior and exterior). String potentiometers were also placed at the 1/4 span and 3/4 span locations in the south span of the bridge. At these locations, one potentiometer was attached to each interior main girder as well as the longitudinal connection. At the north midspan, string potentiometers were placed below the interior girders as well as the flatcar exterior girders comprising the longitudinal connection.

3.3.2 BCB5 Field Load Test

The BCB5 field test consisted of three different load tests. First, as was done with BCB4, two trucks were transversely centered on the bridge, one in each span, to produce a large negative moment at the pier. Due to the similarities of BCB5 to BCB4, a preliminary analysis was not conducted on BCB5; hence, the truck position required to produce the maximum moment had not been determined. Therefore, the trucks were only positioned with the tandems centered at midspan (Figure 3.9).

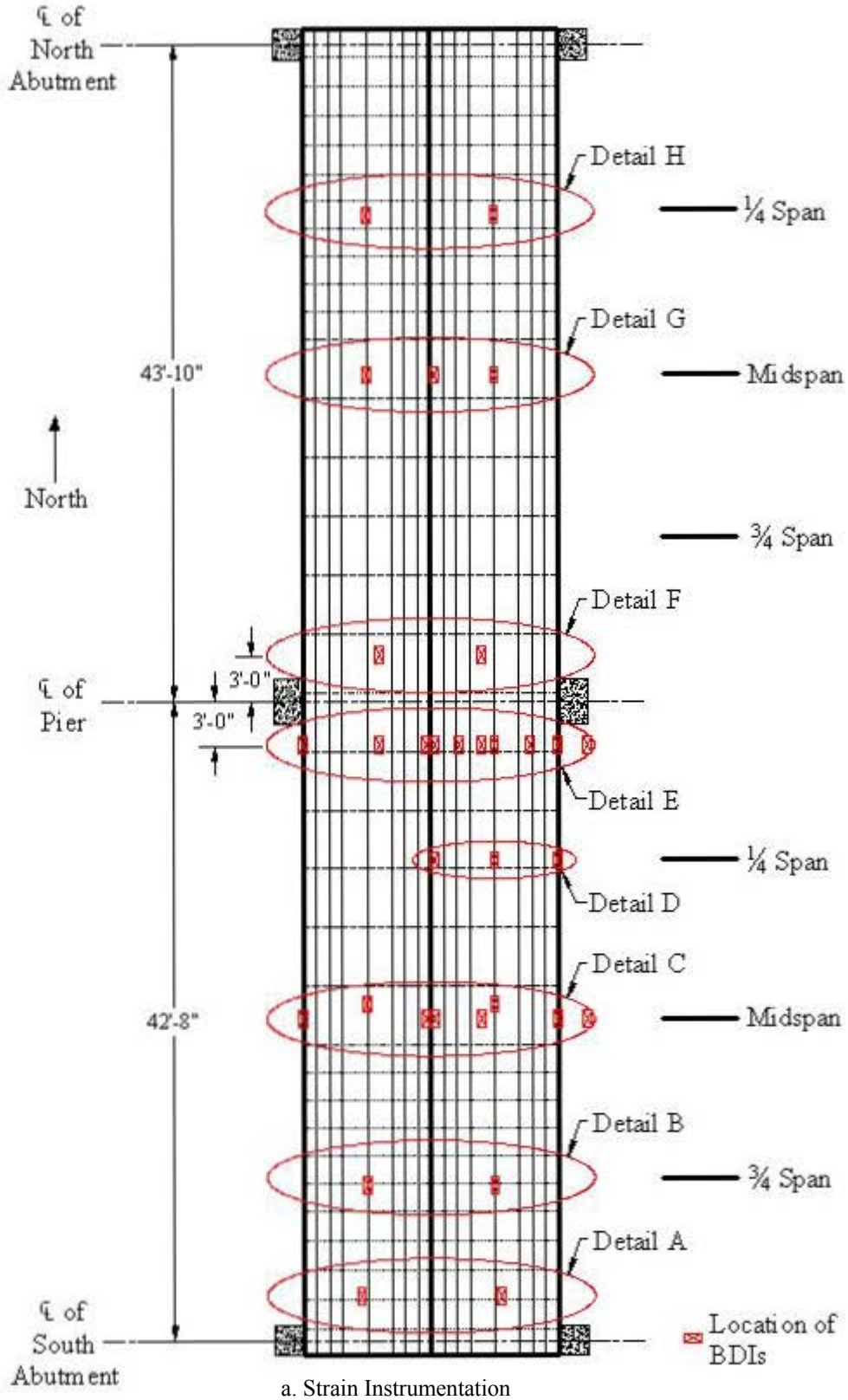

a. Strain Instrumentation

Figure 3.8. BCB5 instrumentation plan

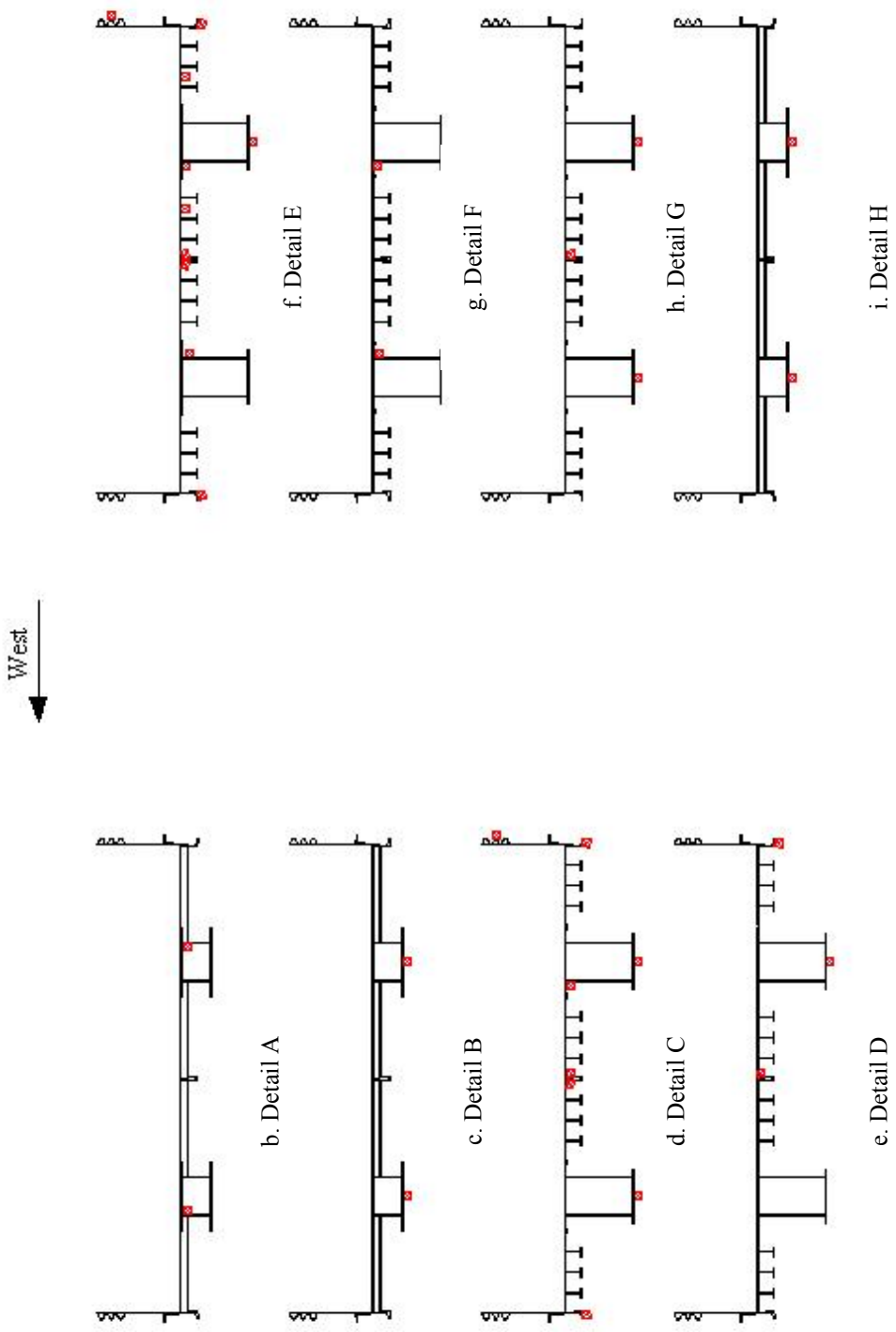

Figure 3.8. Continued

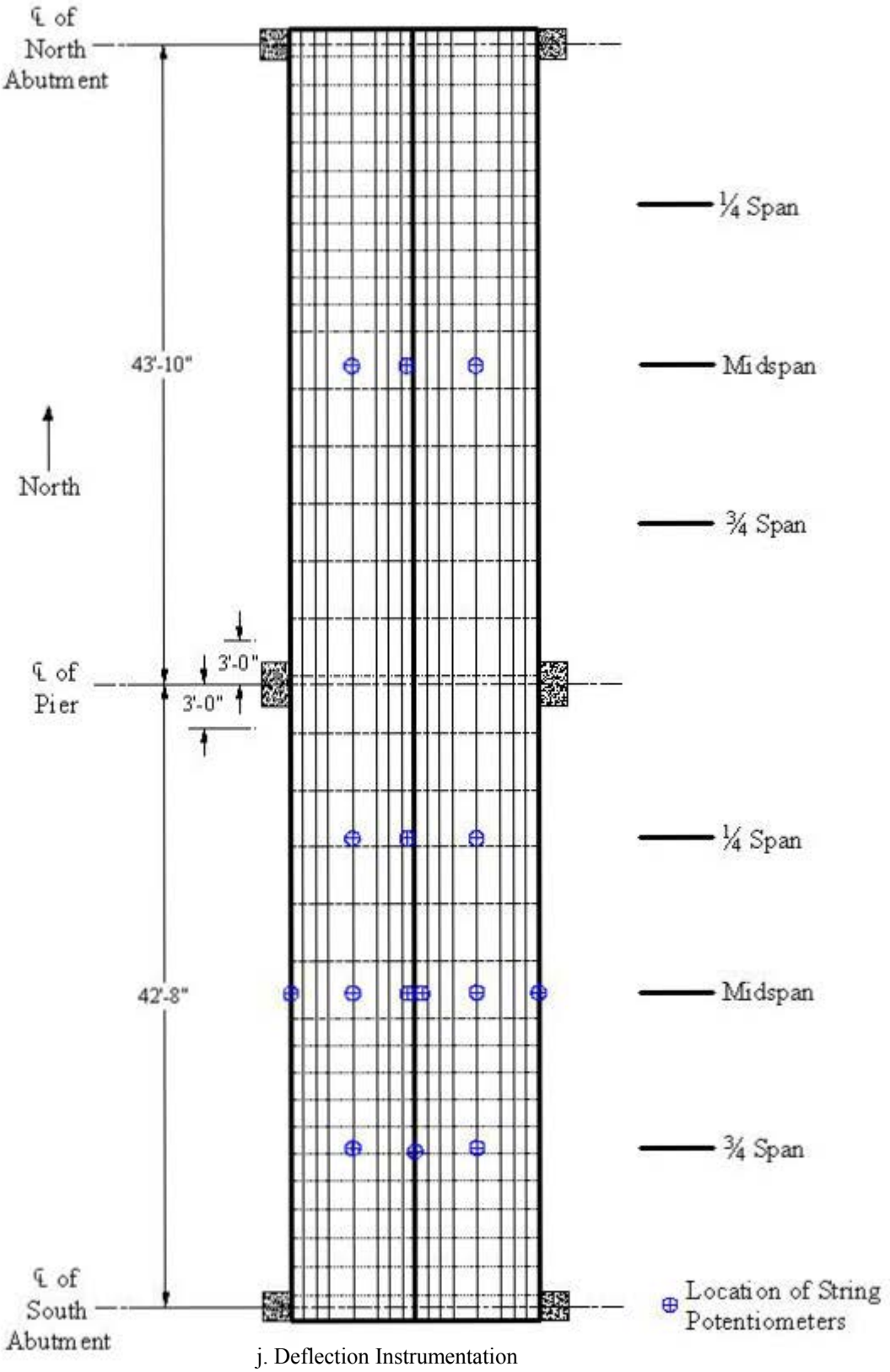

j. Deflection Instrumentation

Figure 3.8. Continued

a. Front view of two-truck load test

a. Side view of two-truck load test

Figure 3.9. BCB5 two-truck load test

Next, pseudo-static tests were conducted with the primary test vehicle traversing the bridge at an idle speed in one of the three test lanes shown in Figures 3.10 and 3.11. The lane assignments were the same for BCB5 as for BCB4, with the outer lanes positioning the center of the outside front wheel line two feet from the exterior girder of the bridge

Finally, a dynamic load test was conducted by driving the test vehicle across the bridge in the center lane (Lane 2) at approximately 30 mph. As was done on BCB4, each load test was conducted twice to investigate the repeatability in the behavior of the bridge and the recorded data.

3.5 BCB4 Dead Load Analysis

The total stresses occurring in BCB5 is the resultant of the live load stresses caused by the test vehicle and the stresses caused by the dead load on the bridge. To determine the total stresses in the bridge, a dead load analysis was completed. As was done in the analysis of previous RRFC

bridges, several assumptions were made to simplify the dead load analysis. Based on the results of a grillage analysis conducted on the 89-ft flatcar as part of TR-444 [4], the entire dead load was assumed to be resisted by the main girders. Also, as was done with previous RRFC bridges, the connected flatcars were assumed to form a rigid cross section. This allows for any additional dead load to be considered uniformly distributed on the bridge.

The dead load for BCB5 is comprised of mainly the driving surface and the weight of the flatcars. Based on previous reports, the flatcar was assumed to weigh 42,000 lbs or approximately 472 lbs/ft. The BCB5 driving surface is comprised of gravel with an approximate depth of 4 1/4 inches. A unit weight of 120 pound/ft^3 was assumed for the gravel driving surface. The guardrail (assumed weight of 100 lbs/ft) also added to the dead load. Adding all the dead loads, the total dead load per car for BCB5 was approximately 935 lbs/ft.

a. Test Vehicle in Lane 1 (West Lane)

b. Test Vehicle in Lane 3 (Middle Lane)

c. Test Vehicle in Lane 1 (East Lane)

Figure 3.10. BCB5 pseudo-static load test

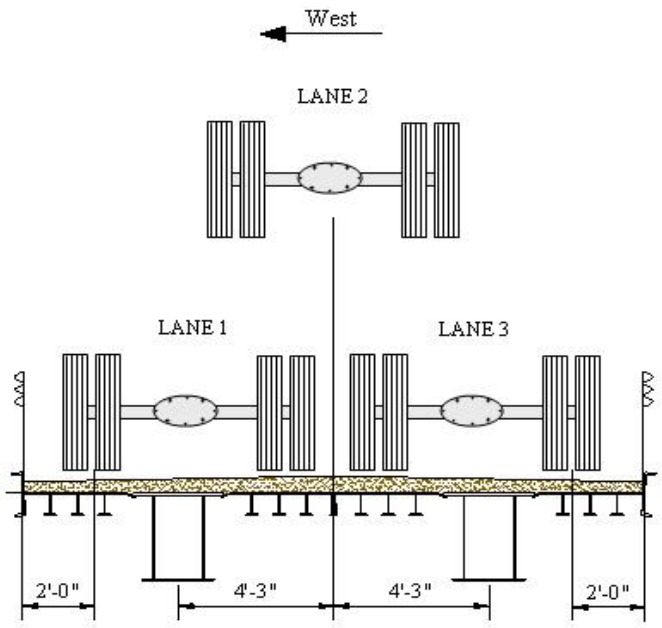

Figure 3.11. BCB5 lane configuration for load tests

To determine the dead load stresses, an idealized model of the bridge was constructed in a structural analysis program. The model was then subjected to a uniform dead load of 935 lbs/ft to determine the resulting moments. At the critical sections – the pier, midspans, and tapers – the dead load moment was divided by the section modulus of the main girder of the bridge. The section modulus of the main girder was found by determining the neutral axis depth based on the entire approximate bridge cross section at the locations of interest. The moment of inertia for the main girder was then found with respect to this neutral axis (instead of the neutral axis for the main girder only). This approach was used to better represent the actual behavior of the bridge. The resulting section modulus was also more conservative. For BCB5, the section modulus was calculated to be 458 in^3. A modulus of elasticity of 29,000 ksi previously discussed was used to convert the dead load stresses to strains. The resulting dead load strains/stresses are shown in Table 3.1 ("+" indicates tension and "-" indicates compressive). Unless noted otherwise, the strains/stresses reported are bottom flange values.

Table 3.1. BCB5 dead load strains (stresses) at critical locations.

	SOUTH SPAN		NORTH SPAN	
Location	Dead Load Microstrain	Dead Load Stress (ksi)	Dead Load Microstrain	Dead Load Stress (ksi)
Shallow End of Taper	+ 231	+ 6.7	+ 260	+ 7.5
Midspan	+ 70	+ 2.0	+ 81	+ 2.4
Pier - Top Flange	+ 67	+ 1.9	+ 67	+ 1.9
Pier - Bottom Flange	- 243	- 7.0	- 243	- 7.0

3.5 BCB5 Field Load Test Results

After completion of the field load tests, the results were analyzed to determine the structural behavior of BCB5. To determine the total stress occurring in BCB5, the live load strain values were converted to stresses using an elastic modulus of 29,000 ksi as determined in previous reports (See Section 1.2.3). The live load stresses were then added to the dead load stresses, as appropriate, to determine the total stresses.

As discussed in Section 2.5, assuming AASTHO limits and a 36 ksi yield strength, the maximum allowable stress for BCB5 is 19.8 ksi (683 microstrain). Although all of the test results were analyzed after completion of the field load test, only the maximum results for the critical sections – tapered transition section (Figure 3.8b and Figure 3.8h), midspans (Figure 3.8c and Figure 3.8g), and at the pier (Figure 3.8e and Figure 3.8f) – will be discussed, as the results at these sections control the bridge's performance. The strain results at other locations were of smaller magnitude and thus not reported.

3.5.1 Static Test Results

After reviewing the static field load test results, the largest live load strains near the shallow end of the tapered section of the RRFC was +264 microstrain (7.7 ksi) in the south span, occurring on the bottom flange of the main interior girder. The dead load stress at this location was calculated to be +231 microstrain (6.7 ksi). Adding the dead load strains to the field test results, the total strain occurring at the shallow end of the tapered transition section is +495 microstrain (14.4 ksi), or approximately 72% of the 19.8 ksi (683 microstrain) allowable limit.

BCB5 is the second RRFC bridge tested by the Bridge Engineering Center to have a significant negative bending moment (BCB4 was the first). For this reason, there was particular interest in the strains occurring in the negative moment region around the pier. At the pier location, the strain instrumentation was placed approximately two feet from the face of the pier (three feet from the pier centerline) to minimize the influence of localized effects due to the support condition at the pier. An adjustment factor was then used to correct the load test data to the pier location. To determine this adjustment factor, the bridge was analyzed in a structural analysis program to determine the theoretical moment envelope for the test vehicle. A moment ratio (i.e. the adjustment factor) was then determined by comparing the moment at the centerline of the pier and at the location two feet from the face of the pier. The adjustment factor for BCB5 was calculated to be 1.07.

Due to the geometry of the RRFC cross section, the strain transducers at the pier could not be placed at the maximum tensile location (i.e. the top of the cross section). To adjust the tensile live load strains, the strain profile of the bridge was determined using the neutral axis location. The live load strains were then extrapolated to the top of the strain profile, assuming a linear distribution.

At the pier, after adjustment for gage location in the strain profile (distance from neutral axis) and proximity to the pier, the maximum live load tensile strain was 140 microstrain (4.1 ksi). After adding the dead load strain of 67 microstrain (1.9 ksi) to the live load strains, the maximum total tensile strain at the pier of BCB5 was 207 microstrain (6.0 ksi). The maximum compressive live load strain

at the pier was -96 microstrain (-3.1 ksi). After adding the dead load strain of -243 microstrain (-7.0 ksi), the maximum total compressive strain at the pier was -339 microstrain -(9.8 ksi), or approximately 50% of the allowable limit of -19.8 ksi (-683 microstrain).

For a continuously bridge structure, the midspan strains/deflections are not the largest in the span due to the continuity over the intermediate supports. However, the instrumentation was placed at the midspan for the BCB5 field load tests to obtain an approximation of the maximum values as the difference between the midspan values and the maximum values is usually minimal.

The strains and deflections measured for each midspan locations are presented in Figures 3.12 – 3.14 for each of the three test lanes. Dashed lines have been added to provide a hypothetical linear trend line between the data points. The maximum midspan live load strain that occurred as a result of the field load test was 412 microstrain (11.9 ksi). Adding the dead load strain (stress) value of 70 microstrain (2.0 ksi) increases the total strain (stress) occurring in the bridge to 482 microstrain (14.0 ksi), which is approximately 71% of the allowable 19.8 ksi (683 microstrain).

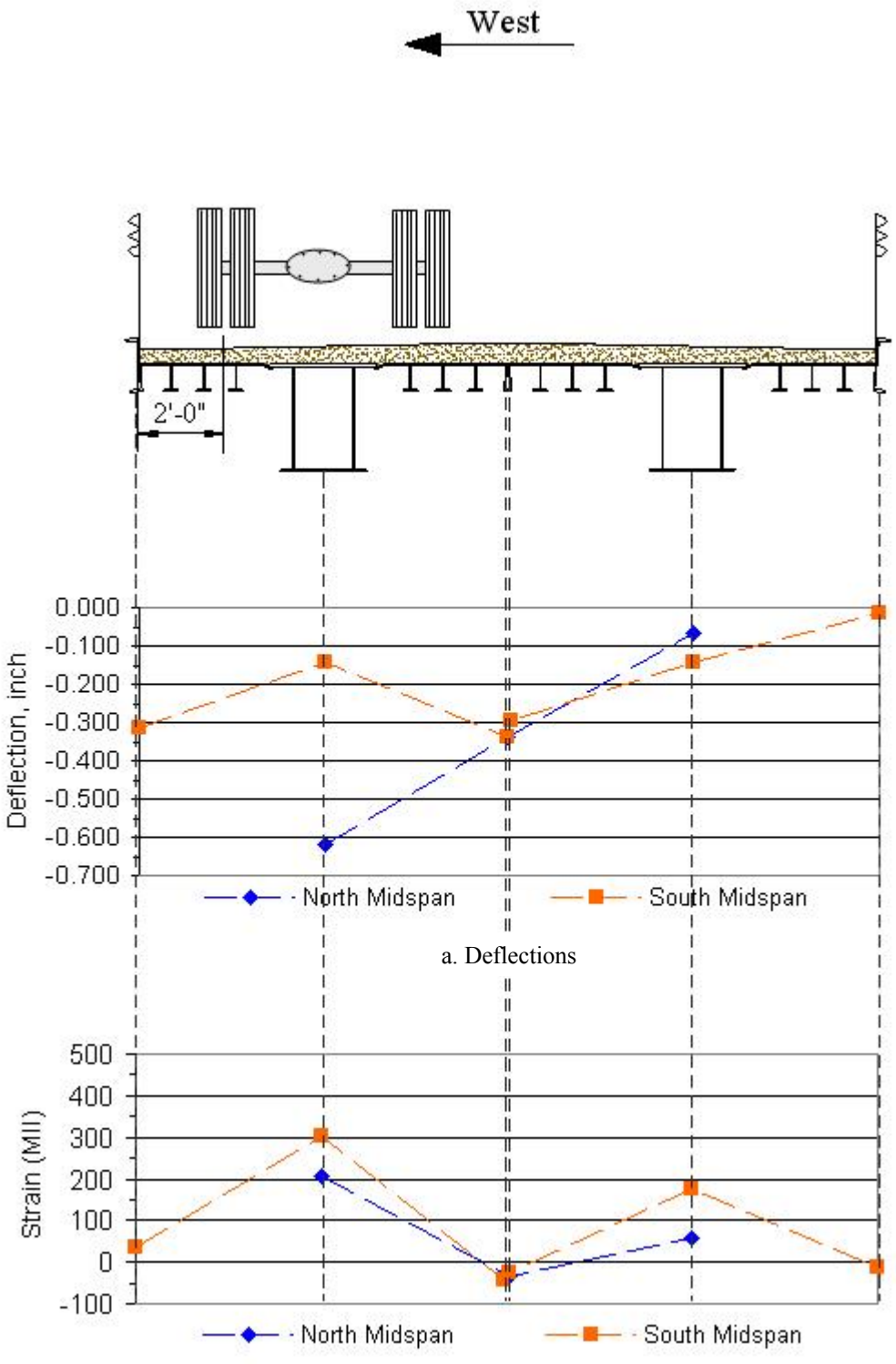

a. Deflections

b. Strains

Figure 3.12. BCB5 Lane 1 midspan live load deflections and strains

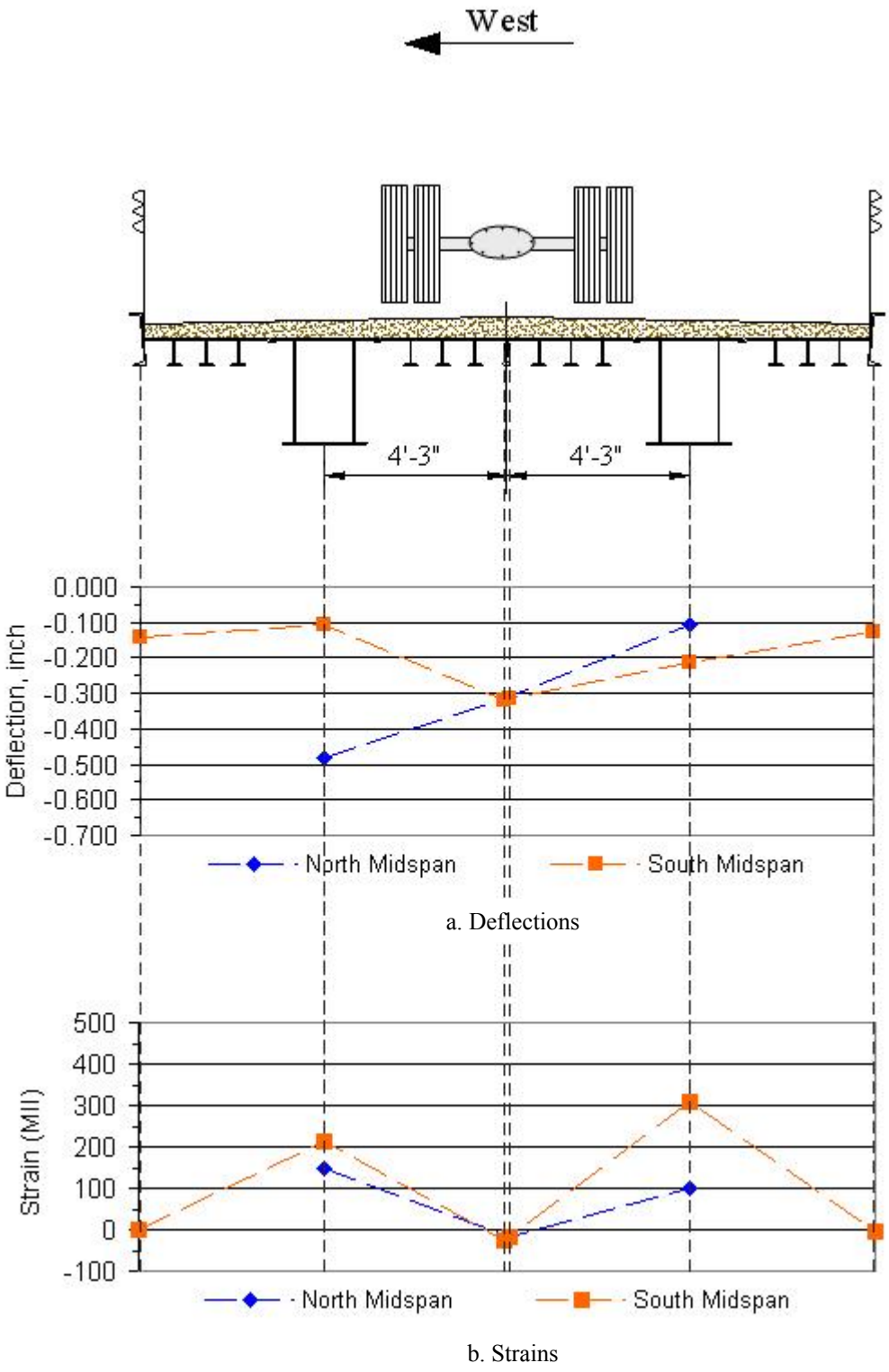

a. Deflections

b. Strains

Figure 3.13. BCB5 Lane 2 midspan live load deflections and strains

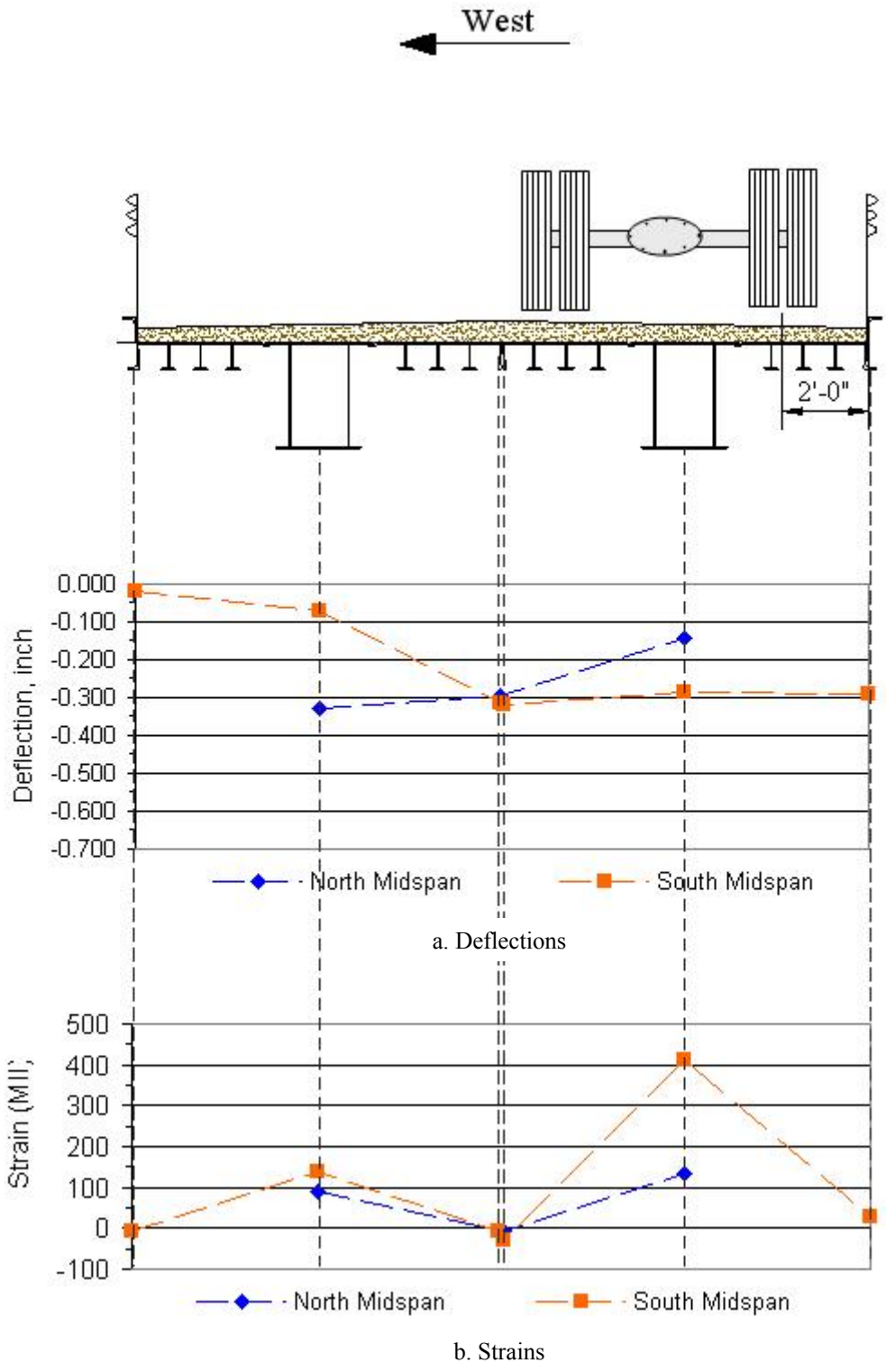

Figure 3.14. BCB5 Lane 3 midspan live load deflections and strains

The 1998 AASHTO *LRFD Bridge Design Specification* recommends a maximum allowable live load deflection of span/800 for legal truck loads [5]. Using this approach, the maximum allowable live load deflection was 0.64 inches for the south span and 0.657 inches for the north span. The maximum midspan live load deflection for the test vehicle, which occurred in the north span, was 0.652 inches, or approximately 99% of the recommended limit. However, as discussed in the subsequent paragraph, this result was believed to be erroneous. Thus, after excluding the erroneous deflection, the maximum deflection was 0.338 inches, occurring at the south midspan. This value is approximately 53% of the recommended allowable limit of span/800 (0.640 inches).

After reviewing the BCB5 data, two discrepancies in the load test results were observed. First, the deflections at the north midspan are not consistent with the strain data when comparing the north span results (both deflections and strains) to the south span results. At the north midspan, the west girder deflection is considerably larger than was expected for the span length. The west girder midspan deflection is also the largest deflection occurring at the north midspan, regardless of the transverse position of the test vehicle. Also, as the test vehicle traverses the bridge in the different test lanes, very little change occurs in east girder displacement. To qualify the questionable deflections, plots were made of the corresponding strain data to investigate if there were similar trends occurring in the strain data as well. However, no discrepancy in the north midspan strain data was observed. As was discussed in Section 2.3.1, questionable deflections were also recorded during the BCB4 load test (the day before the BCB5 load test). Considering that both bridges had questionable deflection and that the companion strains showed no indication of a distribution problem, an instrumentation issue is believed to have been the likely cause, even though no apparent problem was found with the suspected transducers after they were reviewed by the laboratory manager.

The other discrepancy observed in the BCB5 load test results occurred with the south midspan strain data. At the south midspan, strains that were significantly higher than expected (based on the span length and the other data for the bridge) were recorded for the east girder. In an effort to qualify the large strains, data from adjacent locations were plotted to determine if the large strain was unique to the one transducer or a trend that occurred throughout the girder. When plotting the data for the strain transducers at the shallow end of the tapered transition section (which was approximately the 1/4 span location), no values of concern were observed, which indicates a localized problem. As was done with the discrepancy at the north midspan, the corresponding data (deflections in this case) were also plotted to investigate if similar trends were occurring. The deflection data indicated that the deflection of the east girder was larger than the west girder for symmetric loadings, suggesting that the east girder was resisting more load than the west girder at the south midspan of BCB5. If the east girder was resisting more load than the west girder, this could in part explain the high strain data at the south midspan. A visual inspection of the bridge was also made to justify why more load was being resisted by the east girder at the south midspan than the west girder, with the results being inconclusive. However, when comparing the overall performance of BCB5, the controlling section of the bridge was the shallow end of the tapered sections, even with the large live load strain at the south midspan.

As was done in the testing of previous RRFC bridges, an adjustment factor was used to increase the results from the test vehicle to that of an HS-20 truck, the likely design vehicle for the bridge. This adjustment factor was determined using the same methodology as described in Section 2.5.1. The adjustment factor for BCB5 was 1.182. Using this value, along with the adjustment factor discusses in the previous paragraph, the projected maximum total strain for an HS-20 test vehicle on BCB5 becomes 543 microstrain (15.7 ksi). This magnitude is still below the allowable value of 19.8 ksi (683 microstrain). Using the same approach, the maximum live load deflection (not considering the questionable deflections) becomes 0.400 inches, still within the AASTHO guidelines.

The moment fraction, which is the portion of the total transverse live load moment due to the applied load carried by an individual girder or flatcar in this situation, was also determined for BCB5. To determine the moment fraction, the area under the deflection (or strain) curve was determined. The area under the loaded RRFC was then compared to the entire area to determine the moment fraction. For BCB5, the experimental moment fraction was approximately 2/3, similar to the values reported in previous investigations.

As was done with BCB4, an auxiliary vehicle was used in addition to the test vehicle to further investigate the negative moment occurring over the pier. At the pier, after adjustment for gage location in the strain profile (distance from neutral axis), the maximum live load tensile strain was 81 microstrain (2.3 ksi). After applying the dead load strain of 67 microstrain (1.9 ksi), the maximum total tensile strain at the pier of BCB5 due to the two vehicles was 148 microstrain (4.2 ksi). The maximum compressive live load strain at the pier was -117 microstrain (-3.4 ksi). After adding the dead load strain of -243 microstrain (-7.0 ksi), the maximum total compressive strain at the pier was -360 microstrain (10.4 ksi), or approximately 53% of the allowable limit of -19.8 ksi (-683 microstrain).

3.5.2 Dynamic Test Results

As stated earlier, a dynamic load test was conducted by driving the primary test vehicle across the bridge in the center lane (Lane 2) at approximately 30 miles per hour. From this field load test, the structural dynamic properties of the bridge were approximated, as well as the dynamic amplification due to the moving load.

The free vibration oscillations of the bridge were used to approximate the frequency, period, and damping. By observing the oscillations per time, the frequency of BCB5 was approximated as 6.25 hertz which resulted in a natural period of 0.16 seconds. The damping ratio, using a simple logarithmic decrement, was calculated at approximately 1.2 %. The dynamic properties of BCB5 are summarized in Table 3.2.

Table 3.2. BCB5 dynamic properties

Location	Frequency (Hz)	Logarithmic Decrement (δ)*	Damping Ratio (ζ)*
North Span East Girder	6.25	0.062	0.010
North Span West Girder	6.25	0.103	0.016
South Span East Girder	6.25	0.065	0.010
South Span West Girder	6.25	0.076	0.012

* Logarithmic Decrement and Damping Ratio determined over 20 cycles

The dynamic amplification was calculated by comparing the maximum strains in the main girders in each span. The resulting dynamic amplification for BCB5 was determined to be approximately 10%. The dynamic amplification of strains for the East girder at the North midspan location are shown in Figure 3.15.

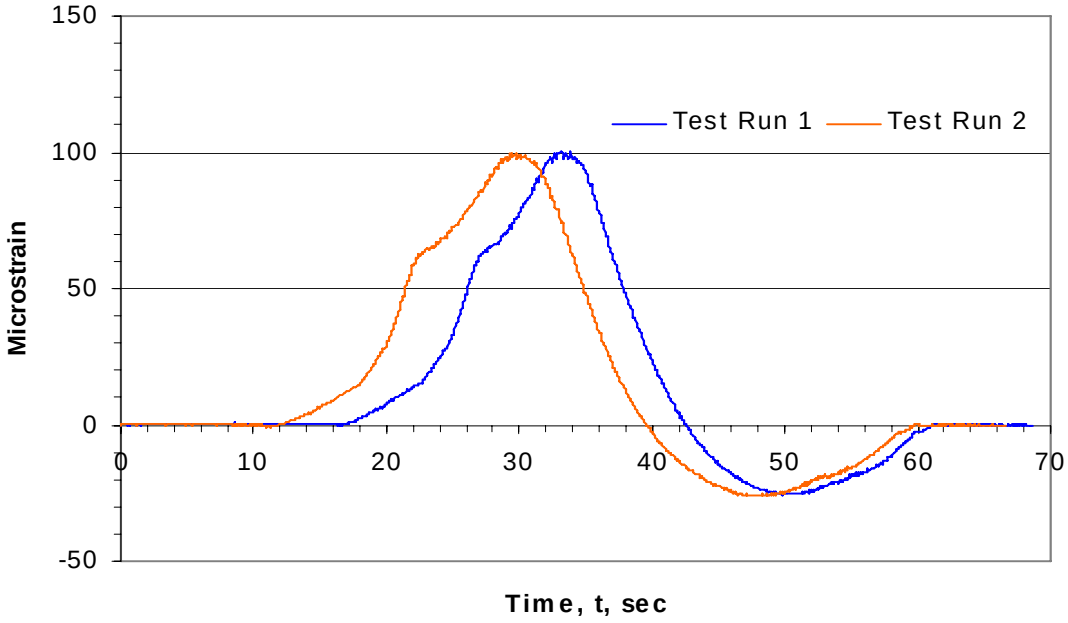

a. BCB5 East Girder Static Strain at North Midspan

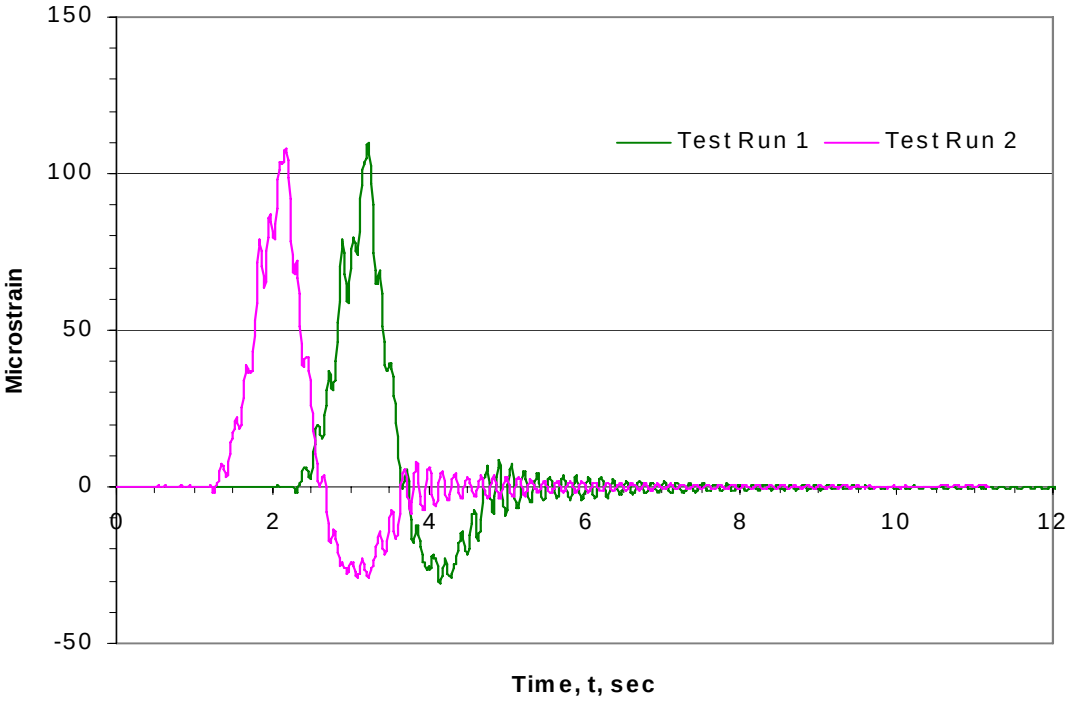

b. BCB5 East Girder Dynamic Strain at North Midspan

Figure 3.15. BCB5 dynamic amplification of strains

4.0 WINNEBAGO COUNTY BRIDGE 3 ON 390TH STREET

4.1 Background

The third RRFC bridge in Winnebago County, Iowa (WCB3) tested by the Bridge Engineering Center is located four miles south of Buffalo Center, Iowa on 390th Street over Little Buffalo Creek (Figure 4.1). The previous bridge at this location (constructed in 1979) was a three span timber bridge 69'-0" in length that was supported on timber piles (Figure 4.2).

Figure 4.1. Location of Winnebago County RRFC Bridge 3 (WCB3) [10]

4.2 WCB3 Design and Construction

Winnebago County Bridge 3 (WCB3) is the third RRFC bridge designed, constructed, and tested in Winnebago County. This bridge was designed and constructed by Winnebago County using guidelines and construction techniques developed in previous RRFC bridge projects. The bridge is identical to WCB1 with the exception of the abutments. For WCB1, new concrete abutments were constructed; while for WCB3, new sheet pile abutments were designed and constructed. Additional

information on the design, construction, and testing of the sheet pile abutments is presented in Appendices A and B.

Figure 4.2. Previous bridge at WCB3 site

Three 89-ft RRFCs were used in the construction of WCB3. WCB3 consists of three spans – one 66'-0" main span and two shorter 11'-6" end spans. New steel piers were constructed at the RRFC bolster location using six HP12x53 A572 Grade 50 piles driven to approximately 55 feet. An HP12x53 was also used for the pier cap. At the piers, a roller condition was established between the pile cap and the RRFCs. This support was constructed in the same manner as was done for previous Winnebago County RRFC bridges. In addition to the piers, new sheet pile abutments were constructed as stated in the previous paragraph. An idealized layout of the bridge with the 1/4 span locations dimensioned is provided in Figure 4.3. The springs shown in Figure 4.3b represent the unknown restraint conditions caused by the sheet pile abutments.

Due to the geometry of the exterior girders in the 89-ft RRFC, the top portion of adjacent girders needed to be removed in order to provide a smooth driving surface. After the top of the adjacent girders was removed, a longitudinal flatcar connection (LFC) between the flatcars could be constructed. As was done with WCB1 and WCB2, a reinforced concrete beam confined by two steel plates was cast in place between the two flatcars (Figure 4.4). Threaded rods were also used to connect the adjacent RRFC exterior girders.

After the flatcars were placed and the longitudinal connection constructed, four inch by twelve inch wooden timbers held in place by angles welded to the exterior girders of the bridge were placed on the bridge deck to provided additional load distribution. Approximately two inches of gravel was then added for the driving surface on the bridge after which a guardrail was attached to the bridge. The finished WCB3 is shown in Figure 4.5.

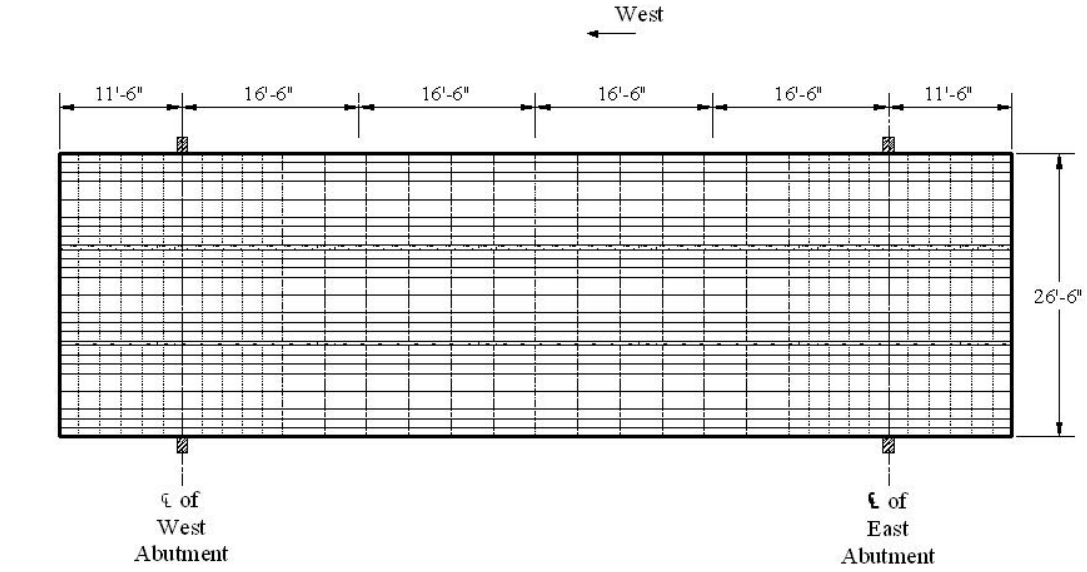

a. Idealized Plan View

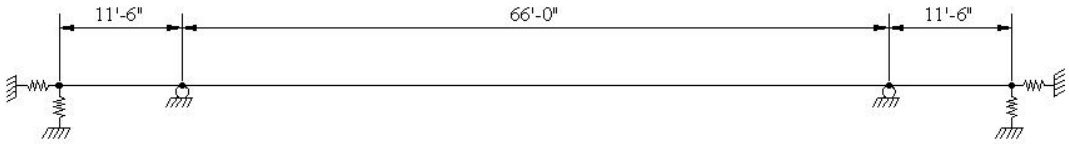

b. Idealized Profile View

Figure 4.3. Idealized layout of WCB3

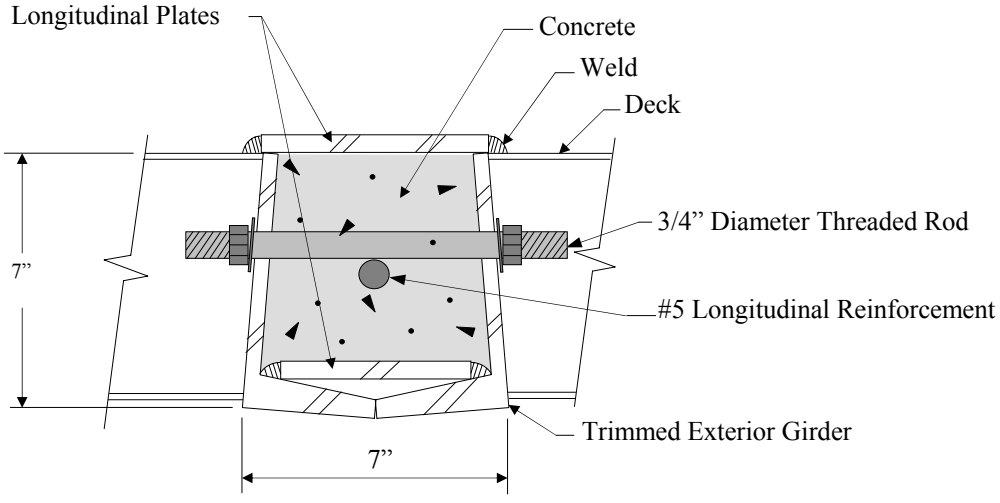

Figure 4.4. WCB3 longitudinal connection detail

Figure 4.5. Completed Winnebago County RRFC Bridge 3 (WCB3)

4.3 WCB3 Field Testing

To determine the behavior of WCB3, a field load test was conducted using Winnebago County Secondary Road Department tandem-axle trucks loaded with gravel. Two trucks were used in the load test – one as the primary test vehicle and one as an auxiliary vehicle that was used in only one of the load tests. The dimensions and weights of the two trucks used are shown in Figure 4.6.

4.3.1 WCB3 Instrumentation

To determine the structural behavior of WCB3, BDI strain transducers and string potentiometers were attached to the bridge. A data acquisition system was then connected to the transducers for recording a continuous data record of the bridge behavior. As the tandem axle of the test truck crossed predetermined reference sections on the bridge, a feature of the data acquisition system was used to "mark" the data for use in the analysis process. The reference sections for WCB3 were at the center of bearing for the abutments and piers as well as the 1/4, 1/2, and 3/4 span locations in the main span for a total of seven reference sections.

The instrumentation plan for WCB3 is shown in Figure 4.7. As shown in Figure 4.7, 21 BDIs were placed at four different cross sections along the bridge; seven string potentiometers were located on the midspan cross section, also shown in the figure.

String potentiometers were attached to the bottom of the main girders midspan of the center span as well as to the exterior girders of the bridge (Figure 4.7f). Potentiometers were also placed below the two longitudinal connections between the adjacent RRFCs at midspan of the center span.

Two locations were investigated for large magnitudes of strain during the load tests – the midspan section and adjacent to the east pier. At the midspan (Detail B in Figure 4.7c), BDIs were placed on the bottom flange of the three main girders to measure tensile strains. One BDI was also placed near

the top of the main girder of the north and middle RRFC for use in determining the location of the experimental neutral axis. BDIs were also placed at midspan on the exterior girders of the bridge as well as the exterior girders of the middle RRFC to measure the strain in the longitudinal connection. A BDI was also attached to the guardrail at midspan to measure the strains occurring in the guardrail, which are proportional to the amount of load being resisted by the guardrail.

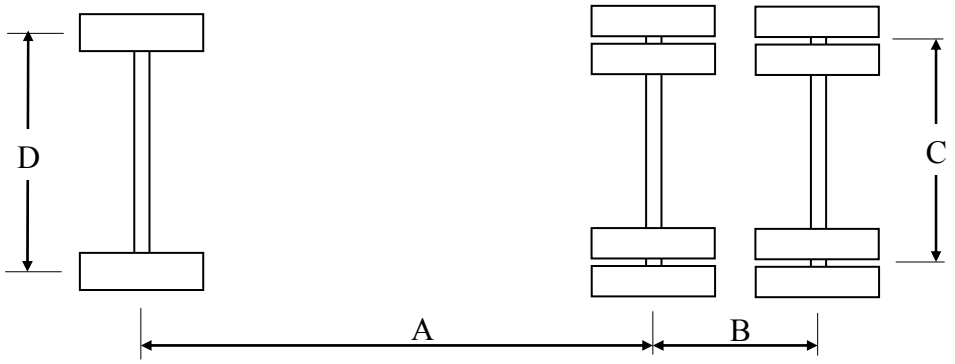

a. Top view

b. Side view

Truck	Dimensions (inches)				Load (lbs)		
	A	B	C	D	F	T	Gross
Primary	178.5	53	72	81	14,200	34,400	48,600
Auxiliary	170	55.5	72	85.5	18,340	33,940	52,280

Figure 4.6. Weights and dimension of WCB3 test vehicles

The pier location was also investigated for the possibility of large strains. WCB3 was instrumented with six BDIs on the west side of the east pier (Detail D in Figure 4.7e). At this location, BDIs were

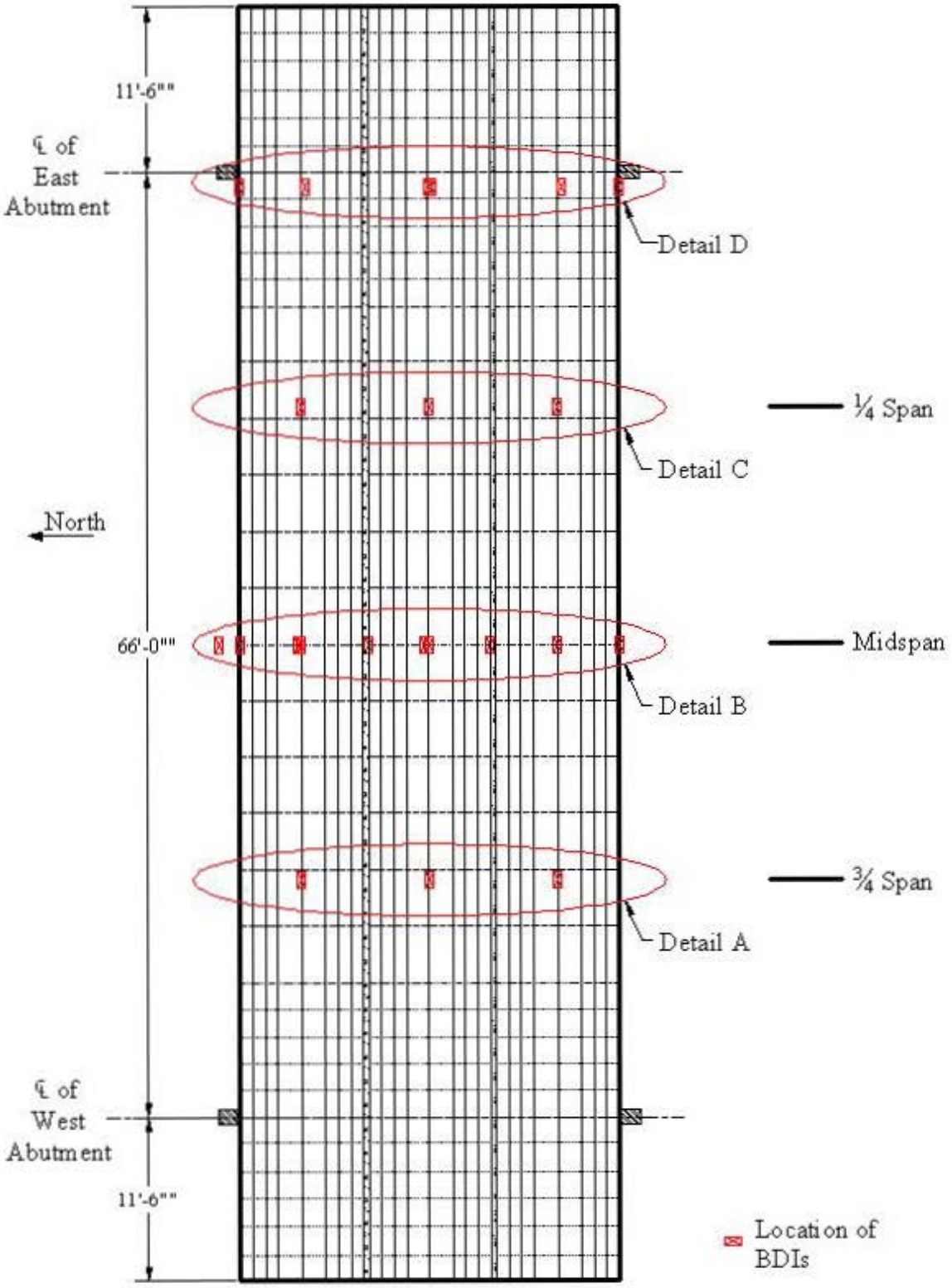

a. Strain Instrumentation

Figure 4.7. WCB3 instrumentation plan

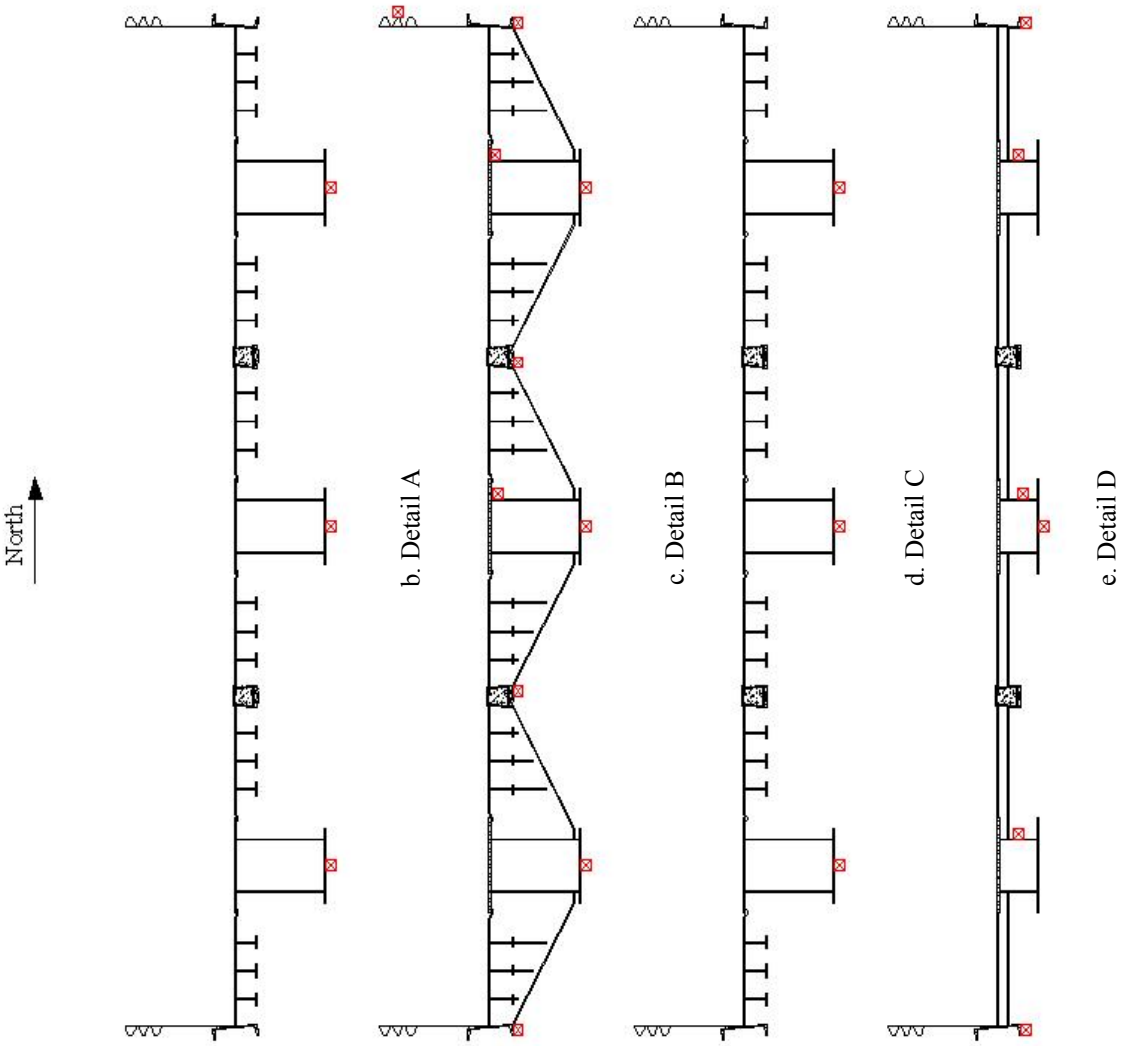

Figure 4.7. Continued

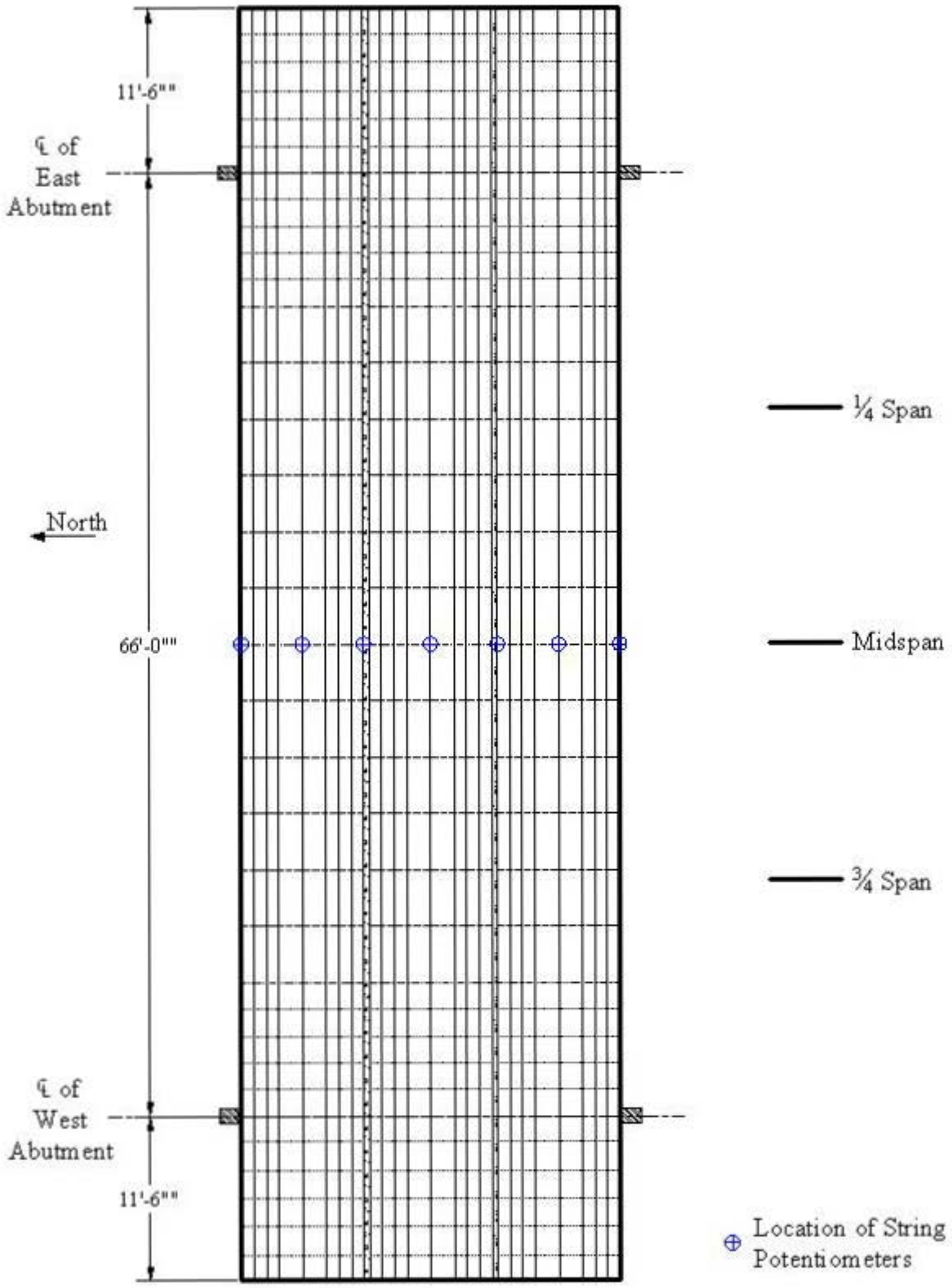

f. Deflection Instrumentation

Figure 4.7. Continued

placed on the north side of the main girders near the bridge deck to measure the strains that occurred due to the negative moment at the pier. A BDI was also placed on the bottom flange of the middle main girder at this location. The purpose of this transducer was two fold. First, it was used to measure the compressive strains in the vicinity of the pier. Secondly, with the tensile strain from the adjacent transducer near the top of the interior girder at this location, an approximation of the neutral axis location could be made. BDIs were also placed on the exterior girders of the bridge as shown in Detail D. The bottoms of the main girders were also instrumented at the 1/4 and 3/4 span locations (Detail A and C in Figure 4.7b and Figure 4.7d, respectively) to determine the overall bridge behavior.

4.3.2 WCB3 Field Load Test

To determine the behavior of WCB3, several field load tests were conducted. First, pseudo-static tests were conducted with the test vehicle traversing the bridge at an idle speed in one of three test lanes (Figures 4.8 and 4.9). The interior lane (Lane 2) placed the truck down the center of the bridge. The other two lanes (Lanes 1 and 3) placed the center of the outside wheel line of the truck two feet from the north and south exterior girders of the bridge, respectively. A dynamic load test was then conducted by driving the test vehicle across the bridge in the center lane (Lane 2) at approximately 25 mph. Each load test was conducted twice to investigate the repeatability in the behavior of the bridge and the recorded data. Several load tests were also conducted to determine the behavior of the sheet pile abutments. Information about these load tests is presented in Appendix B.

a. WCB3 Test Vehicle in Lane 1 (North Lane).

b. WCB3 Test Vehicle in Lane 3 (South Lane).

Figure 4.8. WCB3 pseudo-static load test

4.4 WCB3 Dead Load Analysis

The total stresses occurring in WCB3 is the resultant of the live load stresses caused by the test vehicle and the stresses caused by the dead load on the bridge. To determine the total stresses in the bridge, a dead load analysis was completed. As was done with previous RRFC bridges, several assumptions were made to simplify the dead load analysis. Based on the results of a grillage analysis conducted on the 89-ft flatcar as part of TR-444 [4], the entire dead load is assumed to be resisted by

the three main girders. Also, as was done with previous RRFC bridges, the connected flatcars were assumed to form a rigid cross section. This allows for any additional dead load to be considered uniformly distributed on the bridge.

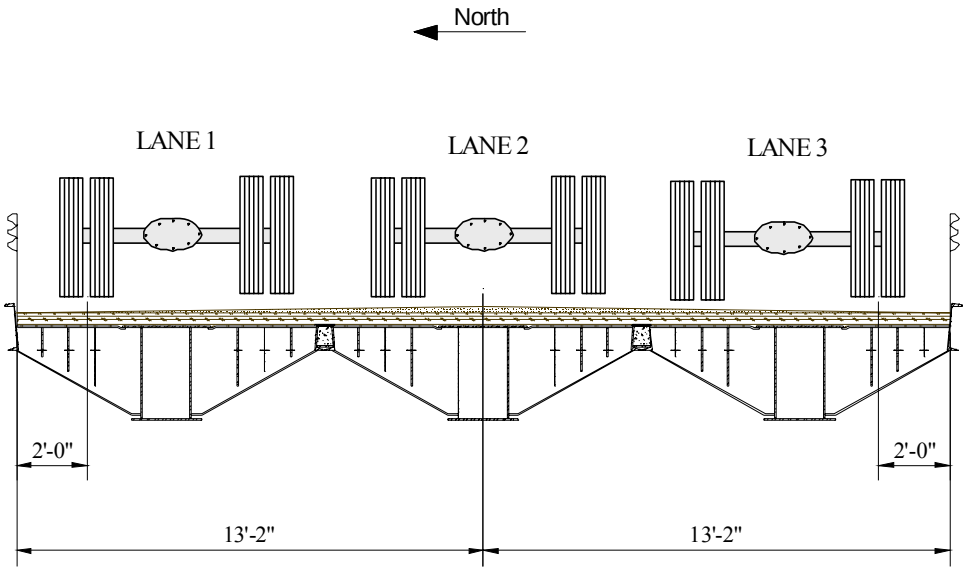

Figure 4.9. WCB3 lane configuration for load tests

The dead load for WCB3 is comprised of mainly the driving surface and the weight of the flatcars. Based on previous work using RRFCs, the individual flatcars were assumed to weigh 42,000 lbs or approximately 472 lbs/ft. The WCB3 driving surface is comprised of approximately two inches of gravel. A unit weight of 120 pound/ft^3 was assumed to determine the dead load that resulted from the gravel. The timber planking was assumed to have a unit weight of 36.3 pound/ft^3. The longitudinal connection and the guardrail also added to the dead load. Adding up all the dead loads, the total dead load per car for WCB3 was calculated to be 740 lbs/ft.

To determine the dead load stresses, an idealized model of the bridge was analyzed using a structural analysis program. The model was then subjected to a uniform load of 740 lbs/ft and an analysis conducted to determine the resulting moments. Because of the restraint uncertainty at the sheet pile abutments, the dead load analysis was conducted twice – once with the connection to the sheet pile modeled as free to rotate (pinned) and once with the connection modeled as fixed against rotation – with the actual restraint being between the two idealized support conditions. For each critical cross section, the model that produced the more conservative results was used. For the midspan location, the maximum dead load moment occurred when the sheet pile connection was modeled as a pinned connection (free to rotate). For the pier location, the maximum dead load moment occurred when the sheet pile connection was modeled as fixed against rotation.

After determining the appropriate dead load moment values at the critical locations, the dead load moment was divided by the section modulus of the main girder of the bridge to determine the corresponding dead load stress. The section modulus of the main girder was found by determining the neutral axis depth based on the entire approximate bridge cross section at the locations of interest. The moment of inertia for the main girder was then found with respect to this neutral axis (instead of the neutral axis for the main girder only). This approach was used to better represent the actual behavior of the bridge. This method also produced a more conservative section modulus. For WCB3, the section modulus was determined to be 458 in^3. A modulus of elasticity of 29,000 ksi was used to convert the dead load stresses to strains. The resulting dead load strains/stresses are shown in Table 4.1 ("+" indicates tension and "-" indicates compressive).

Table 4.1. WCB3 dead load strains (stresses) at critical locations

Location	Dead Load Microstrain	Dead Load Stress (ksi)
Pier - Top Flange	+111	+ 3.2
Pier - Bottom Flange	- 391	- 11.4
Midspan - Bottom Flange	+ 235	+ 6.8

4.5 WCB3 Field Load Test Results

After completion of the field load tests, the results were analyzed to determine the structural behavior of WCB3. To determine the total stress occurring in WCB3, the live load strain values were converted to stresses assuming an elastic modulus of 29,000 ksi as determined previously (See Section 1.2.3). The live load stresses were then added to the dead load stress, as appropriate, to determine the total stresses.

As discussed in Section 2.5, assuming AASTHO limits and a 36 ksi yield strength, the maximum allowable stress for BCB5 is 19.8 ksi (683 microstrain). Although all of the test results were analyzed after completion of the field load tests, only the maximum results for the critical sections – midspan and at the pier – will be discussed, as the results at these sections control the performance of the bridge. Results at other locations were less significant.

4.5.1 Static Test Results

At the pier location, the BDIs were not placed at the maximum strain location (i.e. the deck of the RRFC). Therefore, an adjustment was necessary in the negative moment region to extrapolate the measured strain results to the tensile strains that were occurring at the top of the RRFC section. The same procedure outlined previously for BCB4 and BCB5 was used for WCB3.

After adjusting for gage location in the strain profile (distance from neutral axis), the maximum live load tensile strain was 109 microstrain (3.2 ksi). After including a calculated dead load strain of 111 microstrain (3.2 ksi), the maximum tensile total strain occurring at the pier of WCB3 was 220 microstrain (6.4 ksi), or approximately 32% of the allowable stress of 19.8 ksi (683 microstrain) limit. The maximum live load compressive main girder strain at the pier was -43 microstrain (-1.2 ksi). Adding the calculated dead load strain of -391 microstrain (-11.4 ksi), the maximum compressive

strain occurring at the pier was -434 microstrain (-12.6 ksi), or approximately 64% of the allowable -19.8 ksi (-683 microstrain) limit. However, as presented in the following paragraphs, the flexural bending strains (stresses) at the pier were less than those that occurred in the midspan positive bending moment region.

For a continuously supported bridge structure, the midspan strains/deflections are not the largest in the span due to the presence of the intermediate supports. However, the main span of WCB3 is approximately six times longer than the two end spans (66'-0" vs. 11'-6"); thus the resulting behavior of the main span is similar to that of a single span, with the maximum strains and deflections occurring near midspan (although smaller in magnitude than those that would occur in a simply supported bridge). The strains and deflections measured for the midspan location are presented in Figures 4.10 – 4.12 for each of the three test lanes. Dashed lines have been added to provide a hypothetical linear trend line between the observed data points. As can be seen in the figures, the maximum deflection and strains occur in the RRFC on which the test vehicle is positioned. The transverse distribution of the live load can be seen by the distribution in strain (or deflection) to the unloaded portion of the bridge cross section.

Comparing the results for the three load tests reveals that almost perfect symmetry exists in the distribution of the load. This symmetry is depicted in Figure 4.13, which shows the midspan test results for all three load tests. The maximum live load tensile strain that occurred at midspan as a result of the load test was +243 microstrain (7.0 ksi) with the test vehicle in Lane 1. After applying the calculated dead load strain (stress), +235 microstrain (6.8 ksi), the total tensile strain (stress) occurring in the bridge at midspan increased to +478 microstrain (13.9 ksi), or approximately 70% of the 19.8 ksi (683 microstrain) allowable limit. Midspan compressive strains (both live load and dead load) were significantly less than the tension strains and are therefore not discussed.

The 1998 AASHTO *LRFD Bridge Design Specification* recommends a maximum allowable live load deflection of span/800 for legal truck loads [5]. Using this criterion, the maximum allowable live load deflection for the main span of WCB3 is 0.99 inches. The maximum midspan live load deflection for the test vehicle was 0.613 inches, or approximately 62% of the recommended value.

The moment fraction, which is the portion of the total transverse live load moment due to the applied load carried by an individual girder or flatcar in this situation, was also determined for WCB3. To determine the moment fraction, the area under the deflection (or strain) curve was determined. The area under the loaded RRFC was then compared to the entire area to determine the moment fraction. For WCB3, the experimental moment fraction was approximately 2/3, similar to the values reported in previous investigations.

As was done for previous RRFC bridges, an adjustment factor was used to increase the results from the test vehicle to those of an HS-20 truck, the likely design vehicle for the bridge. This adjustment factor was determined using the same methodology as was used previously in TR-498 Volume 1 [11]. The adjustment factor for WCB3 was 1.443. Using this value, the projected maximum total strain for an HS-20 truck on WCB3 becomes 586 microstrain (17.0 ksi), which is still below the allowable value of 19.8 ksi (683 microstrain). Using the same extrapolation approach, the maximum live load deflection increases to 0.88 inches, still within the AASTHO guidelines.

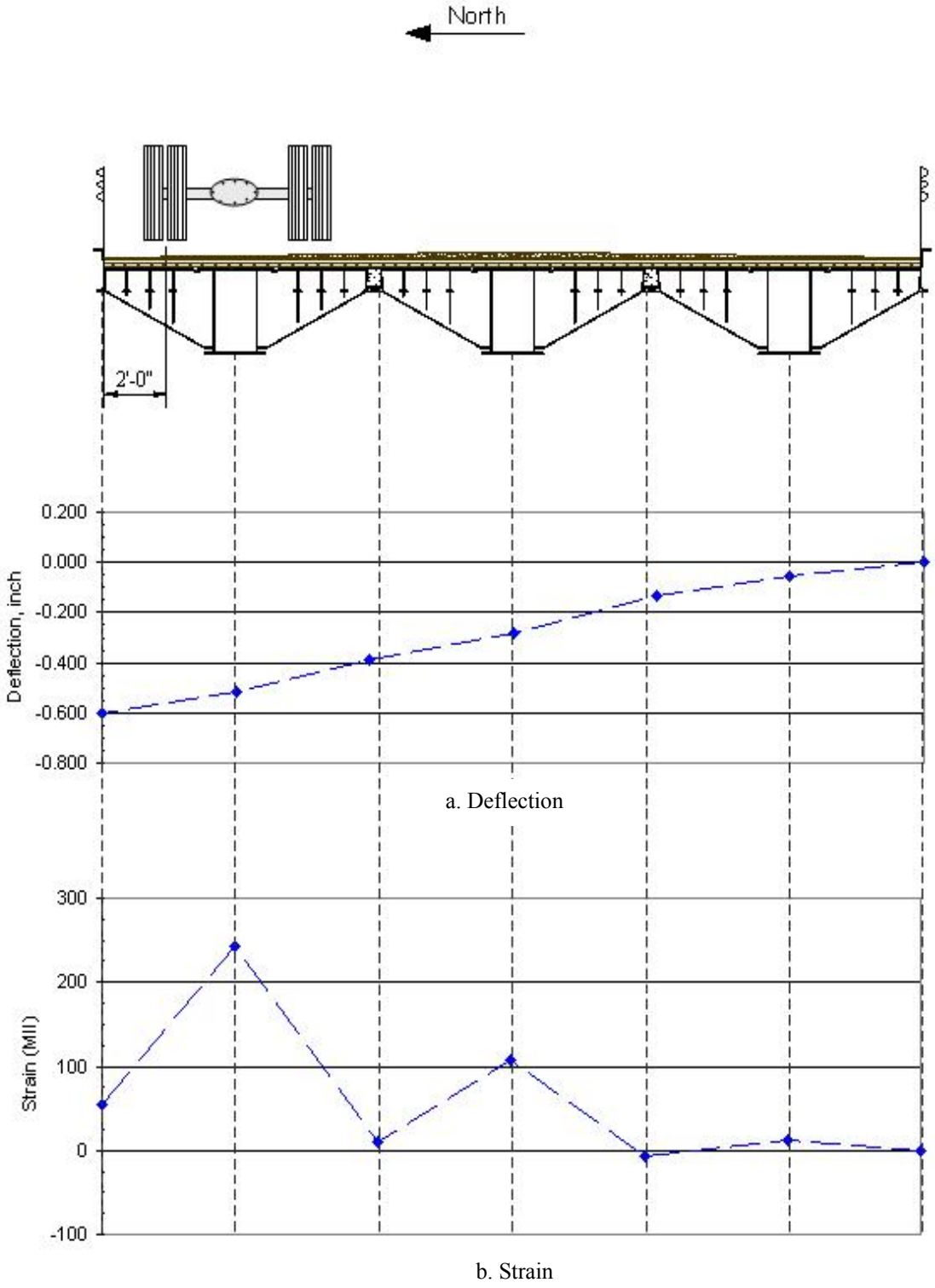

Figure 4.10. WCB3 Lane 1 midspan live load deflections and strains

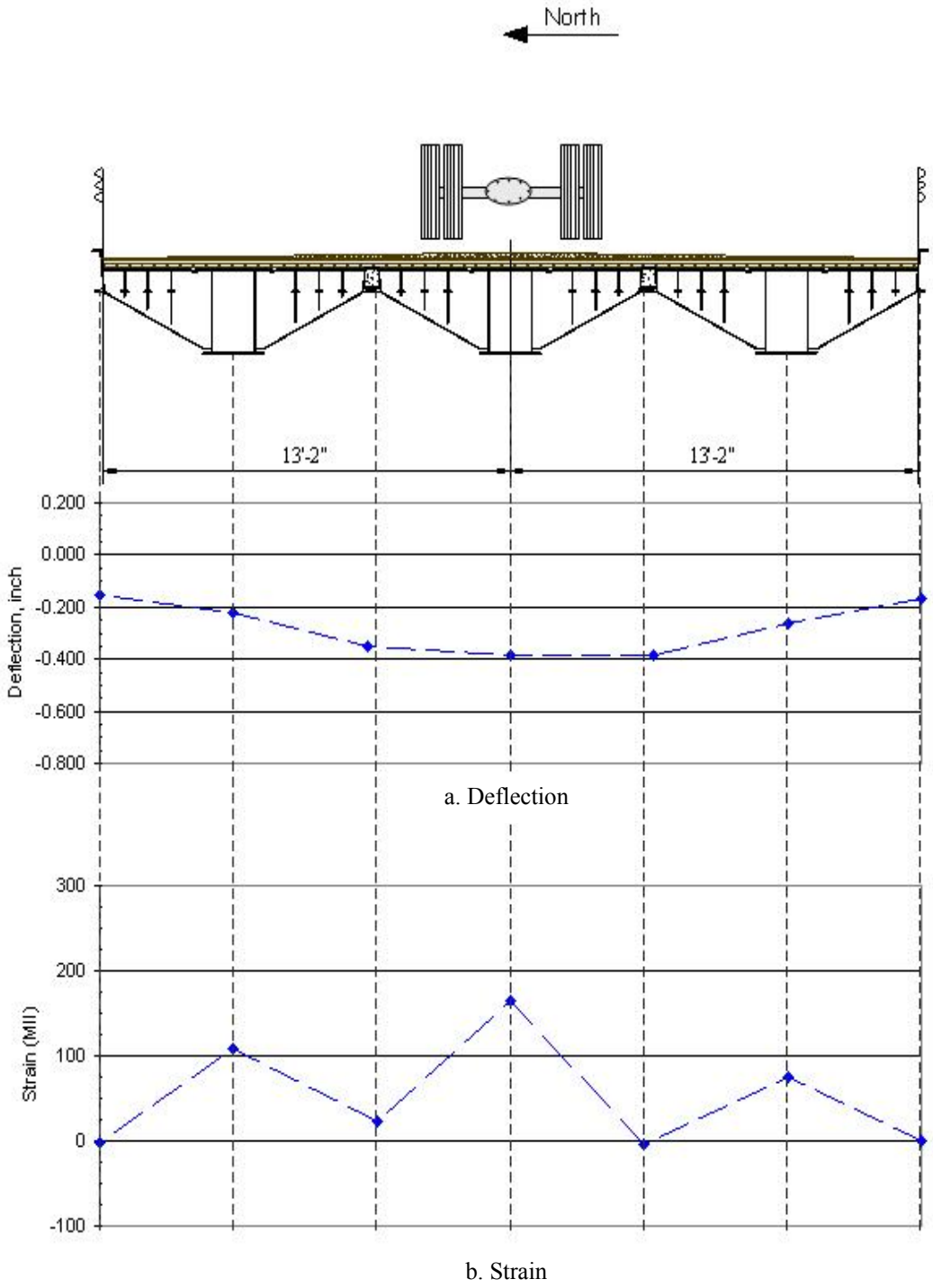

Figure 4.11. WCB3 Lane 2 midspan live load deflections and strains

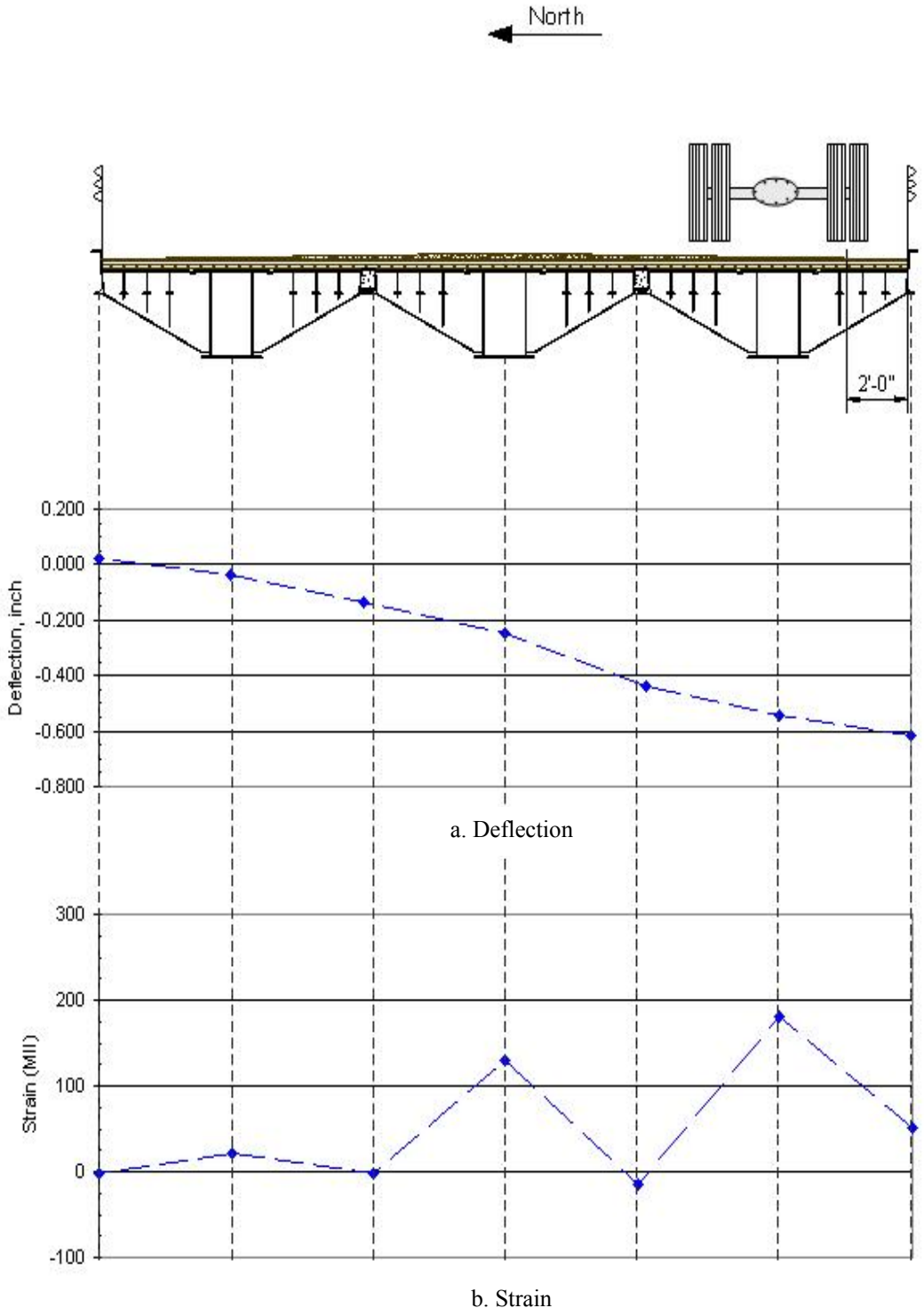

Figure 4.12. WCB3 Lane 3 midspan live load deflections and strains

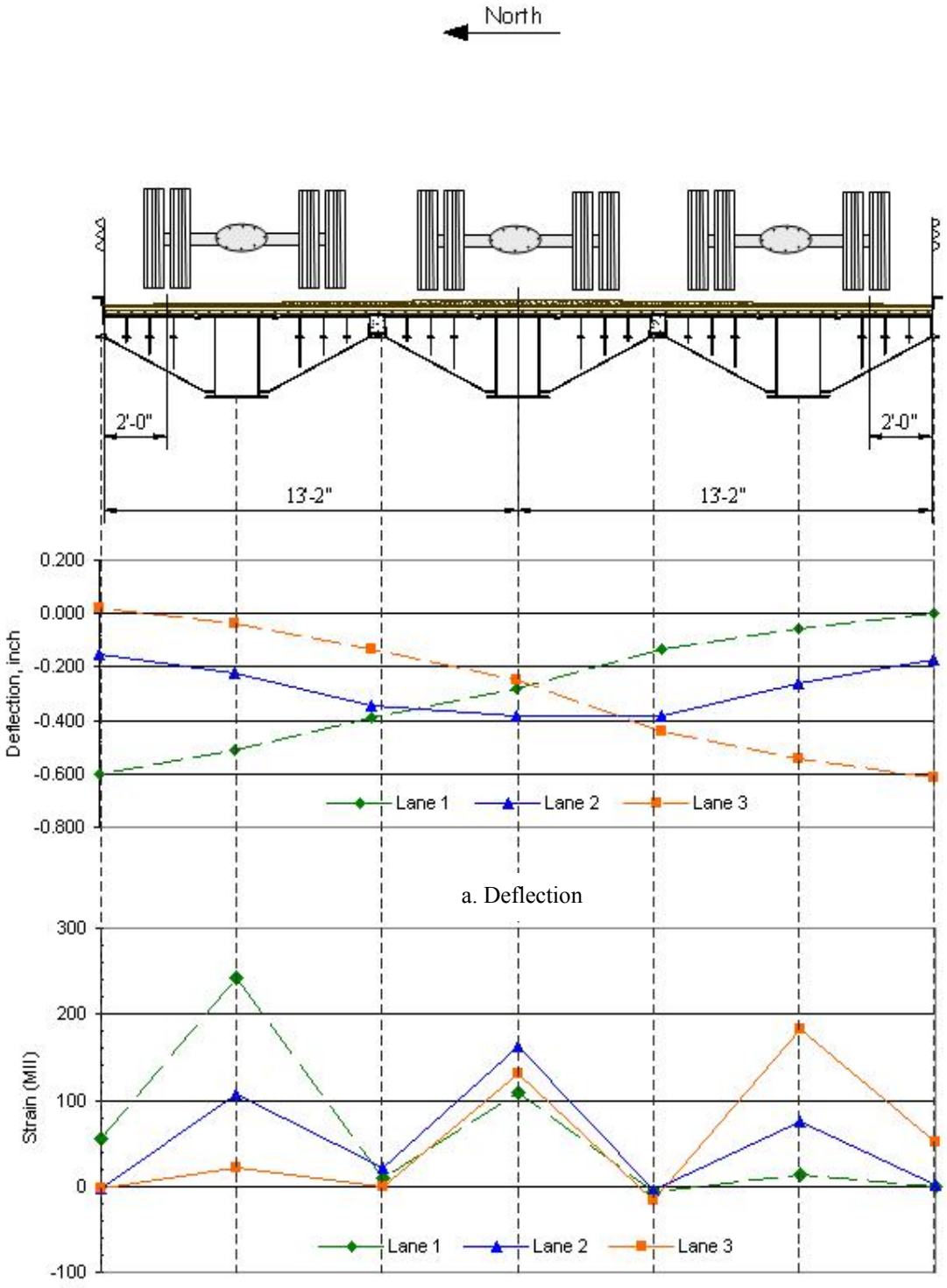

Figure 4.13. WCB3 load distribution symmetry

4.5.2 Dynamic Test Results

As stated earlier, a dynamic load test was conducted by driving the test vehicle across the bridge in the center lane (Lane 2) at approximately 25 miles per hour. However, after reviewing the data from the dynamic field load tests, the data were deemed inconsistent and inconclusive. Therefore, no dynamic characteristics were determined for WCB3.

5.0 THEORETICAL ANALYSIS

To investigate the live load distribution in each of the multiple span RRFC bridges, field test results were compared to the results obtained from a grillage model that was constructed to evaluate the bridges under different loading scenarios. Although a grillage analysis is not the most accurate theoretical analysis, modeling conducted as part of TR-444 [4] concluded that grillage analysis predicts the response of the RRFC bridges with sufficient accuracy.

5.1 Model Construction

For the multiple span RRFC grillage analysis, the same general layout for the 89-ft RRFC previously developed by Doornink in TR-444 [4] was used with only slight modifications to account for the differences in the bridges. By using the same general grillage layout previously developed, it was believed that the same RRFC specific properties could be used with only slight modification, which simplified the analysis and reduced the possibility of errors in calculating the section properties (since the first model has already been validated). However, as discussed in the subsequent section, this was not the case.

In the construction of the model, all of the members (primary and secondary) were represented. As was done in TR-444 [4], the effects of the deck were assumed to minimal; thus the deck was not included in its entirety in the model. However, the deck was considered in the calculation of the moment of inertia values for the various RRFC members.

For BCB4 and BCB5, there is an uncertainty in the degree of rotational restraint present at the abutments. To account for this uncertainty in the model, both pinned and full fixity conditions were investigated for the abutments of BCB4 and BCB5 with the goal of bracketing the field test results. The more conservative (higher-valued) deflection curve was then used to determine the distribution factors. The pier support condition was idealized as a pin in both the BCB4 and BCB5 model. For WCB3, the piers were idealized as pins while the abutments were modeled with full fixity. This condition was assumed to be the most realistic based on the conditions that existed at the bridge site due to the connection between the RRFCs and the sheet pile abutments.

5.2 Model Verification

To substantiate the validity of the grillage models, comparisons were made between the grillage model deflection results and the deflections measured during the field tests where sufficient field test data were available. For WCB3, there was good agreement between the experimental flexural strains in the main girders of the RRFC and those predicted by the model. Although the experimental and theoretical deflections did not agree as well as the strains, they were within acceptable limits. For BCB4 and BCB5, the goal of bracketing the deflections by changing idealization of the support conditions was achieved. However, the models did not satisfactorily predict the strains occurring in BCB4 and BCB5. After lengthy study of the model (and the differences with the WCB3 model), the idealization of several bridge components in the model were suspected for erroneous predictions and were further investigated; however, no definitive problems were discovered in the model.

Several explanations have been proposed as to why the theoretical strains vary from the strains measured in the load tests. As mentioned previously, grillage analysis is not the most accurate

analysis method available. Also, due to the geometric configuration of the 89-ft RRFCs (many small members and a thin steel deck), grillage analysis may not be an appropriate modeling technique. The presence of the transverse timber planking on WCB3 (and WCB1) is believed to have partially negated this problem by provided better load distribution to the larger members as well as a more substantial deck surface.

5.3 Live Load Distribution Factors

Due to the general acceptance of the deflections, theoretical live load distribution factors were developed using the theoretical deflections for the three RRFC bridges. The distribution factors were determined for the load cases that produced the maximum response in the RRFC member being investigated.

To determine the live load distribution factors from the grillage analysis, deflection results were used to develop a ratio of a specific girder deflection to the sum of the deflections of each girder in the respective cross section normalized using the second moment of inertia, as illustrated in Equation 5.1.

$$DF = \frac{\Delta I}{\sum \Delta I} \tag{5.1}$$

where:

DF = distribution factor – portion of the live load resisted by member being investigated

Δ = the theoretical live load deflection from grillage model

I = second moment of inertia of the respective girder

Distribution factors were determined at the midspan (i.e. maximum positive moment location) of all three RRFC bridges tested and also at the pier and tapered sections for BCB4 and BCB5 (i.e. location of the section with a smaller moment of inertia). For BCB4, distribution factors at both midspan locations as well as the pier were almost identical, indicating that the distribution was relatively constant within the main, deeper section of the RRFC. At the tapered transition section, the distribution factors for the interior girders were lower; indicating a smaller percentage of the load was resisted by the interior girders and thus a more even distribution of the load. This was expected as the properties of the main load carrying members were similar at these locations. Similar behaviors were observed for BCB5. For WCB3, distribution factors were only calculated at the midspan of the main (longer) span.

6.0 DESIGN AND RATING OF RRFC BRIDGES

6.1 Design Recommendations

The construction and use of grillage models is very tedious and requires access to computer software with three dimensional capabilities. Therefore, as was done for the RRFC bridges evaluated in the previous research, a simplified RRFC bridge design method for continuous spans was developed. To provide a consistent design process, a similar methodology was developed for the multiple span bridges as was developed in TR-444 [4] and applied in TR-498 Volume 1 [11] for simply supported bridges.

As was discussed in the previous chapters, the maximum strains (stresses) were recorded in the main girder of the bridge on the side where the truck was transversely positioned. The live load moment causing these strains (stresses) for both the positive and negative regions can be calculated using the following equations, which are similar to those previously developed by Doornink in TR-444 [4]:

$$M_{LL} = \lambda \psi \omega M \tag{6.1}$$

where:

M_{LL} = The actual maximum live load moment in the girder being investigated

M = The maximum live load moment at the point of interest in the RRFC bridge from analysis with vehicle center of gravity at midspan

$$\omega = \text{Inertia ratio} = \frac{I_D}{\Sigma I_{RRFC}} \tag{6.2}$$

I_D = Strong-axis moment of inertia for the girder being investigated

ΣI_{RRFC} = Sum of the girders' strong-axis moments of inertia in one RRFC

$$= (2)(I_{EXT}) + I_{INT} \tag{6.3}$$

I_{EXT} = Strong-axis moment of inertia for the exterior girder

I_{INT} = Strong-axis moment of inertia for the interior girder

ψ = Design factor to account for live load distribution, longitudinal connection, and load position

λ = Moment fraction value

The design live load moment value for an individual girder determined from Equation 6.1 is related back to one load position, which positions the center of gravity of the test vehicle(s) at the midspan location of the span being assessed for the positive moment region and on both spans for the negative moment region. In the application of Equation 6.1 to any of the primary girders in a RRFC bridge, the inertia ratio ω is used to account for the different moments of inertia of the girders. To account for the live load distribution, distribution factors were determined for the different bridge geometries using the method presented in Section 5.3. To determine the dead load moment, the dead load should be distributed to the girders as discussed in Sections 2.4, 3.4, or 4.4, with the moment determined accordingly.

In Equation 6.1, the λ-factor represents the moment fraction, which is the portion of the total transverse live load moment due to the applied load carried by an individual girder (or flatcar in this situation). To determine the moment fraction, the area under the deflection (or strain) curve was determined. The area under the loaded RRFC was then compared to the entire area to determine the moment fraction. In TR-444 [4], the moment fraction was determined to be 2/3 for RRFC bridges that were three flatcars wide. Research conducted on simply supported RRFC bridges as part of TR-498 Volume 1 [11] found that the moment fraction was also approximately 2/3 for BCB2 and DCB, which were two flatcars wide.

In previous RRFC bridge research (TR-444 and TR-498 Volume 1), the moment fraction was only determined at the midspan section as the bridges were designed as simply supported bridges and thus the midspan was the controlling section for design. However, as discussed in previous sections of this investigation, the shallow end of the tapered transition section exhibited high strain values and possibly is the controlling section (as was the case for BCB4 and BCB5). Therefore, the moment fraction was also calculated at the tapered section. For the midspan locations as well as the pier location, the average moment fraction, as reported in earlier sections of this investigation, was approximately 2/3, agreeing with the results from the previous investigations. The average moment fraction at the tapered section was determined to be approximately 3/5. This lower value was expected, as there is a more uniform load distribution at the tapered sections, as discussed previously.

In Equation 6.1, the ψ-factor represents a design factor used to account for different longitudinal flatcar connections, span configuration (single span vs. multiple span), and a simplified load position. For the multiple span RRFC bridges analyzed during this investigation, the ψ-factor was determined according to Equation 6.4.

$$\psi = \frac{DF}{\lambda\omega}\beta \qquad (6.4)$$

where:

DF = distribution factor determined from Equation 5.1

λ = Moment fraction value for location of interest

ω = Girder inertia ratio from Equation 6.2

β = Modification factor to account for load position

The β-factor used in Equation 6.4 represents a purely empirical value determined by matching predicted strains to the live load strains measured during the field load tests for each of the three RRFC bridges tested (BCB4, BCB5, and WCB3). The β-factors were also selected to provide some conservatism.

Design factors (ψ) for seven RRFC bridge configurations tests are provided in Table 6.1. These design factors, in addition to Equation 6.1 and the related equation parameters represent a complete design procedure for RRFC bridges. Table 6.1 lists the adjustment factors for the different bridge configurations and where the supporting information is located. As shown in Table 6.1, the RRFC design factors can be separated in to four categories, with the type of longitudinal connection being the variable. A detailed description of each connection type is provided in Appendix C of this investigation. Two values are presented for the 56-ft v-deck RRFC midspan exterior girder for the Type 1 connection because two different sized connections were investigated (see Appendix C). The larger value (1.1) corresponds to the wider connection while the smaller value (0.8) corresponds to the narrower connection.

A parametric study of the multiple span RRFC bridges was not conducted. All of the bridges that were analyzed and field tested were constructed from 89-ft RRFCs positioned side-by-side. Although there was some variation in the RRFC properties from bridge to bridge (BCB5 had different transverse members), the primary girders had essentially the same structural properties. Therefore, the results presented for distribution factors as well as the multiple span RRFC bridge simplified design procedure presented are not universal and apply only to 89-ft flatcars with primary girders that have essentially the same structural properties as those evaluated.

6.2 RRFC Bridge Rating Procedure

To determine the safe load carrying capacity of the multiple span RRFC bridges tested in this investigation, an inventory load rating was determined for each of the three RRFC bridges. For consistency with previous reports [7] and with the field information gathered, the allowable stress method was used to determine the rating factor. Using the AASHTO *Manual for Condition Evaluation of Bridges* (Rating Manual) [12], the rating factor is equal to:

$$RF = \frac{C - A_1 D}{A_2 L (1 + I)} \quad (6.5)$$

where:

RF = the rating factor for the live load carrying capacity

C = the capacity of the member

D = the dead load effect on the member

Table 6.1. Summary of Design Factors (ψ)

	RRFC Connection			
	Type 1	**Type 2**	**Type 3**	**Type 4**
Brief Description of Connection	Concrete Beam w/threaded rods	Concrete beam w/timber planks	Bolted through exterior flange	Welded plates
RRFC Bridge where connection was used	BCB1, BCB2, BCB4	WCB1, WCB2, WCB3	BCB3, BCB5	DCB
Referenced Report / **Type of RRFC**	TR-444 [4] TR-498 Vol 1&2 [11]	TR-444 [4] TR-498 Vol 1&2 [11]	TR-498 Vol 1 [11]	TR-498 Vol 1 [11]
56-ft RRFC Single Span				
Midspan Exterior Girder	0.8 - 1.1 *	----	----	----
Midspan Interior Girder	0.8	----	----	----
89-ft RRFC Single Span				
Midspan Exterior Girder	----	0.6	0.4	0.4
Midspan Interior Girder	----	1.2	1.2	0.9
89-ft RRFC Multiple Span				
Midspan Exterior Girder	0.5	0.8	0.8	----
Midspan Interior Girder	1.5	1.0	2.0	----
Pier Exterior Girder	0.9	----	0.8	----
Pier Interior Girder	0.8	----	0.8	----
Taper Exterior Girder	----	----	----	----
Taper Interior Girder	0.9	----	1.0	----

* Two differenced configurations were evaluated. See Appendix B for more information on the connections.

L = the live load effect on the member

I = the impact factor to be used with the live load effect = 0.33

A_1 = factor for dead loads = 1.0 for allowable stress method

A_2 = factor for live loads = 1.0 for allowable stress method

To determine the capacity of the member being rated using the allowable stress method, the yield stress of the material is multiplied by an appropriate factor, as determined using tables provided in the Rating Manual and material properties. For bridges in which the bridge material is unknown, the allowable stresses should be established by the engineer who is conducting the bridge rating, determined by field investigation, and/or by material testing [12].

The dead load effect on the member is calculated using conventional bridge analysis methods and is based on the condition of the bridge at the time of rating. Guidelines are provided in the appendices of the Rating Manual for determining the live load effect on bridge components of typical highway bridges. However, due to the many differences between RRFC bridges and typical highway bridges (e.g. slab on girder), a different approach must be used to determine the live load effect for RRFC bridges. For RRFC bridges, the live load effect on a member, L, was determined by multiplying the maximum live load effect by a distribution factor which represents the percentage of the live load resisted by the member being rated. For consistency with previous reports [7], this distribution factor is assumed to be the same distribution factor used in the simplified design procedure (Equation 6.1). The distribution factor to determine the live load effect on a member is:

$$DF_{LL} = \lambda \psi \omega \qquad (6.6)$$

The definitions of the variables in Equation 6.6 are the same as those presented for Equation 6.1.

To determine the live load effect, the three RRFC bridges were analyzed under loading from five different rating vehicles. The rating vehicles used were: HS-20, Type 3, Type 3S2, Type 3-3, and Type 4. For each rating vehicle, the vehicle was positioned on the bridge span with the vehicle center of gravity at the midspan location (or on both spans for the negative moment region). The moment envelope was then developed, from which the maximum live load moment at each critical location (at pier or in span) could be determined. To determine the live load effect, the maximum moment value was multiplied by an appropriate distribution factor determined through the application of Equation 6.6 to determine the moment resisted by each girder. This distributed live load moment was then divided by the section modulus of the bridge cross section to determine the live load stress.

The rating factor (RF) may be used to determine the rating of the bridge member being evaluated in tons by multiplying the rating factor by the weight (in tons) of the truck used to determine the live load effect. The rating of the bridge is controlled by the member with the lowest rating. An example of the rating procedure is presented in Appendix D of TR-498 Volume 1 [11].

For all three RRFC bridges evaluated during this investigation, the HS-20 load produced the largest live load response. By applying Equation 6.5 at the critical sections of the bridge, rating factors and

subsequently load ratings were developed for BCB4, BCB5, and WCB3. For BCB4 and BCB5, the controlling section of the bridge was the tapered transition section of the main girder, agreeing with the results from the field load testing. For WCB3, the controlling section of the bridge was at midspan. The rating factors and load ratings for the three RRFC bridges is summarized in Table 6.2.

Table 6.2. RRFC rating factors and load ratings

Bridge	Critical Section	Rating Factor (RF)	Load Rating (tons)
BCB4	shallow end of taper	1.61	115.7
BCB5	shallow end of taper	1.05	75.6
WCB3	midspan	1.09	78.8

7.0 SUMMARY AND CONCLUSIONS

7.1 Summary

In this investigation, the application of multiple span railroad bridge superstructures for use on low volume roads was examined. Specific objectives included investigating construction variables such as the use of sheet pile abutments; testing of multiple span RRFC bridges to determine live load strains (stresses) and deflections; refining the simplified design procedure developed in previous research; and developing a load rating procedure for multiple span RRFC bridges. These objectives were achieved by field testing three multiple span bridges – two in Buchanan County, Iowa and one in Winnebago County, Iowa – and analyzing the data obtained from the tests. In addition to the previously noted objectives, the research team also tested a RRFC bridge in Winneshiek County in which the RRFCs had been strengthened. By adding steel plates 23" wide by 5/8" thick to the RRFCs, it was possible to use existing abutments in the replacement bridge. Additional information on this bridge and test results may be found in Appendix D.

The BCB4 bridge is comprised of two 89-ft RRFCs positioned on existing concrete abutments and a new concrete pier with an longitudinal connection between the adjacent RRFCs consisting of an eighteen inch wide by 24 inch deep reinforced concrete cast-in-place beam with 5/8 inch diameter threaded rods on 24 inch centers through the exterior girders of the adjacent flatcars. BCB4 has center to center of support span lengths of 40'-3" and 39'-3" with 4'-1" and 4'-11" end overhangs at the abutments for a total superstructure length of 89'-0". The BCB5 bridge is also comprised of two 89-ft RRFCs situated on existing concrete abutments and a new concrete pier. However, unlike BCB4, the longitudinal connection between the adjacent consists of 5/8 inch diameter bolts on 36 inch centers along the length of the connection. BCB5 has no overhangs at the abutments which results in longer center to center of support spans of 42'-8" and 43'-10" for the same total superstructure length of 89'-0". The WCB3 bridge is composed of three 89-ft RRFCs supported by two new steel capped piers at the bolster locations and two new sheet pile abutments. The longitudinal connection between the adjacent flatcars is comprised of a five inch wide by seven inch deep reinforced concrete beam in addition to 3/4 inch threaded rods on 24 inch centers through the exterior. Timber planks were also added to the bridge deck to aid in the transverse load distribution. WCB3 has three spans – a 66'-0" main center span and two 11'-6" end spans for a total superstructure length of 89'-0".

To determine the structural behavior of the three bridges during pseudo-static field load tests, strain and deflection instrumentation was attached to the bridges at several critical locations on the primary girders (both exterior and interior) as well as on the longitudinal connection girders in the positive and negative moment regions. Instrumentation was also placed at the 1/4 and 3/4 span locations in addition to midspan for all three RRFC bridges. For BCB4 and BCB5, some instrumentation was placed near the shallow end of the tapered transition section of the primary interior girders. During the field load tests, a data acquisition system was used in conjunction with the instrumentation to generate a continuous data record of the behavior of the bridge. The use of the data acquisition system also allowed the data to be "marked" at specific reference times for use in analyzing the data records. For the pseudo-static load tests, the data records were marked when the center of the test truck tandem axle was at the center of bearing, 1/4, 1/2, and 3/4 span locations.

For the pseudo-static load tests, the bridges were divided into three lanes in which the test truck traversed the bridge. When the test truck was in Lane 1 and Lane 3, the outside wheel line of the test truck was positioned approximately two feet from the edge of the bridge. Lane 2 positioned the truck transversely in the center of the bridge. Dynamic testing was also completed for the three bridges. For

BCB4 and BCB5, the test truck traversed the bridge in Lane 2 at approximately 30 mph, while for WCB3, the test truck traversed the bridge in Lane 2 at approximately 25 mph.

In the demonstration project, TR-444 [4], tensile tests conducted on a steel coupon from the 89-ft RRFC determined that the modulus of elasticity and yield strength of the steel from which the RRFC is constructed was 29,000 ksi and 40 ksi, respectively. However, a conservative yield strength of 36 ksi was assumed for the RRFC bridges tested as part of this investigation since no additional material testing was conducted. Using the 2003 AASHTO *Standard Specification for Highway Bridges* [6] and the 36 ksi yield strength, an allowable flexural stress of 19.8 ksi, 55% of the yield strength, was determined for the RRFC members. The 1998 AASHTO *LRFD Bridge Design Specification* [5] was used to determine the recommended live load deflection limit of span/800. The field test results for the three RRFC bridges tested were then compared to these two criteria.

To determine the total stresses in the RRFC bridges, a dead load analysis was completed. The resulting dead load stresses were then added to the live load stresses from the field load test to determine the total stresses occurring in the respective bridge. A grillage analysis conducted as part of the demonstration project [4] determined that for the 89-ft RRFC, almost all of the dead load is resisted by the interior primary girders. For this reason, in this investigation the dead load was assumed to be resisted by only the interior primary girders and not the exterior girders.

Field load test results, both deflections and strains, were below the AASHTO recommended limitations. After adding in the dead load stresses as appropriate, the total stress values were still below the maximum allowable stress of 19.8 ksi. However, the test vehicles used in each field test weighed less than the likely design vehicle for the bridges, which was assumed to be an HS-20 designated truck. To correct for this, an adjustment factor was determined to increase both the live load strains and deflections in proportion to the difference in bridge response from the HS-20 and the test truck loadings. After applying the HS-20 adjustment factor, maximum stresses were still below the 19.8 ksi allowable stress limit and projected deflections were less than the span/800 recommended limitation. The damping and frequency of the BCB4 and BCB5 was also determined. Dynamic characteristics were not determined for WCB3 due to inconsistent data.

A grillage analysis was also conducted for the three RRFC bridges tested, using field load test results to validate the model. From the grillage analysis, live load distribution factors were determined for use in the simplified design procedure developed in conjunction with the demonstration project, TR-444 [4].

After the determination of the distribution factors, a rating procedure for multiple span RRFC bridges was developed. This rating procedure follows the allowable stress rating equation presented in the 1994 AASHTO *Condition Evaluation of Bridges* rating manual [12]. Live load distribution factors from the simplified design procedure were used to determine the live load effect on the RRFC members because of the non-traditional structural geometry of the RRFCs.

6.2 Conclusions

The following conclusions have been drawn from the data collected and subsequent analysis that was completed as part of this investigation on the use of multiple span RRFC bridges:

- Multiple span bridges constructed using the 89-ft RRFC (or a comparable flatcar) are an effective replacement bridge for use on low volume roads.
- For multiple span RRFC bridges constructed similarly to BCB4 and BCB5, the critical section to be analyzed for flexure will likely be at the region at the shallow end of the tapered section.
- Strains/Stresses and deflections in the bridges tested in conjunction with this investigation were below the allowable limits as set forth by AASHTO.
- Distribution factors are consistent through similar sections of the RRFC profile (are the same at midspan and pier).
- Through developing additional design factors for multiple span RRFC bridges, the simplified design procedure developed in previous investigations for single span RRFC bridges was expanded to include multiple span RRFC bridges.
- Multiple span RRFC bridges may be rated using the AASHTO Manual for Condition Evaluation of Bridges [12] with the use of appropriate distribution factors as determined at part of this investigation.
- The preliminary investigation in to the use of sheet pile abutments indicates that the use of such abutments is a viable alternative for low volume roads for a compatible superstructure.
- Sheet pile sections needed to be designed and selected for not only the geotechnical and structural load requirements, but also to withstand forces incurred during installation.

8.0 REFERENCES

1. 2006 Bridge Inventory. Better Roads Magazine. http://betterroads.gcnpublishing.com/content/fileadmin/user_upload/issues/pdfs/Bridge_Inventory/bridge2006.pdf. Accessed April 1, 2007.

2. US Census Bureau. 2005 Census Estimate. http://factfinder.census.gov/servlet/GCTTable?_bm=y&-geo_id=01000US&-_box_head_nbr=GCT-T1-R&-ds_name=PEP_2005_EST&-format=US-9S. Accessed March 8, 2006.

3. Wipf, T. J., F. W. Klaiber, and T. L. Threadgold. *Use of Railroad Flat Cars for Low-Volume Road Bridges*. Iowa DOT Project TR-421. Iowa Department of Transportation. August, 1999. 141 pp. May be accessed electronically at http://www.dot.state.ia.us/materials/research/reports/ihrb_by_topic/transportation_structures.html

4. Wipf, T. J., F. W. Klaiber, J. D. Witt, and J. D. Doornink. *Demonstration Project Using Railroad Flatcars for Low-Volume Road Bridges*. Iowa DOT Project TR-444. Iowa Department of Transportation. February 2003. 193 pp. May be accessed electronically at http://www.dot.state.ia.us/materials/research/reports/ihrb_by_topic/transportation_structures.html

5. American Association of State Highway and Transportation Officials (AASHTO). *AASHTO LRFD Bridge Design Specifications, Second Edition, Customary US Units.* Washington, D.C. 1998.

6. American Association of State Highway and Transportation Officials (AASHTO). *Standard Specifications for Highway Bridges, 17th Edition.* Washington, D.C. 2003.

7. Palmer, K. S. *Field Testing of Railroad Flatcar Bridges*. M.S. Thesis, Iowa State University, 2005.

8. Boomsma, H. A. *Field Testing of Railroad Flatcar Bridges on Low-Volume Roads*. M.S. Thesis, Iowa State University, 2005

9. Iowa Department of Transportation, Highway Division. Standard Designs. *Abutment Details 0° skew – Steel Piling*, Standard No., J30C-17-87. December 2004.

10. DeLorme Topo USA 5.0. DeLorme. Yarsmouth, Maine. 2004.

11. Wipf, T. J., F. W. Klaiber, K. S. Palmer, and H. A. Boomsma. *Field Testing of Railroad Flatcar Bridges*. Iowa DOT Project TR-498 Volume 1. Iowa Department of Transportation. Not Yet Published.

12. American Associate of State Highway and Transportation Officials (AASHTO). *Manual for Condition Evaluation of Bridges*. Washington D.C. 1994.

13. Doss, Robert E. and Mary Hauber. *Subsurface Exploration Bridge L-7-N Winnebago County, Iowa*. TEAM No. 1-1368. TEAM Services: Soil, Environmental, and Material Consultants. March 29, 2004. 12pp.

14. U.S. Army Corp of Engineers. *Design of Sheet Pile Walls Engineer Manual 1110-2-2504*. Department of the Army. Washington D.C. March 31, 1994. pp. 74.

15. Anderseon, J. B., F.C. Townsend, and B. Grajales. *Case History Evaluation of Laterally Loaded Piles*. Journal of Geotechnical and Geoenvironmental Engineering, American Society of Civil Engineers (ASCE). March 2003. pp. 188.

16. Bowles, Joseph E. *Foundation Analysis and Design*. 5th Edition. New York: The McGraw-Hill Companies, 1996.

17. Wipf, T. J., D. J. White, F. W. Klaiber and R. R. Evans. *Modified Sheet Pile Abutments for Low Volume Bridges*. Iowa DOT Project TR-568. Iowa Department of Transportation. In preparation.

APPENDIX A. DESIGN OF SHEET PILE ABUTMENTS

In this appendix the feasibility and design of sheet pile abutments for RRFC bridges on low-volume roads are presented. A brief overview of the advantages of constructing sheet pile abutments and selected case studies of their use in both Europe and the United States are outlined. Design considerations and recommendations obtained from previous research are also included. Last, a sample design of a sheet pile wall abutment using the WCB3 site conditions and an 89 ft, three-span RRFC bridge will be discussed.

A.1 Background

As previously noted, the main objectives of this project were to investigate possible design and/or construction variables along with improving performance, constructability, and cost for the RRFC bridge concept. One way to accomplish these objectives is to create an alternative, cost effective, abutment design that provides adequate bearing capacity and is easy to construct.

In previous RRFC bridge construction, steel sheet piles have been driven behind abutments only if required for soil retainment; they have not been utilized for bearing purposes. These structures, however, also possess the ability to support vertical load. Therefore, it is possible to eliminate the conventional pile abutments and utilize the bearing capacity and flexural rigidity of a steel sheet pile wall to serve as both the bridge abutment and as an earth retaining structure. It has been documented that using steel sheet piling for both bearing and earth retention has been used in Europe for years and its use in the United States is increasing.

A.1.1 Sheet Pile Abutment Feasibility

Using steel sheet piling for bridge abutments have numerous advantages over conventional methods. Sheet piles can resist both bridge bearing loads and lateral earth forces, thus eliminating the need for foundation piles. Construction may be completed sooner because the amount of earthwork is reduced, fewer materials are needed to construct the abutment, and formwork is not required since the piles are driven. Scour, a significant issue with bridges, may be prevented with driven steel sheet piles. Through the combination of these attributes, other advantages of sheet pile abutments include substantial cost savings, less traffic disruption due to quicker construction, simplified construction, and reduced environmental impact [A1].

A.1.2 Case Studies of Sheet Pile Abutments

The use of sheet pile walls for bridge abutments has been practiced in Western Europe extensively for decades in both rural and urban areas; in the past 35 years, some of these structures have been used in highway bridges over railroads, highways, and waterways. Sheet pile abutments have been built in the United States, but have been limited to mostly low volume road bridges in rural areas. In the following case studies, various designs and wide applications of steel sheet pile abutments for bridges are presented [A1].

A.1.2.1 Highway Bridge over a Branch of the Moselle - Europe

In this application, a sheet pile abutment with a concrete cap and bridge seat supports the bridge superstructure. The steel sheet pile wall abutment penetrates through various soil stratums including backfill, gravel, and sand, while the sheet pile is embedded in stiff marl (a mixture of crumbly clays,

shells, and calcium and magnesium carbonates). Tie rods are spaced 6 ft – 7 in. on centers along the length of the wall for additional support [A1].

A.1.2.2 Highway Bridge over a Railroad - Europe

Due to the high elevation of bedrock, the required depth of penetration was greatly reduced. A concrete footing within the bedrock was constructed. The toe of each sheet pile was embedded into a steel channel placed in the footing which transferred the vertical loads into the reinforced concrete. The sheet pile abutments were capped with an integral reinforced concrete beam and tied back using a 2 1/2-in. diameter tie rod 46 ft long [A1].

Railway transportation is widely used in European countries; hence, the swiftness of installing sheet pile abutments is a significant advantage because of train frequency. Installation of the sheet piles for this highway bridge over a railroad was performed between the passing of trains and eliminated the disruption of train schedules [A1].

A.1.2.3 Highway Bridge over a Port Facility - Europe

Large bearing forces from the 233-ft long truss bridge were resisted by a set of steel sheet pile walls. The first row of sheet piles were continuous, while the second row of sheet piles were intermittently spaced 13 ft – 9 3/5 in. apart and were utilized for added bearing resistance. A 66-ft driven and grouted batter pile was tied to the top of the sheet pile abutment and was extended into layers of sand and medium firm marl for supplementary support [A1].

A.1.2.4 Taghkanic Creek Bridge, Columbia County, New York – United States

Steel sheet piling abutments were used for the 42-ft single span highway bridge. The sheet piling was driven into granular soils to an embedment depth required for adequate bearing strength (16 ft). The sheet piles were capped with a reinforced concrete beam bearing on a steel plate. Wing walls were constructed using cantilevered steel sheet piles driven to the same depth as the abutments, and were capped with steel channels [A1].

A.1.2.5 Banks Road Bridge, Tompkins County, New York – United States

The 65 ft single span bridge was supported on steel sheet abutments embedded to a required depth of 45 ft at the east abutment and 22 ft at the west abutment. A total of 16 sheet pile sections were used for the abutment, but only 10 were needed to support the vertical bridge loads. The remaining six sheets were driven to a more shallow depth required for soil retainment. A steel channel overlain by a steel beam was used to cap the sheet pile abutment piles. Tie backs were used to stabilize both the steel sheet pile abutments and wing walls [A1].

A.1.2.6 Sprout Brook Bridge, Paramus, New Jersey – United States

In 2000, A.G. Lichtenstein & Associates constructed the Sprout Brook Bridge (48-ft span length; 13 traffic lanes for a width of 209 ft) using permanent sheet piling abutments in an effort to reduce construction cost and time. The sheet pile abutment construction reduced the project cost by over $200,000 and resulted in a completion date 10 weeks earlier than originally anticipated. Original construction plans included cast-in-place concrete abutments and wingwalls on piled footings which would have required temporary cofferdams along with significant excavation and dewatering for the driving of piles and footing construction. Permanent sheet piles were installed instead to support both the vertical bridge loads and the horizontal earth pressures. Installing steel sheet pile abutments eliminated the need for excavation of the existing channel, which lessened the economic impact and reduced traffic rerouting from six lane changes to only two. Steel sheet piles were driven to refusal into sandstone bedrock and stabilized with a tie back near the top attached to a deadman system. The sheet piling was imbedded 1ft – 0 in. into a cast-in-place reinforced concrete cap which was designed to transfer the 15 kip/ft of axial load from the bridge to the abutment. Design moments of 45 kip-ft/ft from earth pressures and an additional 150 kip-ft/ft for seismic activity were also considered [A2,A3].

A.1.3 Analysis and Design

When analyzing and/or designing a sheet pile wall abutment, both the lateral earth pressures and the bearing capacity of the abutment must be considered. Designing for lateral earth forces on sheet pile walls has been widely documented since sheet piles are commonly used for soil retainment. However, calculating the pile resistance of the steel sheets is more difficult to determine and, consequently, the use of sheet piles for bearing is less common.

To proceed with design calculations for the steel sheet pile wall, an accurate subsurface investigation must first be conducted. Soil borings near each abutment are required since soil conditions may vary across the channel. Data obtained should include the water table depth, along with soil classifications, water content, blow count, and unit weight throughout the boring depth. In poor soil conditions, adequate bearing strength may not be achieved in shallow depths; therefore, borings should extend sufficiently deep to ensure a complete soil profile for the entire depth of the sheet pile.

Lateral earth pressures on the sheet pile walls are dependent upon soil conditions, location of the water table, embedment depth, and if cantilever or anchored sheet piles are used. Guidelines for the design of steel sheet piles for use as retaining walls are documented in the United States Steel (USS) Steel Sheet Piling Design Manual [A4]. Cantilevered sheet piles are designed by creating a zero net lateral pressure on the wall, thus resulting in stability of the sheet pile wall. The design lateral forces exerted on a cantilevered sheet pile assuming granular backfill and penetration into clay are illustrated in Figure A.1. As described in the Design Manual previously noted, cantilevered sheet piles may be designed by a conventional method (Figure A.1a) or a simplified method (Figure A.1b). The Fixed Earth and Free Earth Support Methods are the basic methods of sheet pile design, with the Free Earth Support Method being the most commonly used due to its simplicity. The Fixed Earth Support Method assumes a hinge (zero bending moment) at the point of contraflexure, and the portions above and below this point are treated as separate freely supported beams. The Free Earth Support Method assumes that there is no pivot point below the dredge line. A sketch of the design lateral forces acting on an anchored sheet pile in cohesive soil backfilled with granular soil using the Free Earth Support Method is shown in Figure A.2 [A4].

Pile bearing capacity is composed of both the point resistance and the skin frictional resistance of the pile (See Figure A.3). The point resistance is a function of the cross sectional area of the pile, while the skin fiction is proportional to the perimeter of the pile throughout the embedment depth. The behavior of steel sheet piles may be compared to that of a steel H-pile whereas the cross section is not a boxed or circular section, but instead is an open cross section. A plug situation may be created in the void areas of the cross section when penetrated into cohesive soil conditions; however, a complete plug situation is unlikely to occur. Therefore, it is difficult to determine the effective area and perimeter of the cross section that is effective for calculating the point and frictional resistance of a sheet pile.

A.1.3.1 Point Resistance

The sheet pile cross sectional area bearing the lateral forces has been defined in numerous ways. Bustamante and Gianeselli [A5] describe the bearing cross sectional area as the entire inside area bounded by the flanges of the profiles as shown in Figure A.4. However, McShane [A6] considers the instance in which complete plug conditions may not exist; hence, in cohesive soils it is suggested 50% of the gross area (steel sheet pile cross sectional area + soil plug area) be considered.

A.1.3.2 Frictional Resistance

As with point resistance, there are various methods for calculating the sheet pile area used in determining the frictional resistance. Bustamante and Gianeselli [A5] define the area as the developed area of the wall (i.e. perimeter) (See Figure A.4); whereas, McShane [A6] recommends using a surface of up to 80% of the perimeter when plug formation is not considered.

A.2 Sheet Pile Abutment Design

The WCB3 site was selected for the theoretical design of sheet pile abutments. Three, 89-ft RRFCs were used for a 3-span bridge (See Figure A.5): the middle span was 66 ft and each end span was 11 ft – 6 in. from bolster to the end of the RRFC. Sheet pile wall abutments were designed based on soil borings taken at the east and west abutment locations. The sheet pile abutments were designed for soil retainment and to transfer bridge bearing forces to the underlying soil.

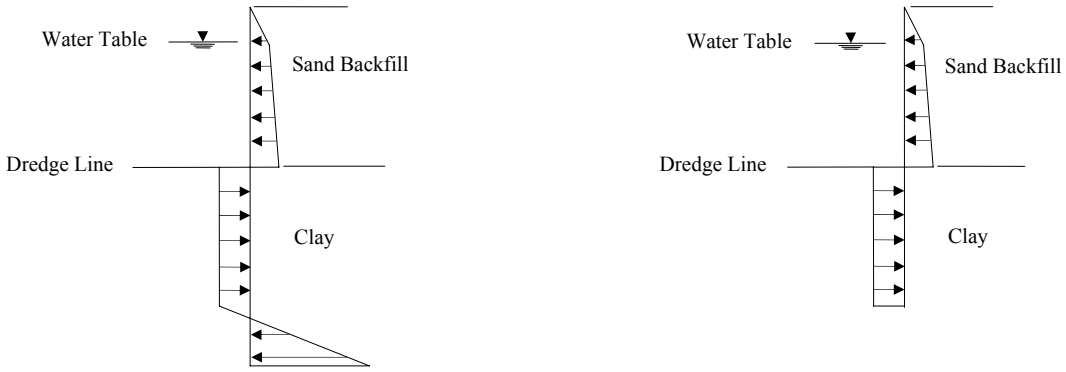

a. Conventional Method

b. Simplified Method

Figure A.1. Design lateral forces for a cantilevered sheet pile [A4]

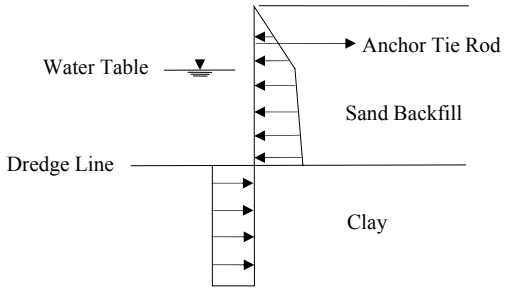

Figure A.2. Design lateral forces for an anchored sheet pile using free-earth method [A4]

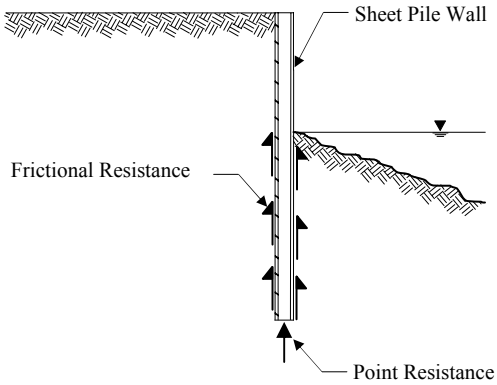

Figure A.3. Point and frictional resistance

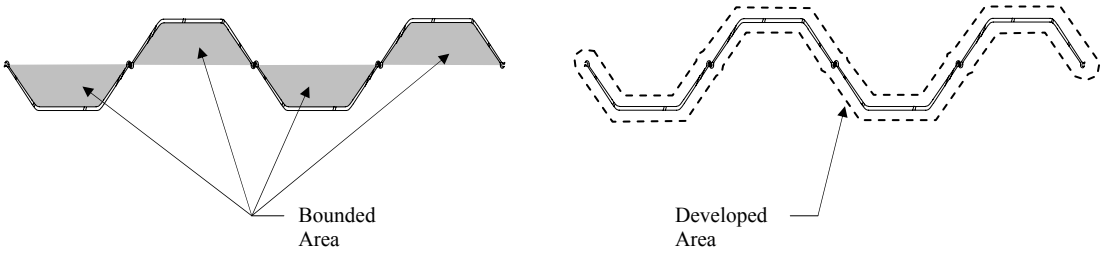

Figure A.4. Bounded and developed areas

A.2.1 Soil Properties

Borings near each existing abutment determined that fill material extended to about 5 ft below the existing road grade. Alluvial deposits extending to approximately 19 ft below existing road grade at the east abutment consisted of sandy lean clay and fine sand with silt. The alluvial deposits at the

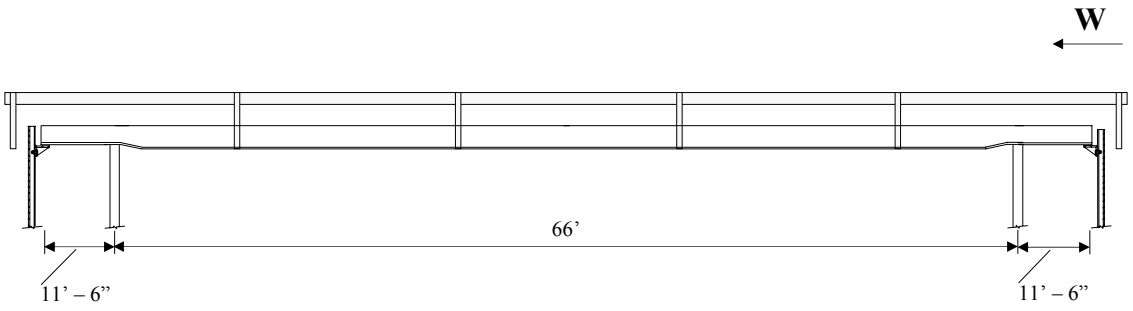

Figure A.5. Theoretical WCB1 dimensions

west abutment consisted mostly of a thin lean clay layer underlain by a peat layer extending from 7 ft to 19 ft – 6 in. below existing road grade, followed by silty or fine sands to a depth of 44 ft – 6 in. below existing grade. Below the alluvial deposits at both abutments were supraglacial sediments and subglacial tills consisting of stiff or very stiff sandy lean clays to a depth of about 65 ft – 6 in. below existing road grade. Supraglacial deposits typically consist of nearly equal parts of sand, silt, and clay with traces of larger particle sizes such as gravel, cobbles, or boulders. Subglacial tills have been preconsolidated by glacial activity; hence, they typically have a high density and shear strength [A7]. Hence, both supraglacial and subglacial soils would provide strong bearing if embedment depths were required to extend into these layers.

Unit weights, undrained shear strength, and soil friction angles of the various soil layers were not available from the boring test results; therefore, correlations between Standard Penetration Test (SPT) blow count numbers (N values) and these unknown properties were used. The USS Steel Sheet Piling Manual was referenced for its tables relating N values and unit weights of both cohesive and cohesionless soils [A4]. A relationship established by Karl Terzaghi and Ralph Peck for estimating

undrained shear strength of cohesive soils from SPT blow counts was used, and Peck's estimate of soil friction angel using SPT blow counts in cohesionless soils was also utilized [A8].

A.2.2 Earth Pressures

The sheet pile wall was designed for lateral earth pressures, including a surcharge load specified in article 6.5.2.4 of the Iowa Department of Transportation Bridge Design Manual [A9], and an external moment resulting from eccentric loading of the RRFC onto the abutment (See Figure A.6). A required penetration depth was found and a 40% increase, as specified in the USS Sheet Piling Design Manual [A4], was applied for a safety factor to obtain the design embedment depth. The calculated stresses in the retaining wall were then used to select a required steel sheet pile section.

A.2.3 Pile Design

Pile designs for the steel sheet pile walls were performed considering both end bearing and skin frictional resistance since layered soils existed throughout both abutment profiles. The west abutment of the WCB1 was bearing in a sand layer, while the east abutment was in firm glacial clay. Skin friction for the sand layers in both profiles and bearing resistance of the sand layer at the driven distance for the west abutment were calculated using equations given in AASHTO 10.7.3.4.2 correlating these values to SPT blow counts. The skin friction of the cohesive clay layers at both abutments and bearing resistance for the cohesive clay layer at the east abutment embedment depth were found using AASHTO 10.7.3.3 Semiempirical Estimates of Pile Resistance [A10]. A factor of safety of 4.0 [A11] was applied to all bearing and friction resistance values because of the soil property correlations that were utilized to obtain values used in the design.

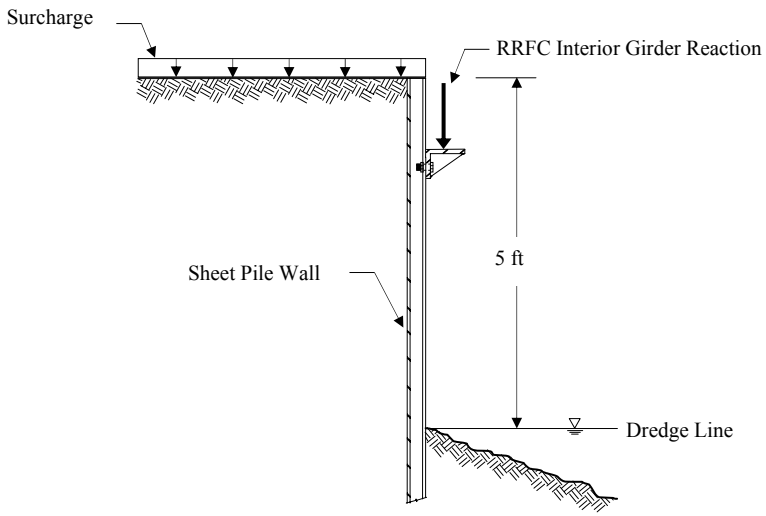

Figure A.6. Sketch of sheet pile analysis

Material properties for 5-Gage metric sheeting from Contech Construction Products Inc. were used for design, including both bearing capacity and frictional resistance of the sheet piles. Because sheet

piling does not have a solid cross section, like that of an H-pile, the amount of surface area in contact with the soil is unknown. Since a complete plug situation is unlikely to occur, the cross sectional area used for bearing capacity calculations was the cross sectional area of the steel sheets given in the Contech Construction Products Inc. Metric Sheeting brochure [A12], and the surface area used for frictional resistance was twice the laying width, which was approximately 86% of the total surface area of each steel sheet.

The maximum required depth from the earth pressure analysis and pile design calculations was used for determining the embedment depth of each steel sheet pile section located under a bearing point. The bearing points at the sheet pile abutments were the location of the three interior girders, the two concrete beam locations, and the two exterior girder locations at the outer edges of the bridge. Three sheet pile sections were designed to carry the bearing under the most critical bearing locations: the interior girders. The reaction forces under the remaining locations were much less; therefore, only one sheet pile section was required for bearing at the exterior members and concrete beam bearing regions. Sheet piling must be continuous for soil retainment; hence, the sheets not required for bearing under the interior girders would be driven to a lesser depth. It is recommended that the sheet piling be extended below the peat layer at all locations in the west abutment because of the soil's low strength. The west abutment, due to the substantial peat layer, would have a significantly deeper embedment than the east abutment to ensure a strong soil base for bearing. Design drawings of the steel sheet pile abutments for the theoretical 89-ft Winnebago County Bridge are presented in Figure A.7.

The upper surface of the sheet pile wall is not a suitable base for bearing; therefore, an attached angle support was designed to provide the required bearing. As stated in Section A.1.2, previous use of sheet pile wall abutments has involved attaching an inverted channel shape on the top of the sheet pile wall to create an adequate bearing surface. However, for RRFC bridges, this approach may not be suitable since the open cross-section would not retain backfill material. This problem may be prevented by attaching a stiffened angle to the side of the wall along the length of the sheet pile to create the bearing surface (See Figure A.8). In this instance, the sheet pile wall would still retain the backfill material and would also resist the bearing forces.

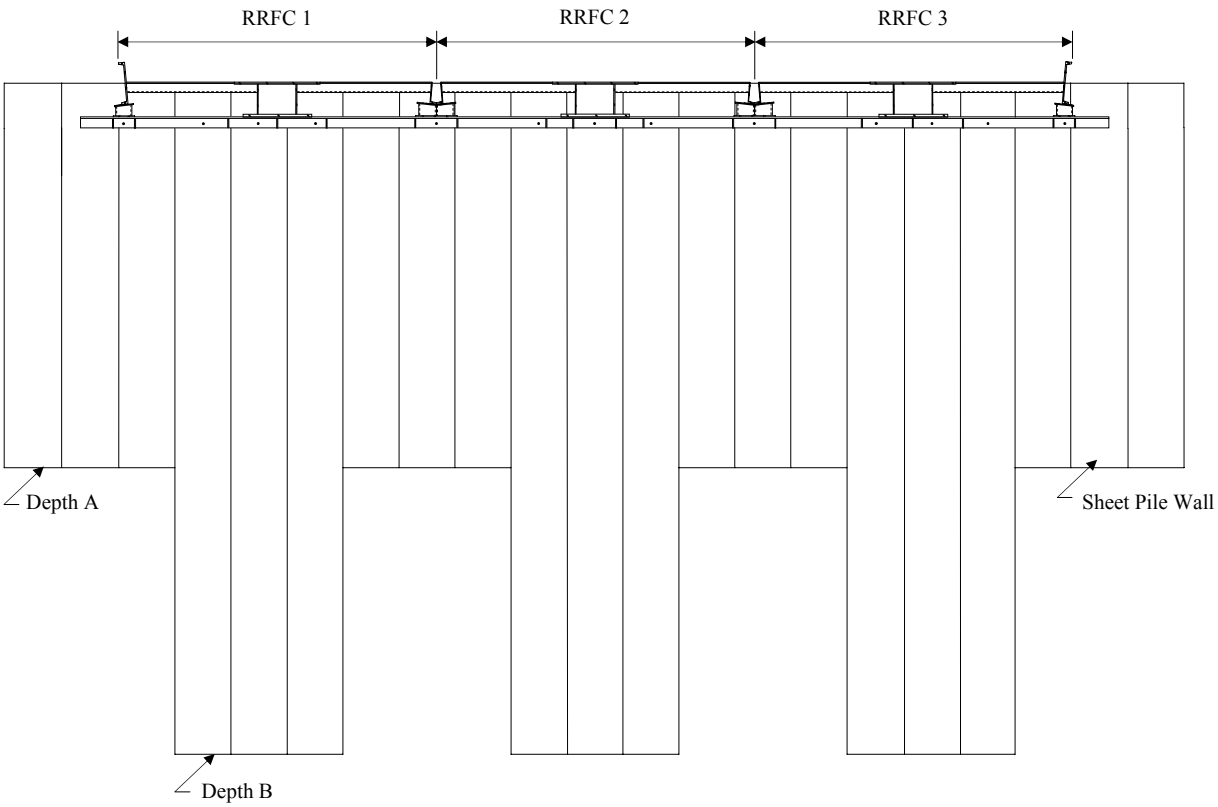

	Depth A	Depth B
East Abutment	11 ft	25 ft
West Abutment	20 ft	35 ft

Materials Summary:

East Abutment
9 pieces of Gage 5 steel sheets, 25 ft long
12 pieces of Gage 5 steel sheets, 11 ft long

West Abutment
9 pieces of Gage 5 steel sheets, 35 ft long
12 pieces of Gage 5 steel sheets, 20 ft long

Figure A.7. Sheet pile abutment design for the theoretical WCB1

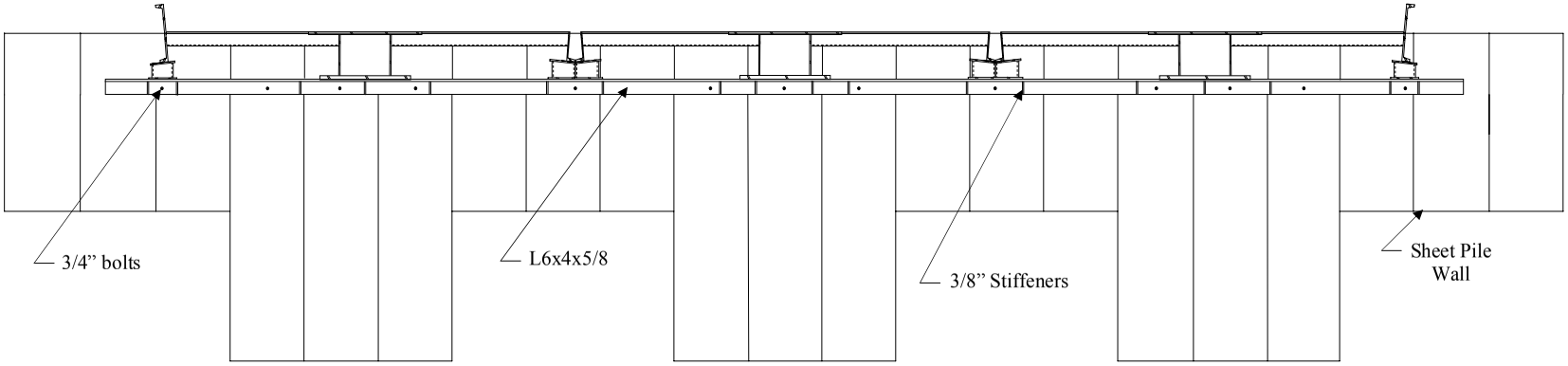

a. Cross sectional view of the RRFC stiffeners and bolt locations at the sheet pile abutments

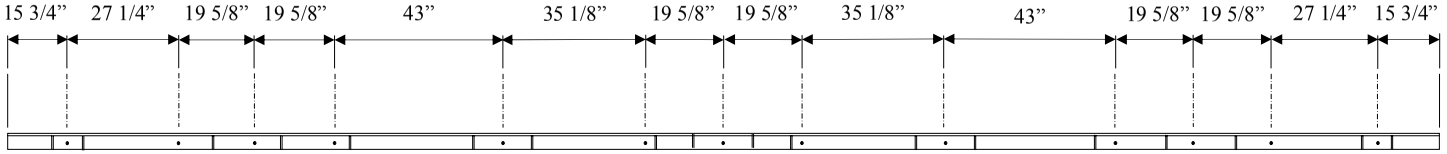

b. Approximate spacing between centerline of bolt holes*

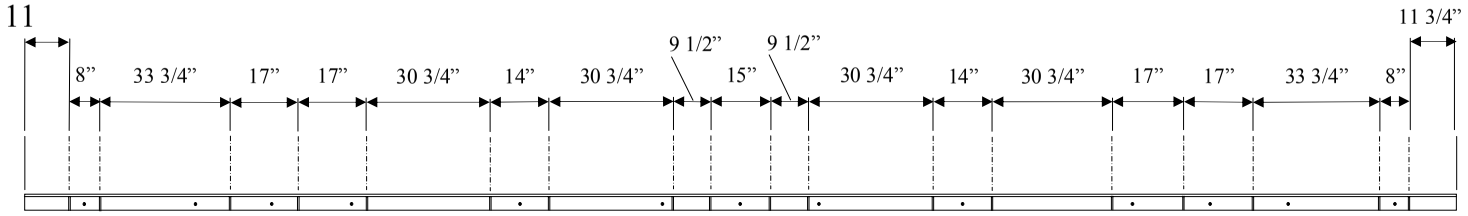

c. Approximate spacing between centerline of angle stiffeners*

*Dimensions may need to be adjusted for field conditions.

Figure A.8. Theoretical WCB2 sheet pile abutment bearing support design

A.3. References

A.1. Carle, R., and S. Whitaker. Sheet Piling Bridge Abutments. Deep Foundations Institute Annual Meeting, Baltimore, Maryland. Oct. 1989, 16 pp.

A.2. Skyline Steel, LLC. Case Histories: Sprout Brook Bridge: Permanent Sheet Piling provides the Answer. Online article: http://www.skylinesteel.com/info_ch1.htm.

A.3. Sassel, R. Fast Track Construction with Less Traffic Disruption. Structural Engineer, October 2000. pp. 1-2.

A.4. United States Steel Corporation. USS Steel Sheet Piling Design Manual. Federal Highway Administration (FHWA). July 1984, 132 pp.

A.5. Bustamante, M., and L. Gianeselli. Predicting the Bearing Capacity of Sheet Piles Under Vertical Load. Proceedings of the 4th International Conference on Piling and Deep Foundations. Stresa, Italy. April 1991, 8 pp.

A.6. McShane, G. Steel Sheet Piling Used in the Combined Role of Bearing Piles and Earth Retaining Members. Proceedings of the 4th International Conference on Piling and Deep Foundations, Stresa, Italy. April 1991.

A.7. Doss, Robert E. and Shiping Yang. Subsurface Exploration Bridge G-2-N Winnebago County, Iowa. TEAM No. 1-1361. TEAM Services: Soil, Environmental and Material Consultants. March 1, 2004, 12 pp.

A.8. Anderson, J.B., F.C. Townsend, and B. Grajales. Case History Evaluation of Laterally Loaded Piles. Journal of Geotechnical and Geoenvironmental Engineering, American Society of Civil Engineers (ASCE). March 2003, pp. 187-189.

A.9. Office of Bridges and Structures. Bridge Design Manual. Iowa Department of Transportation. January 28, 2004.

A.10. American Association of State Highway and Transportation Officials (AASHTO). AASHTO LRFD Bridge Design Specifications, Second Edition, Customary US Units. Washington, D.C. 1998.

A.11. Das, Braja M. Principles of Foundation Engineering, 4th Edition. Brooks/Cole Publishing Company. 1999, p 598.

A.12. Contech Construction Products, Inc. Metric Sheeting. Middletown, Ohio. 1989.

APPENDIX B. SHEET PILE ABUTMENTS IN WCB3

In an effort to maximize the economy of bridge design and construction for low volume roads, an investigation was made into the use of sheet pile abutments. This appendix includes details on the design and construction of the sheet pile abutments for the WCB3 RRFC bridge. Also included are test results and corresponding preliminary data analysis along with an interpretation of the resulting trends. Additional information on the feasibility and application of sheet pile abutments can be found in Appendix A.

B.1 Analysis and Design

The Winnebago RRFC Bridge 3 (WCB3) is located four miles south of Buffalo Center, Iowa on 390th Street over Little Buffalo Creek (Figure 4.1). Three 89-ft RRFCs were used to construct WCB3 (see Figure B.1.1). The bridge has a 66'-0" main span and 11'-6" end spans. Sheet pile abutments were designed based on soil borings from both the east and west abutment locations, taking into account both soil retention and the transfer of the bridge bearing forces to the underlying soil.

Figure B.1. Winnebago County RRFC Bridge 3 (WCB3)

B.1.1 Soil Properties

Soil boring logs for the approximate location of each abutment were provided by Winnebago County. At both abutment locations, the soil borings indicated fill to a depth between four and eight feet. Beneath the fill were supraglacial sediments and tills consisting of stiff to hard lean clays, sandy lean clays, and silt. These materials extended to the bottom of the bore sample (approximately 65 feet from the existing grade). No boulders or cobbles were noted in the boring logs. However, due to the

nature and origin of the soil, there is a possibility that boulders and cobbles may be present in the vicinity of the bridge [13].

Soil properties were not provided on the borings logs so correlations were needed between the standard penetration test (SPT) blow count numbers (N values) and the required properties. The Army Corp of Engineer *Design of Sheet Pile Walls* was referenced for tables that related the unit weight of both cohesive and non-cohesive soils to N values [14]. A relationship developed by Karl Terzaghi and Ralph Peck was used to estimate the undrained shear strength for the cohesive soils based on N values [15]. An expression developed by Peck was also used to relate friction angles to N values [15].

B.1.2 Sheet pile Design

Lateral earth pressures were determined for the sheet pile design by using conventional methods and the approximate properties determined from the blow count numbers reported in the boring logs. For layers with multiple N values, the values were averaged to determine the approximate soil properties of the entire layer. To determine the lateral earth pressure, the "at-rest" lateral pressure coefficient (K_o) was used. The at-rest coefficient was conservatively used in place of the active pressure coefficient (K_a) because the presence of the bridge restrained the lateral displacement of the sheet pile. Therefore, the displacement necessary to develop the active pressure situation was assumed not to have developed. A dredge depth of four feet was used for the sheet pile design based on the previous RRFC bridges constructed in Winnebago County. The water table was assumed to be located at a depth of four feet based on conversations with Winnebago County officials. A factor of safety of approximately 1.5 was applied to the design of the sheet pile wall in regards to soil retention as recommended by Bowles [16].

After the required section modulus was determined, the design was checked using a finite element program developed by Joseph Bowles [16]. Both the Bowles program and the hand calculations produced similar results.

B.1.3 Pile Design

In addition to soil retention, the sheet pile sections needed to be designed to provide axial resistance to the bridge reactions. The 1998 American Association of State Highway Transportation Officials (AASHTO) *LRFD Bridge Design Specification* was used to provide a methodology for the pile design. For the tip resistance calculation, the actual end area of the sheet pile section was used in conjunction with AASHTO LRFD Section 10.7.3.3.3.3 [5] as suggested in Appendix A. AASHTO LRFD Section 10.7.3.3.2 [5] was used to calculate the resistance due to skin friction. For the surface area calculations, twice the width of the sheet pile section multiplied by the depth was used as the surface area exposed to skin friction. This conservative estimate of skin area is noted in Appendix A.

The design axial load on the sheet pile section was determined using a HS-20 truck loading and the dead weight of the RRFC bridge. For preliminary calculations, the axial load from the bearing points (under the three main girders, the exterior girders of the bridge, and the longitudinal connections) was assumed to be distributed to approximately two sheet pile sections, using the RRFC-sheet pile connection and friction between adjacent sheet pile to transfer the load. At the main girder locations, the full reaction from a computer analysis (24 kips) was used as the design axial load. At the longitudinal flatcar connections and the exterior girders of the bridge, the axial load was reduced by half (12 kips). Since the actual load distribution in the bridge was not known at this time, this

approach was used as an initial conservative approach. A factor of safety of 3.75 was applied to the axial capacity of the sheet pile abutments.

B.1.4 Connection Design

The connection between the RRFC superstructure and the sheet pile sections was as designed in Appendix A with one slight modification. The original design consisted of a continuous 6 inch x 4 inch x 5/8 inch angle stiffened with 3/8 inch plates and 3/4 inch diameter bolts. After some discussion with the Winnebago County, it was decided that constructability would be easier if the angles were not continuous. No additional calculations were made for the new design. Both the original continuous angle design as well as the new discontinuous angle design is shown in Figure B.2 and B.3, respectively.

B.2 Construction

Construction of the sheet pile abutments started after the placement of the RRFCs on the two piers. As shown in Figure B.4, the sheet piles sections were driven directly adjacent to the bridge superstructure, eliminating any expansion joint. This was done to increase the constructability and with the belief that the soil retained by the sheet pile as well as the flexibility of the sheet pile itself would allow the abutment to move as needed for expansion and contraction (approximately 1/2 inch of movement was needed at each end of the bridge assuming a 100 degree temperature change).

The sheet pile sections used for the WCB3 abutment were approximately 0.21 inches in thickness. These sections were readily available to Winnebago County and satisfied the requirements for the stresses that resulted from soil retention. However, when construction started on the abutments, it was soon realized that the sections were not substantial enough to withstand the forces that the vibrating pile driving equipment was exerting on the sections. This inadequacy resulted in two things. First, extra care had to be taken not to buckle the portion of the sheet pile sections within the jaws of the vibrator (Figure B.5). Second, it was not possible to drive the sheet pile sections to the design depth. Instead, the sections were driven to rejection (just before the portion in the jaws buckled). This was deemed satisfactory by on-site personnel as the rejection depth varied only plus/minus two feet from the original depth. Figure B.6 shows the sheet pile sections at the east abutment just after driving. After the pile sections were driven, the sections were cut off to provide a level top section.

Due to a misunderstanding between the parties involved, a 5 inch x 3 inch x 1/2 inch angle was welded to the bottom of the deck of the RRFCs (Figure B.7) before the placement of the flatcars. This angle was proposed to represent the connection between the bridge superstructure and the abutments. However, after review by Iowa State University, additional stiffened angles 4 inch x 4 inch x 1/2 inch were added below the main bearing points (girders and longitudinal connections) as shown in Figure B.8. These angles were smaller than the angles discussed in Section B.1.4 because the top angle took a portion of the load. No connection was made between the additional angles and the bridge superstructure.

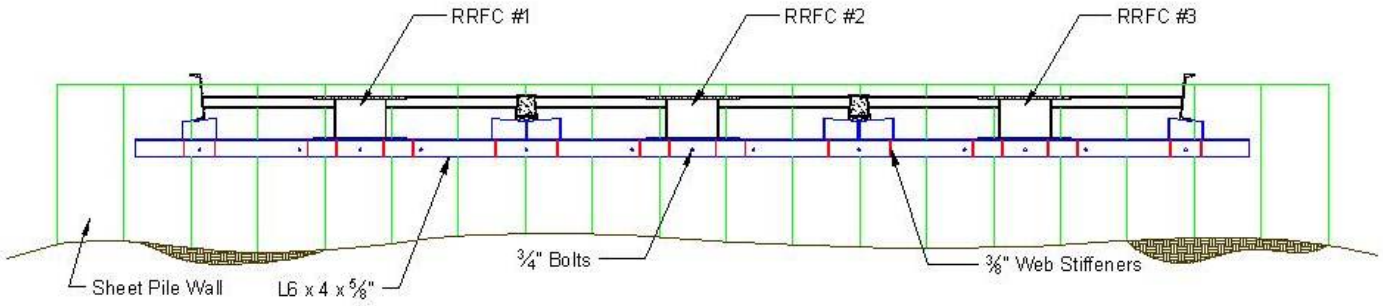

a. Profile view of connection

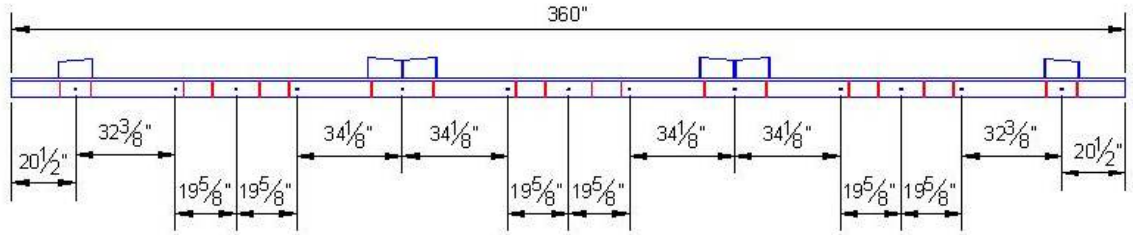

b. Approximate spacing of 3/4" bolts

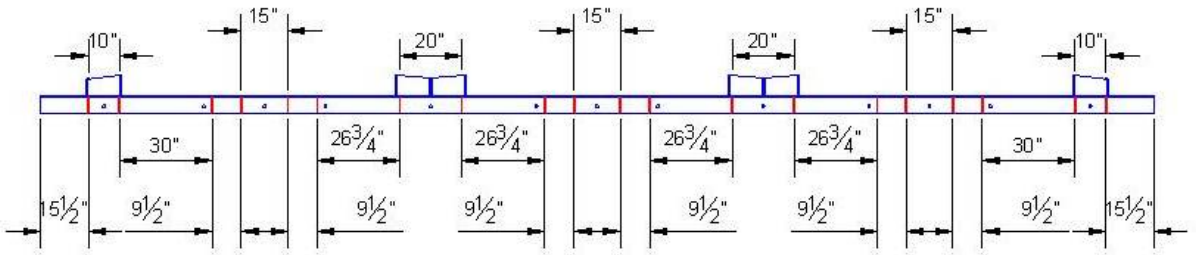

c. Approximate spacing of 3/8" angle stiffeners

Figure B.2. Details of continuous sheet pile connection angle

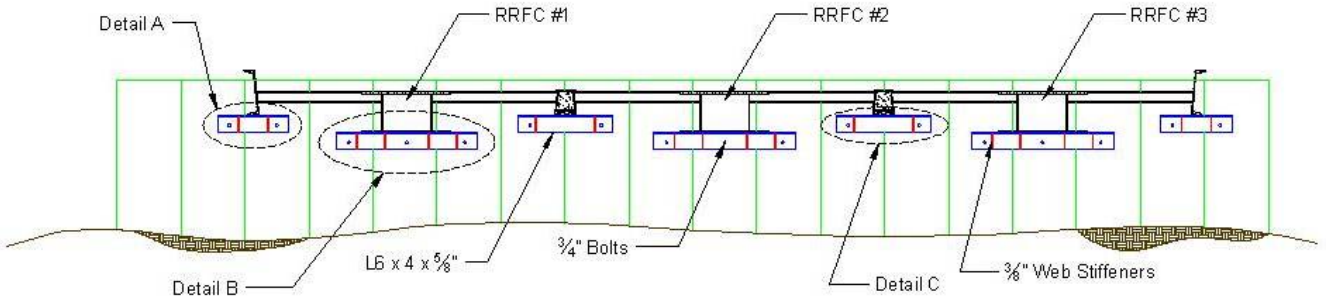

a. Profile view of connection

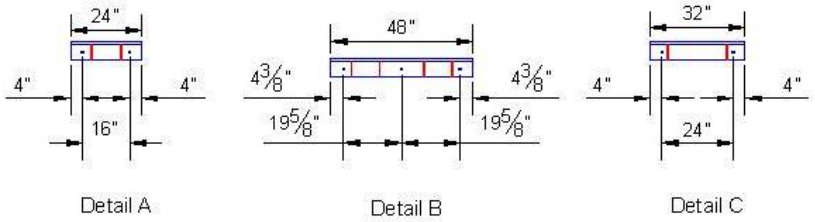

b. Approximate spacing of 3/4" bolts

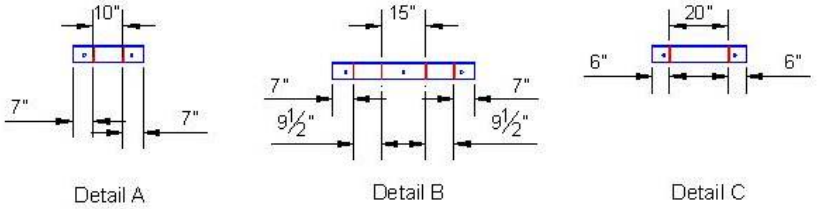

c. Approximate spacing of 3/8" angle stiffeners

Figure B.3. Details of discontinuous sheet pile connection angle

Figure B.4. Sheet pile abutment construction with no expansion joint provided

Figure B.5. Buckled sheet pile section due to driving equipment

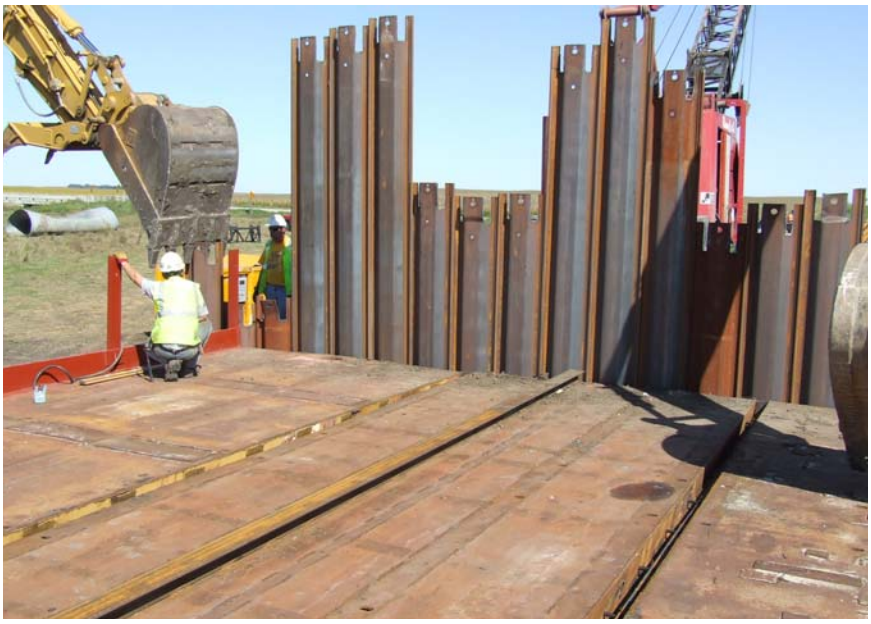

Figure B.6. East abutment after driving

Figure B.7. Angle welded to bottom of RRFC deck

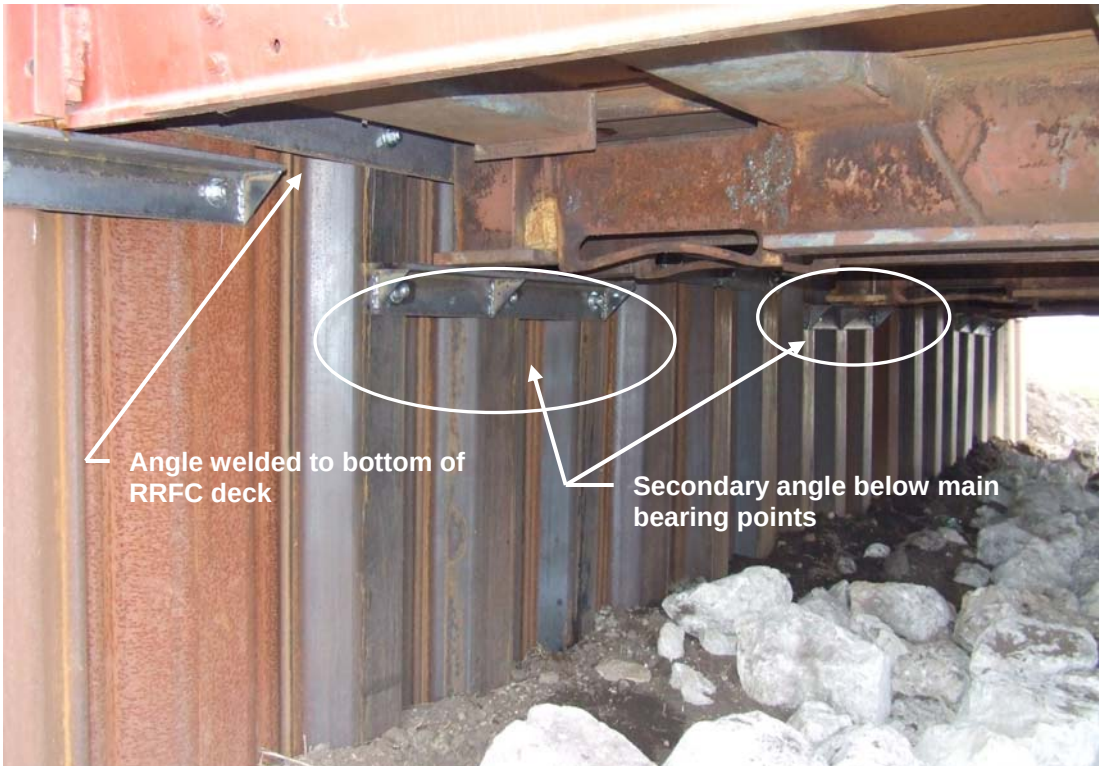

Figure B.8. Secondary angle attached below main bearing points

After the placement of the angles and before the placement of the backfill material, 3/4 inch diameter bolts were used to connect the angles to the sheet pile sections. No protection was provided for the bolts against the environment. In future bridges, it is recommended to provide some type of protection for the bolts to reduce (or eliminate) corrosion due to the contact with the backfill material. After the bolts were tightened, the abutments were backfilled with fill available on site. A recommendation for future sheet pile abutments would be the use granular select fill for backfill.

After the placement of the angles and before the placement of the backfill material, 3/4 inch diameter bolts were used to connect the angles to the sheet pile sections. No protection was provided for the bolts against the environment. In future bridges, it is recommended to provide some type of protection for the bolts to reduce (or eliminate) corrosion due to the contact with the backfill material. After the bolts were tightened, the abutments were backfilled with fill available on site. A recommendation for future sheet pile abutments would be the use granular select fill for backfill.

B.3 Field Testing

A field test was conducted on the sheet pile abutments simultaneously with the field load test of WCB3. The same test vehicles were used for the field load test on the sheet pile abutments as were used for testing of the RRFC bridge. See Section 4.3 of this investigation for the specifics on the trucks used for these field tests.

B.3.1 Instrumentation Plan

To determine trends in the structural behavior of the sheet pile abutments, BDI strain transducers and string potentiometers were attached to the abutments. The instrumentation plan for the two abutments is shown in Figures B.9 and B.10. Several areas of interest were investigated to better understand the behavior of the sheet pile abutments. At the east abutment three strain transducers were placed vertically under the main girder of the north RRFC (BDI 4825, 4785, and 4781 in Figure B.9). Data from these transducers were used to determine live load bending stresses as well as the vertical load distribution. Three strain transducers (BDI 4783, 6084, and 4780) were orientated vertically in a horizontal line on the east abutment below the north longitudinal connection to investigate the horizontal distribution in the three sheet pile sections beneath the connection. Three strain transducers orientated to measure vertical strains were also placed vertically in a horizontal line under the middle RRFC main girder on the east abutment for the same reason (BDI 4829, 4782, and 4703). One strain transducer was placed under the north exterior girder to investigate the magnitude of the load being transferred from the exterior girder (BDI 1177). Four strain transducers were also placed on the west abutment under the main girder of the middle RRFC in an inverted T shape arrangement as shown in Figure B.9. These transducers were used to investigate the horizontal and vertical load distribution at the west abutment and to validate the pile strain distribution at the east abutment.

As shown in Figure B.10, several deflection transducers were also attached to the abutments. At the west abutment, a string potentiometer (70368) was attached to the support angle under the main girder of the middle RRFC to measure the vertical deflection. At the east abutment, string potentiometer (50371) was attached to the support angle of the exterior girder to measure the movement of the sheet pile perpendicular to the flow of traffic (Figure B.11). String potentiometers were also attached to the supporting angle for the main girder of both the north and middle RRFC to measure the vertical displacement of the east abutment at these locations (70369 and 70371). Two string potentiometers were also placed under the main girder of the north RRFC at the east abutment. These transducers were orientated to measure the displacement in the direction of the bridge (Figure B.12). One string potentiometer was placed near the top of the abutment (70362) and one was placed near ground level (70360) to measure differential movement in the abutment. A final string potentiometer (70363) was placed near the top of the east abutment under the middle RRFC main girder (in line with the corresponding transducer for the North RRFC). This transducer was also orientated to measured movement in the direction of the bridge.

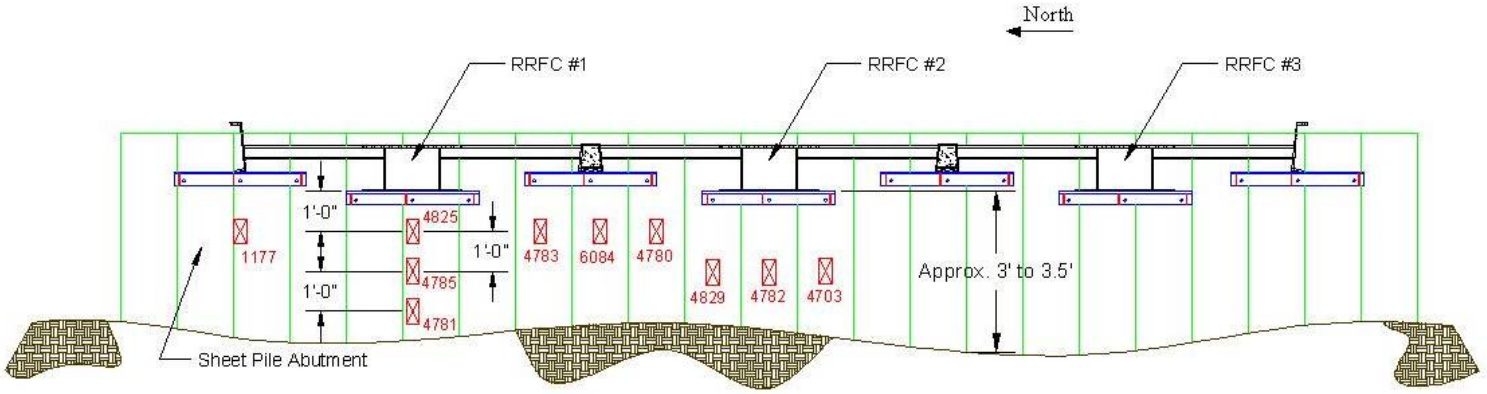

a. East abutment

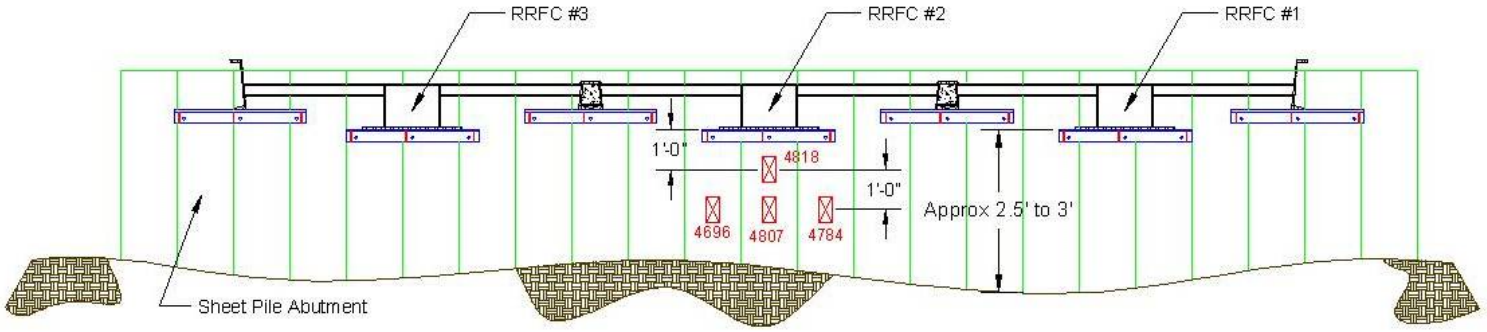

b. West abutment

Figure B.9. Strain instrumentation for WCB3 sheet abutments

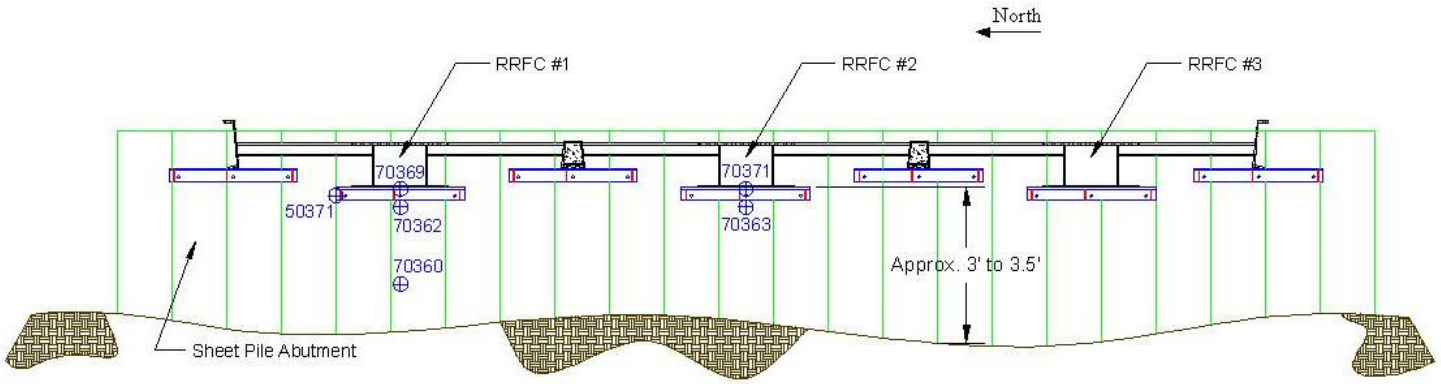

a. East abutment

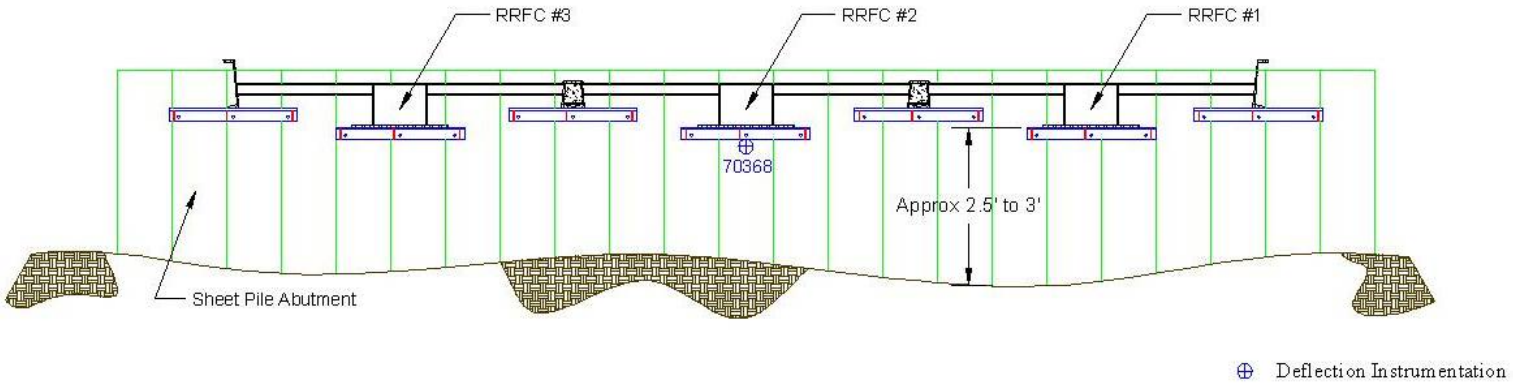

b. West abutment

Figure B.10. Deflection instrumentation for WCB3 sheet pile abutments

Figure B.11. Instrumentation measuring displacement perpendicular to traffic

Figure B.12. Instrumentation measuring displacement in the direction of the bridge

B.3.2 Field Load Test

As previously stated, the field load test of the abutments was conducted simultaneously with the field load test of WCB3. However, after completion of the primary bridge tests, four additional load tests were conducted specifically for determining the behavior of the sheet pile abutments. In the first three tests, the test vehicle was parked with the rear tandems of the vehicle on the edge of bridge first at the east end of the bridge and then at the west end to apply a large concentrated load to the abutment (Figure B.13). For each of these tests, the test vehicle was positioned in one of the three lanes as described in Section 4.3.2 of this investigation. The final test consisted of both the primary test vehicle and the auxiliary vehicle to produce a large axial load on the sheet pile abutments (Figure B.13). In this test, the vehicles were parked in Lanes 1 and 3, first on the east end of the bridge and then on the west end of the bridge as was done in the three previous tests. The test vehicle was in the south lane and the auxiliary vehicle was in the north lane. For all four tests, the test vehicles were traveling from east to west, as shown in Figure B.13.

a. Truck parked at east abutment in Lane 1

b. 2 trucks parked at east abutment

c. 2 trucks parked at west abutment

Figure B.13. Sheet pile abutment load tests

In all the field load tests, the data were marked at certain reference sections. For load tests where the truck was parked, the data were marked when the truck was in the desired position. For the tests were the truck was moving at an idle (pseudo-static), the data were marked when the center of the truck's rear tandem axle crossed a predetermined reference section. For the moving tests, the reference points were: east abutment, center of east pier, 1/4 span, midspan, 3/4 span, center of west pier, and west abutment. These reference sections are shown on the data trend graphs in Section B.4 as dotted lines.

B.4 Field Load Test Results

Since the testing of the sheet pile abutments provided only a limited amount of data, only general data trends are presented. Additional research has been scheduled for a more in-depth investigation in to the use of sheet pile abutments [17].

Due to the limitations of the available equipment, dead load strains can only be approximated using general assumptions and basic geotechnical theory. Therefore, the dead load strain (stress) results are not reported because of the degree of uncertainty. Also, since the instrumentation was attached to only the exposed side of the sheet piles, no distinction can be made between flexural strains and strains due to axial load; the strains and deflections presented are for the test vehicles used and not an HS-20 design vehicle (See Figure 4.6 for truck weights and dimensions).

After reviewing the WCB3 abutment field load test data, several behavioral attributes were observed. First, a "soil push" phenomenon was observed at the east abutment. As the test vehicle approached the abutment (but was not yet on the bridge), the truck "pushed" the underlying soil in the direction that the truck was moving, which in turn flexed the abutment. Figure B.14 displays the soil push displacing the abutment inward as well as the corresponding strains as the truck approaches the bridge. As the front axle of the truck approached the abutment, the abutment flexed in the direction the truck was moving. The resulting displacement and tensile strain (which indicates that the abutment is flexing and not moving as a rigid body) are indicated by the first spike in the data trend, which occurs at approximately twelve seconds. As the front axle of the truck crosses over the abutment, the displacement decreases and the strain becomes compressive. This cycle repeated as the rear tandem axle approached and then crossed over the abutment, with the entire truck on the bridge at approximately 26 seconds.

Horizontal and vertical load distribution was also investigated. For vertical load distribution, two vertical lines of BDI strain transducers were analyzed. As stated in the instrumentation plan, three strain transducers were placed on the east abutment below the main girder of the north RRFC (BDI 4825, 4785, and 4781 in Figure B.9). These transducers are spaced vertically at one foot increments from the top of the support angle. The strain trends for these three strain transducers are plotted in Figure B.15. As the distance between the connection point and the strain transducer increases, the strain experienced by a particular sheet pile section decreases as the load was transferred to the surrounding piles. A similar behavior was observed for the two strain transducers (BDI 4818 and 4807 in Figure B.9) at the west abutment and thus the results from these two transducers will not be discussed.

To investigate the horizontal load distribution, three lines of horizontally spaced BDI strain transducers were analyzed. At the east abutment, two horizontal lines of strain transducers existed – one below the north longitudinal connection and one below the main girder of the middle RRFC. For the instrumentation group below the north longitudinal connection, the strain transducer that was

closest to the loaded RRFC experienced the largest strain, with the other strain transducers experiencing lesser amounts of strain (See Figure B.16). For the instrumentation group below the middle RRFC, shown in Figure B.17, the middle strain transducer (BDI 4782 in Figure B.9) in the instrumentation group experienced the largest strain due to the load path of the RRFCs. Strains measured by the transducers on either side of the center transducer (BDI 4829 and 4703 in Figure B.9) were of similar magnitude, indicating symmetry of the load distribution. Strains at the west abutment exhibited comparable behavior and thus are not presented.

A comparison in the strain trends was also made, comparing the east and west abutments. Presented in Figure A.18 are the strain trends for three transducers below the main girder of the middle RRFC for both the east and west abutments (BDI 4829, 4782, and 4703 at the east abutment and BDI 4696, 4807, and 4784 at the west abutment). At both abutments, good agreement existed between the strain magnitudes as well as the strain data trends.

Overall, the recorded live load strains and deflections were small. For the load tests conducted, the measured live load strains were all below an absolute value of 75 microstrain (2.2 ksi). The maximum vertical deflection was -0.011 inches, occurring at the west abutment. For deflections other than the vertical deflections (i.e. displacements transverse to traffic flow and in the direction of the bridge), the maximum deflection was -0.012 inches, occurring at the east abutment in the direction of the bridge (due to soil push).

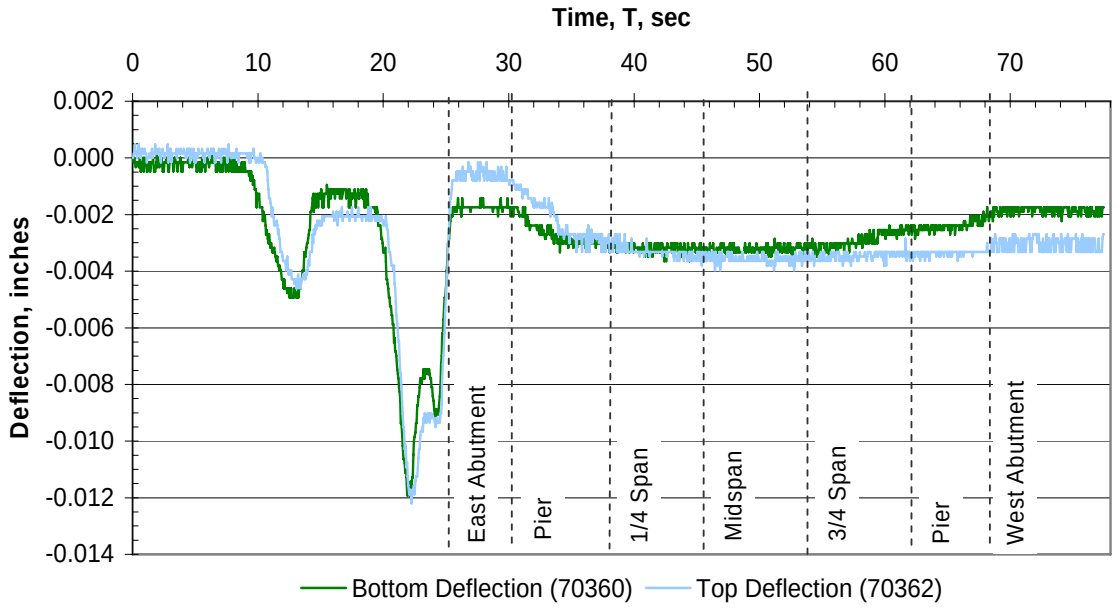

a. Lane 1 longitudinal deflections

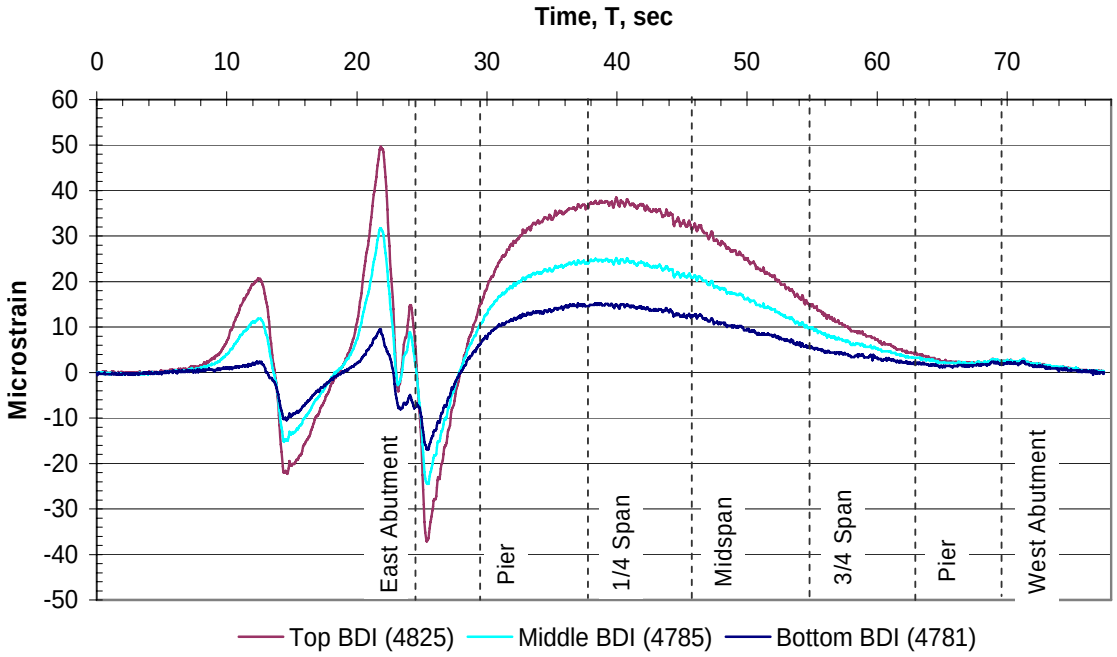

b. Lane 1 microstrain

Figure B.14. Soil push at east abutment

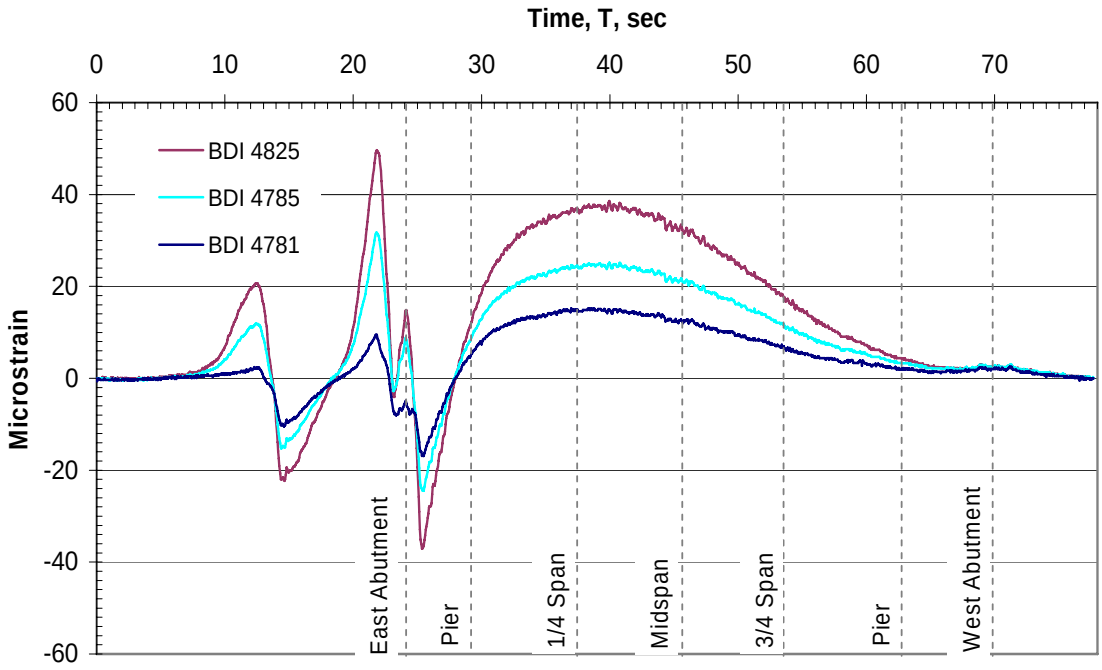

a. Sheet pile vertical load distribution – Single truck in Lane 1

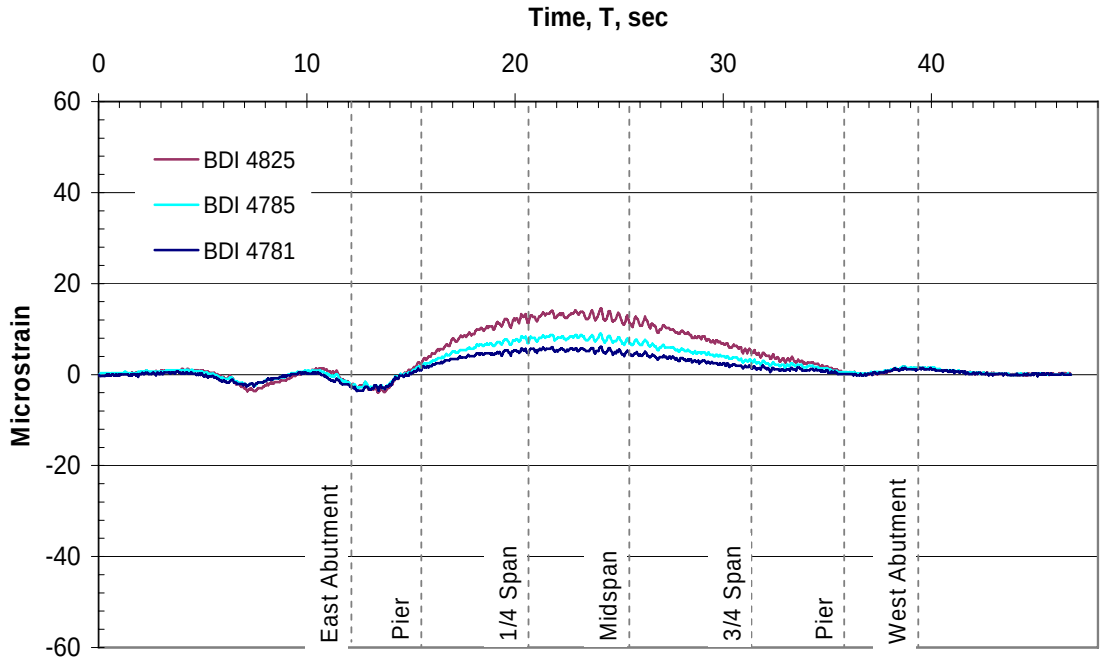

b. Sheet pile vertical load distribution – Single truck in Lane 2

Figure B.15. Sheet pile vertical load distribution at east abutment

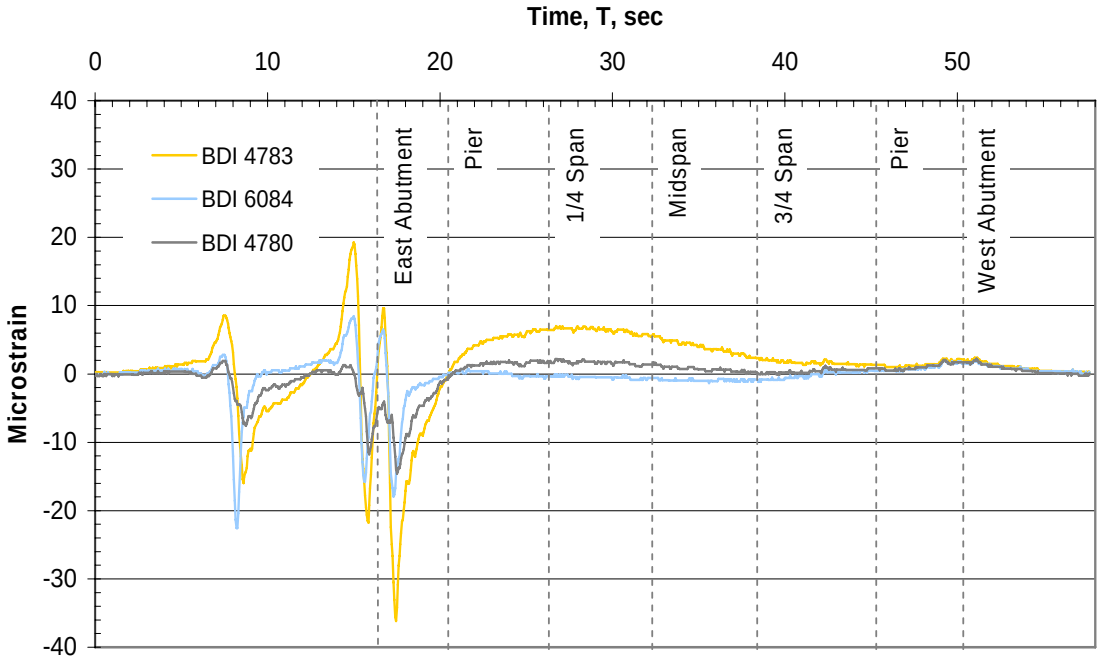

a. Sheet pile horizontal load distribution – Single truck in Lane 1

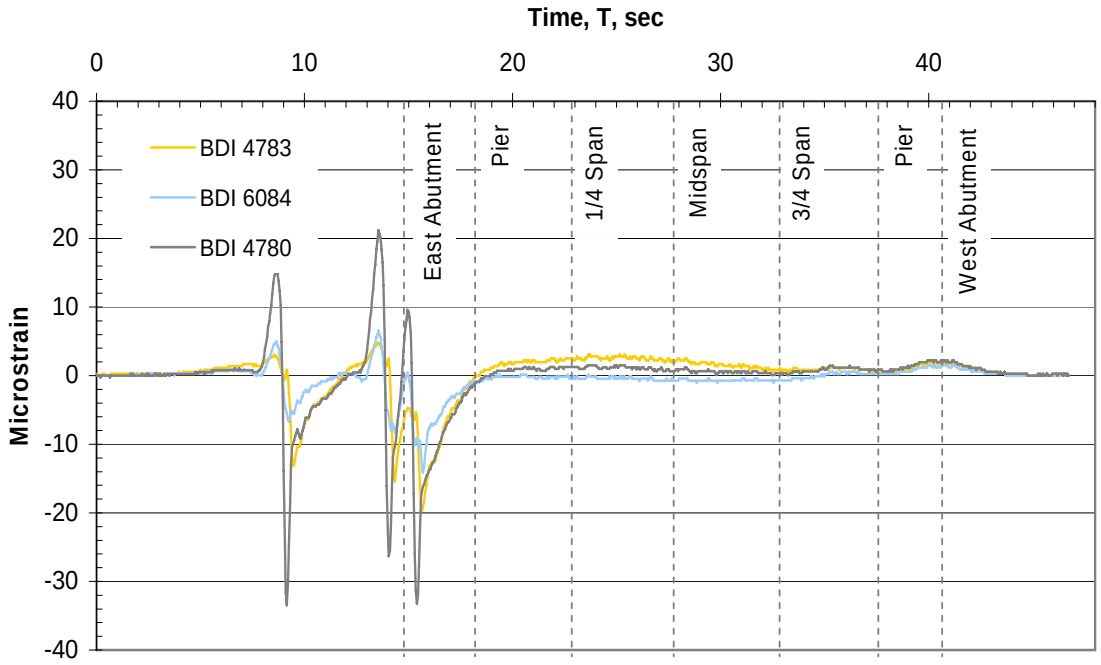

b. Sheet pile horizontal load distribution – Single truck in Lane 2

Figure B.16. Sheet pile horizontal load distribution below north longitudinal connection at east abutment

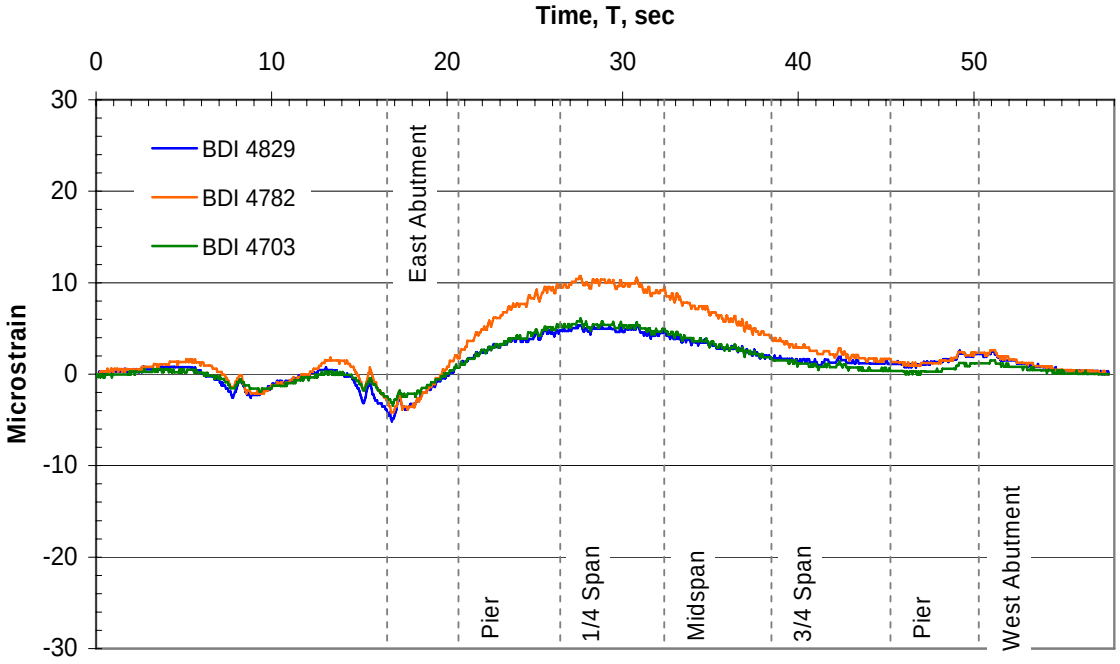

a. Sheet pile horizontal load distribution – Single truck in Lane 1

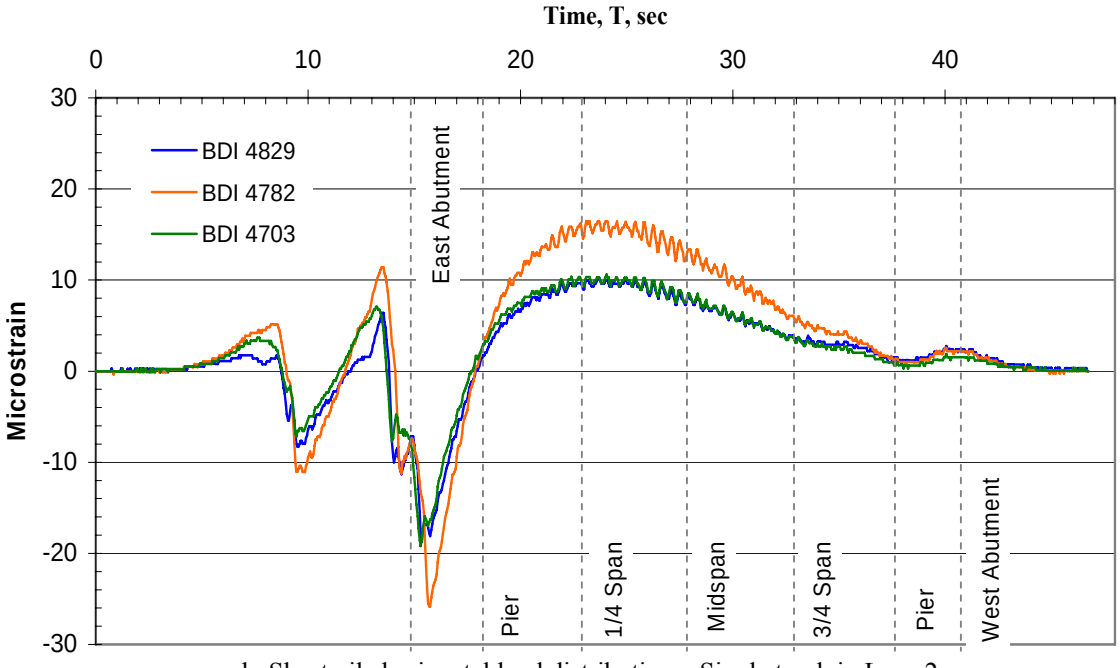

b. Sheet pile horizontal load distribution – Single truck in Lane 2

Figure B.17. Sheet pile horizontal load distribution below middle RRFC main girder at east abutment

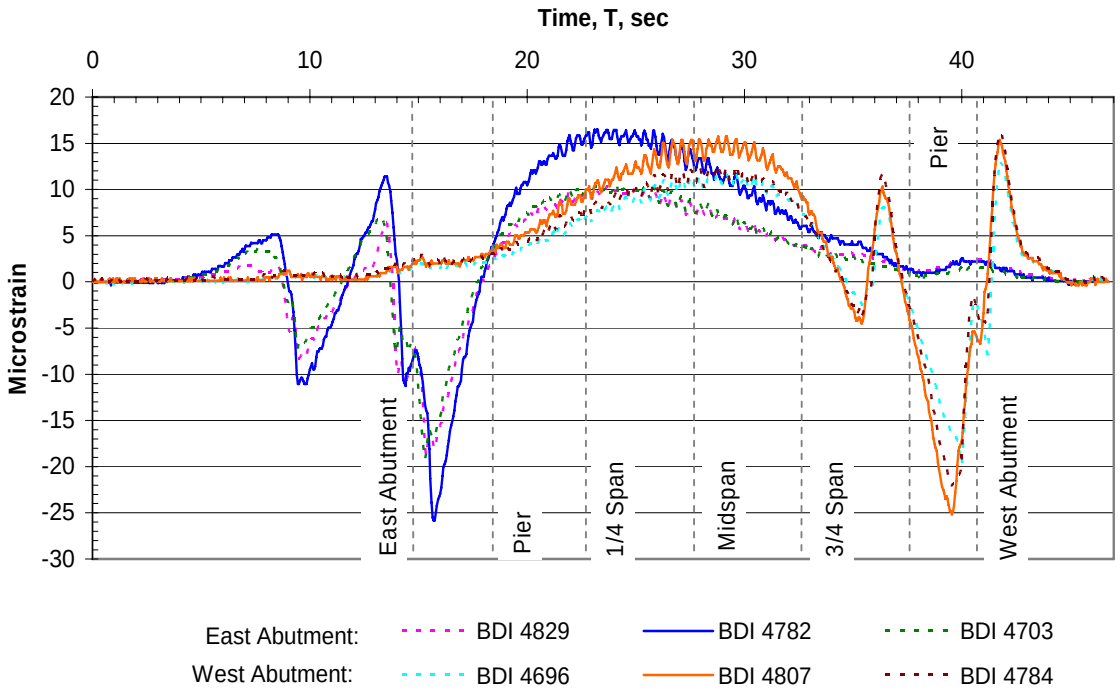

Figure B.18. Strain comparison for east and west abutments

B.5 Observations

Live load strains and deflections in the sheet pile abutments constructed in Winnebago County were small. The field load test data trends confirm assumptions about the load transfer mechanism of the sheet pile sections as well as the distribution of the load through the sheet pile sections. However, due to limited data, only trend observations of the data can be made. Additional research is needed for the development of a more precise model of sheet pile abutment behavior and the soil/structure interaction.

APPENDIX C. RRFC BRIDGE SIMPLIFIED DESIGN PROCEDURE—CONNECTION TYPES

Several different types of longitudinal flatcar connections have been utilized in the RRFC bridges investigated conducted by the Iowa State University Bridge Engineering Center. These connections can be separated into four main categories as noted in Section 6.1. The connection categories are:

Type 1: Reinforced concrete beam with threaded rods (used in BCB1, BCB2, and BCB4)

Type 2: Reinforced concrete beam confined with steel plates, threaded rods, and transverse timber planks (used in WCB1, WCB2, and WCB3)

Type 3: Bolted exterior webs (used in BCB3 and BCB5)

Type 4: Welded plates (used in DCB)

Three different configurations of the Type 1 connection were investigated. First, a narrower connection was used for BCB1 with the 56-ft v-deck RRFC (Figure C.1a). A wider connection was used for BCB2, again with the 56-ft v-deck RRFC (Figure C.1b). For BCB4, a modification to the connection was made to accommodate the use of a different RRFC (89-ft instead of 56-ft) and still maintain a sufficient depth, which was achieved by adding angles below the exterior girders of the adjacent RRFCs (Figure C.1c).

For each connection category, design factors (ψ) were developed for use in the simplified design procedure as outlined in Section 6.1 of this investigation. The following figures (Figures C.1-C.4) display samples of each type of connection.

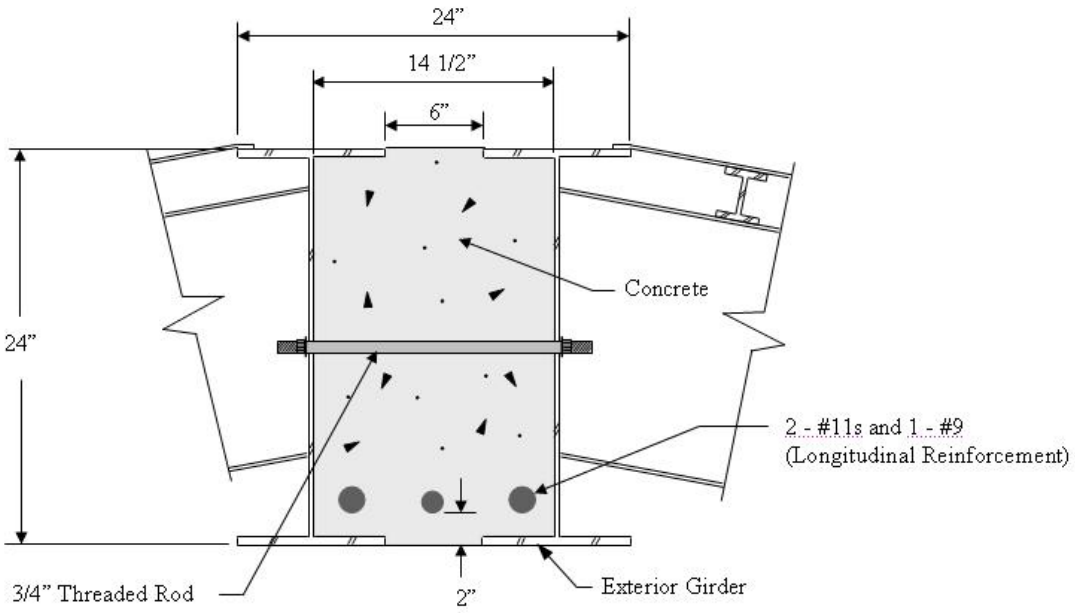

a. Smaller Type 1 Connection used with 56-ft V deck RRFC (BCB1)

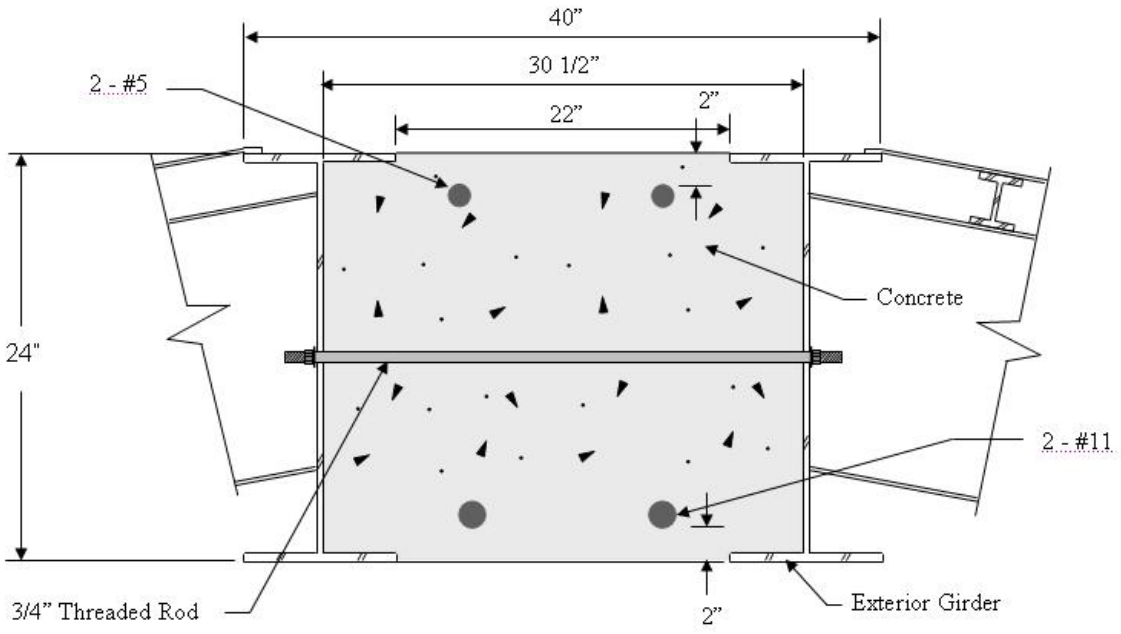

b. Wider Type 1 Connection used with 56-ft V deck RRFC (BCB2)

Figure C.1. Type 1 longitudinal flatcar connection (BCB1, BCB2, & BCB4)

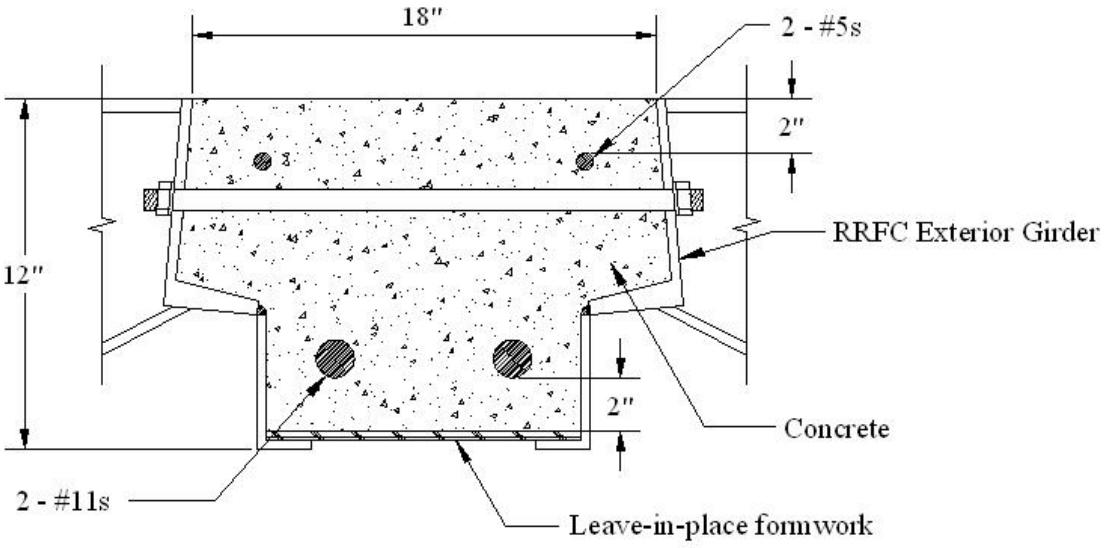

c. Modified Type 1 Connection used with 89-ft RRFC (BCB4)

Figure C.1. Continued

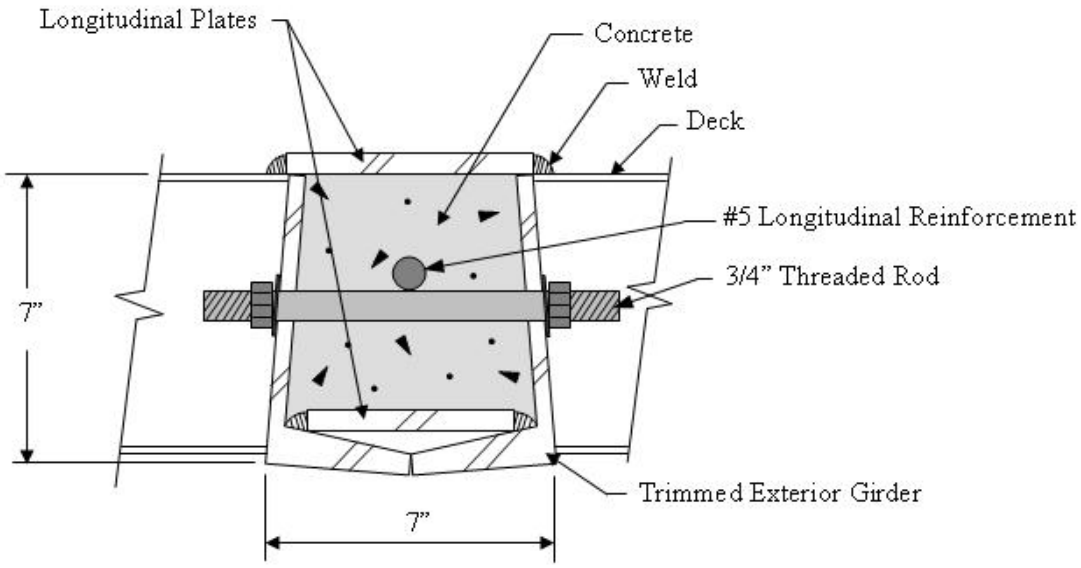

Figure C.2. Type 2 longitudinal flatcar connection (timber planking not shown) (WCB1, WCB2, & WCB3)

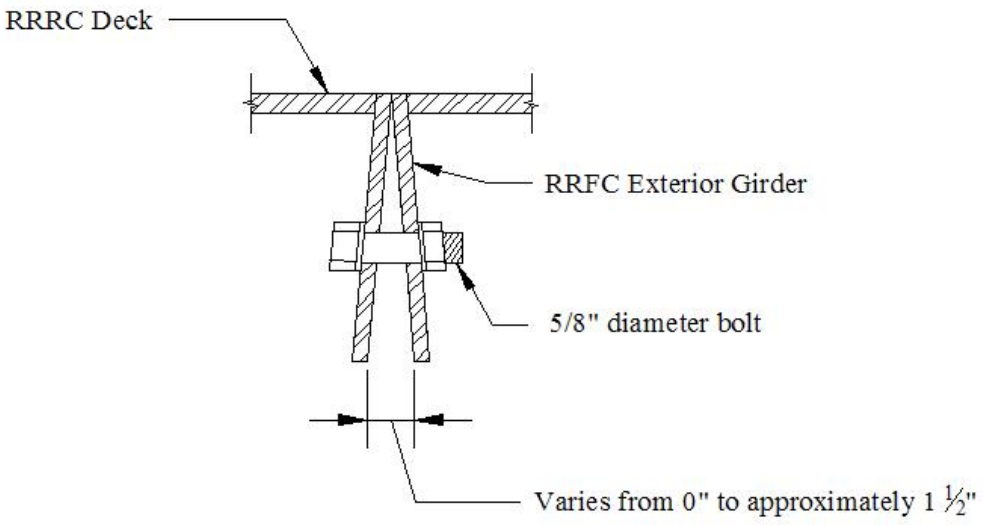

Figure C.3. Type 3 longitudinal flatcar connection (BCB3 & BCB5)

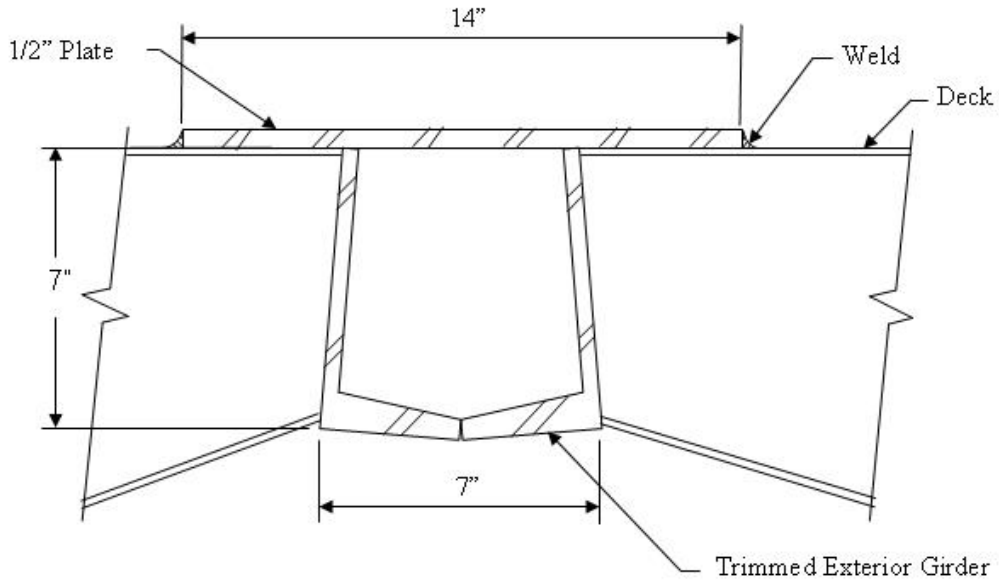

Figure C.4. Type 4 longitudinal flatcar connection (DCB)

APPENDIX D. FIELD TESTING OF STRENGTHENED WINNESHIEK COUNTY, IOWA RRFC BRIDGE

Presented in this appendix are the field testing and analysis of a single span RRFC bridge located in Winneshiek County, Iowa, that features integral abutments as well as a built up sections to allow for the longer span length.

D.1 Winneshiek Bridge Site

The Winneshiek County, Iowa RRFC (WINNRRFC) was constructed in late 2006 approximately eight miles east of Decorah, Iowa on Coon Creek Road over the Trout River, a tributary of the Upper Iowa River (See Figure D.1). The previous bridge at this site had collapsed after a truss member was struck by a pickup truck in June of 2006. A RRFC bridge was chosen for this site by Winneshiek County officials because of the short construction time and the economy associated with RRFC bridges.

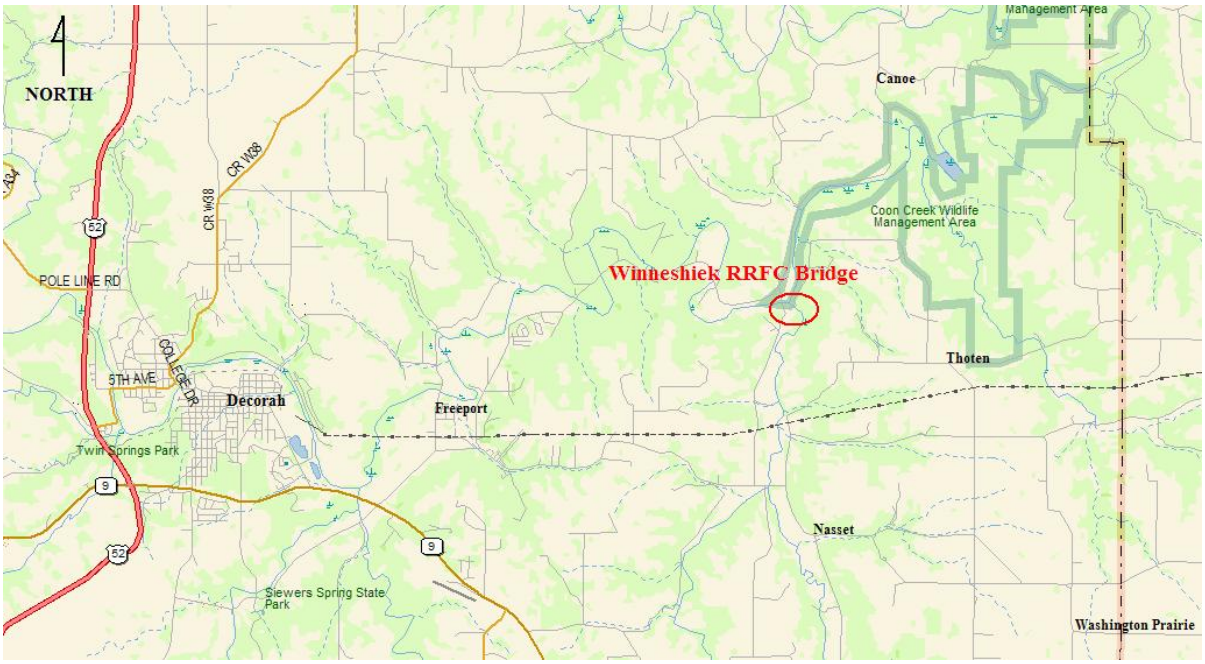

Figure D.1. Location of Winneshiek County RRFC bridge [2]

D.2 Winneshiek RRFC Bridge Design

Previous RRFC research has suggested a maximum single span of 66'-0" results in strains (stresses) and deflections that are below recommended limits set forth by the American Association of State Highway and Transportation Officials (AASHTO) [1]. However, the geometry of the WINNRRFC bridge site required a single span bridge of 69'-0" center of abutment to center of abutment; therefore, modifications were required to strengthen the RRFCs to provide acceptance in regards to the aforementioned AASHTO criteria. The engineering firm Shuck-Britson Consulting Engineers of Des Moines, Iowa, was hired by Winneshiek County to design the WINNRRFC bridge, which included sufficiently strengthening of the RRFCs.

Two 89 ft RRFC were selected for use in the WINNRRFC bridge. As was done in previously constructed RRFC bridges, the 89 ft RRFCs were trimmed to the required overall length of 71'-0" by removing similar amounts of material at each end of the RRFC. To provide the additional strength required to accommodate this span length, a 5/8 inch thick plate 23 inches wide and 38 feet long was attached to the bottom of the interior primary girders of the RRFCs by 5/16 inch fillet welds along the longitudinal edges of the plate. The plates were welded to the girders prior to the installation of the RRFCs at the bridge site to simplify construction.

The WINNRRFC bridge superstructure is supported by new integral concrete abutments that were constructed on existing steel H-pile. The existing timber wing and backwalls were also used. An idealized plan and side view of the bridge with pertinent dimensions are provided in Figure D.2.

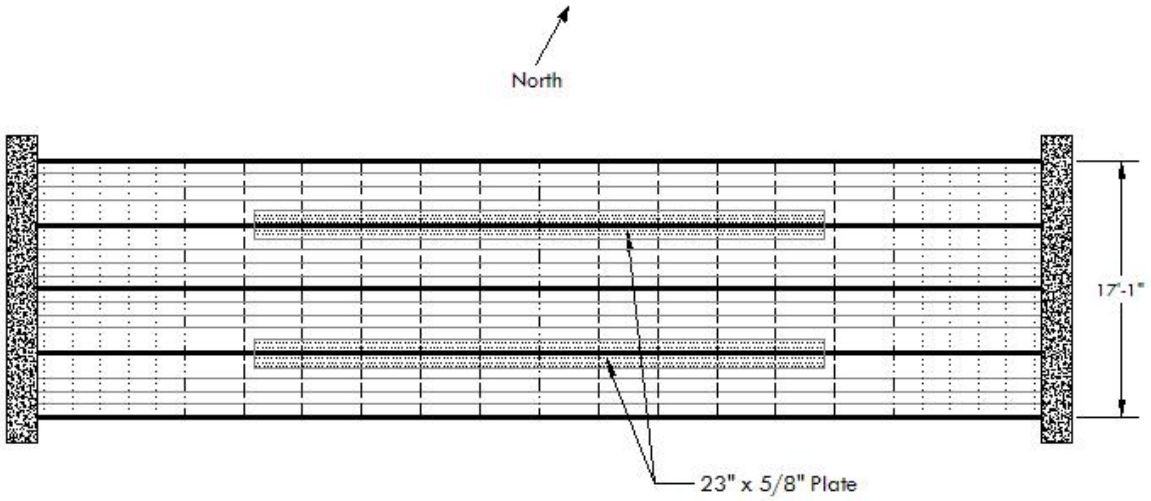

a. Idealized Plan View

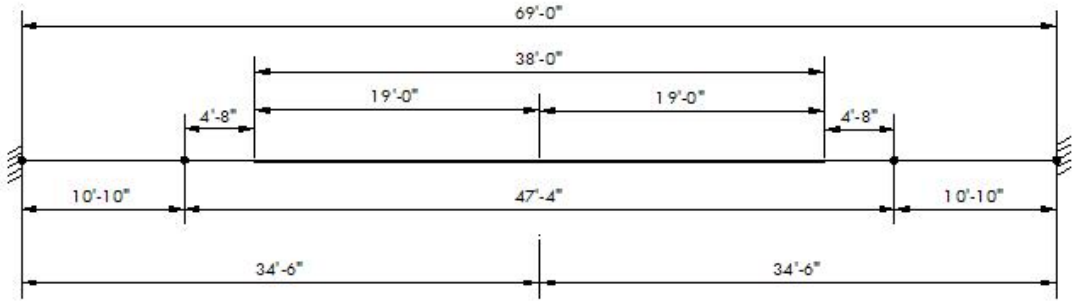

b. Idealized Side View

Figure D.2. Idealized view of WINNRRFC

Due to the geometry of the exterior girders in the 89 ft RRFC, the top portion of adjacent girders needed to be removed in order to provide a "flush" driving surface. After the top of the adjacent girders was removed, a longitudinal flatcar connection (LFC) between the flatcars was constructed. Previous RRFC bridges investigated by the Bridge Engineering Center employed LFCs that were one of two main types, a bolted connection or reinforced concrete beam. For the WINNRRFC bridge, the bolted connection was utilized. To construct the LFC connection, the bottom flange of the exterior girder of the two adjacent RRFCs was removed. The remaining webs were then bolted together with 3/4 inch diameter bolts four inches long spaced on 72 inch centers. Due to difficulties in constructing the LFC connection and the shape of the RRFC exterior girders, frequently a small gap develops between the tips of the adjacent girder webs. On the WINNRRFC bridge, this gap ranged from being almost non-existence to about one and one half inches, with the majority of the gap being approximately three quarters of an inch. The gap, as well as an idealized view of the connection, is shown in Figure D.3. A guardrail was attached to the bridge (shown in Figure D.4) and approximately four inches of gravel was added for the driving surface on the bridge. The finished WINNRRFC is shown in Figure D.5.

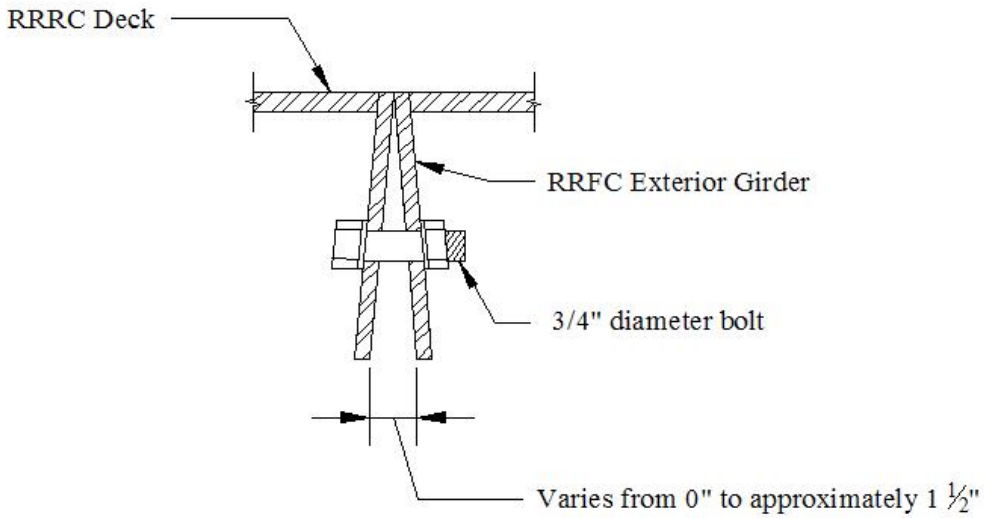

a. WINNRRFC LFC idealized cross section

Figure D.3. WINNRRFC longitudinal connection detail

b. LFC gap between adjacent girder webs

c. LFC bolted connection

Figure D.3. Continued

a. Guardrail post

b. Guardrail connection to RRFC

Figure D.4. WINNRRFC guardrail system

Figure D.5. Completed Winneshiek RRFC bridge

D.3 Field load testing

To determine the behavior of WINNRRFC, a field load test was conducted using a Winneshiek County Secondary Road Department tandem-axle truck loaded with gravel. The dimensions and axle weights of the vehicle used in the load test are shown in Figure D.6.

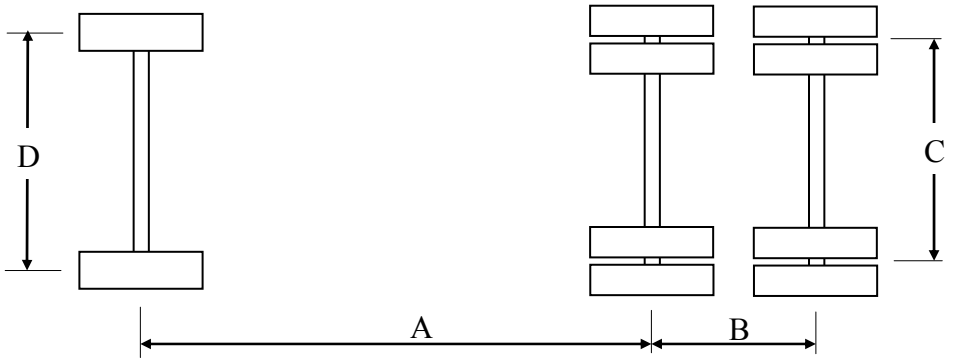

a. Top view

b. Side view

Truck	Dimensions (inches)				Load (lbs)		
	A	B	C	D	F	T	Gross
Test	192	54.5	72	85	16,900	32,800	49,700

Figure D.6. WINNRRFC test vehicle weights and dimensions

D.3.1 Instrumentation

To determine the structural behavior of the WINNRRFC bridge, BDI strain transducers and string potentiometers were attached to the bridge. A data acquisition system was then connected to the instrumentation to record a continuous data record of the bridge behavior during the field load tests. As the tandem axle of the test truck crossed predetermined transverse reference sections on the bridge, a feature of the data acquisition system was used to "mark" the locations of the truck for later

use in the data analysis process. The reference sections for the WINNRRFC bridge were at the center of bearing for the abutments as well as the 1/4, 1/2, and 3/4 span locations for a total of five reference sections. The data record was also marked when the front axle of the truck entered on to the bridge.

Two critical regions were investigated for strains (stresses) during the load test – the midspan region and the region adjacent to the termination of the plates that were added for strengthening. The instrumentation plan for the WINNRRFC bridge is shown in Figure D.7. The instrumentation plan used for the WINNRRFC bridge consists of five string potentiometers and twelve BDI strain transducers.

At the midspan, seven BDI strain transducers were placed on the bridge cross section as shown in Detail B of Figure D.7. One BDI was placed on the bottom flange of each exterior girder of the bridge. One BDI was also placed on the web of each RRFC exterior girder at the longitudinal connection between the two adjacent flatcars. BDI strain transducers were also placed on the bottom of the interior primary girder (i.e. on the added plate) of each RRFC at the midspan location. A BDI was also placed near the top of the south interior primary girders at the midspan location. Data from this transducer were used in conjunction with the companion transducer on the bottom of the girder to determine the location of the experimental neutral axis.

To verify the adequacy of the strengthening measures applied to the bridge (i.e. the 23" x 5/8" plates), BDI strain transducers were also placed approximately nine to twelve inches from either end of the plate to verify that AASHTO requirements for strain were satisfied at these regions (Detail A and C in Figure D.7). One BDI was also placed on the south RRFC approximately 30 inches from the face of the east abutment to assess the behavior of the integral abutment (Detail D in Figure D.7).

At the midspan, five string potentiometers were placed on the bridge cross section as shown in Figure D.7f. One potentiometer was placed on each exterior girder of the bridge. One string potentiometer was also placed on the south side of the longitudinal flatcar connection at midspan. String potentiometers were also placed beneath each of the interior primary girders as shown in the instrumentation plan.

C.3.2 Field Load Test

To assess the structural performance of the WINNRRFC bridge under traffic loading, three pseudo-static field load tests were conducted (Figure D.8). To perform the field load tests, three lanes were identified on the bridge, as has been customary with other RRFC bridges tested by the Bridge Engineering Center. The two outside lanes (Lane 1 and Lane 3) positioned the outer wheel line of the test vehicle approximately two feet from the exterior girder of the bridge. The remaining lane, Lane 2, centers the test vehicle transversely on the bridge. A schematic of the lane configurations is shown in Figure D.9. For each test run, the test vehicle traversed the bridge at an idle speed, producing a pseudo-static record of the bridge behavior (strains and deflections) which were then analyzed to determine response of the bridge. Each load test was conducted twice to investigate the repeatability of the bridge's response.

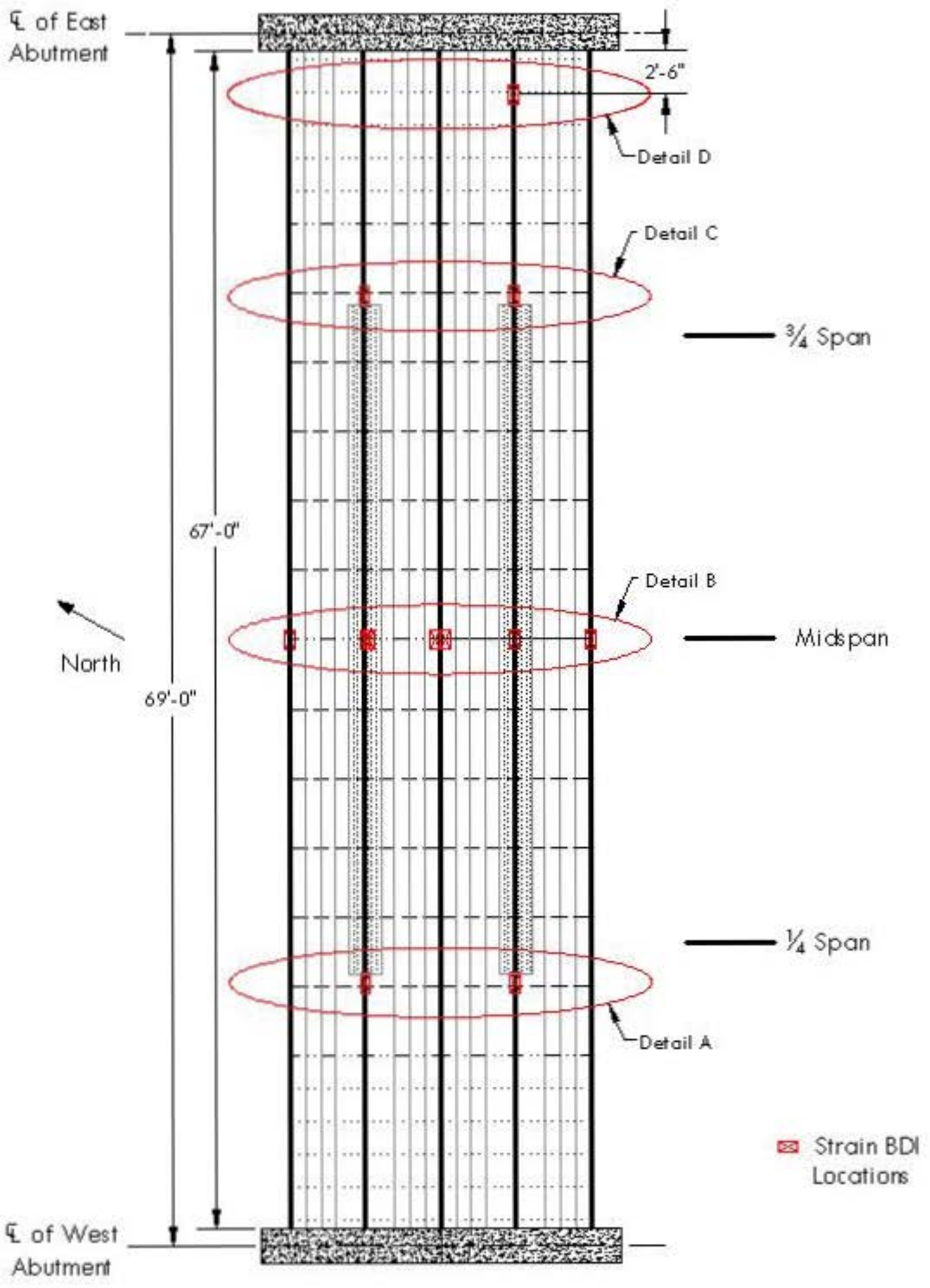

a. Strain Instrumentation

Figure D.7. WINNRRFC instrumentation plan

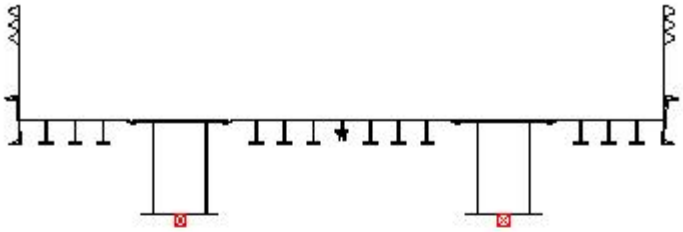

b. Detail A

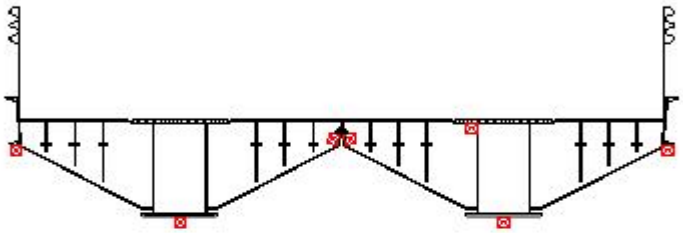

c. Detail B

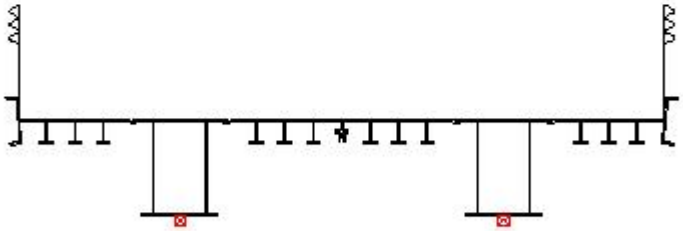

d. Detail C

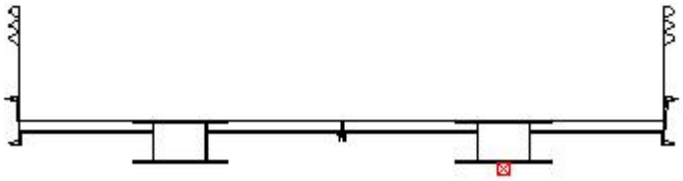

e. Detail D

Figure D.7. Continued

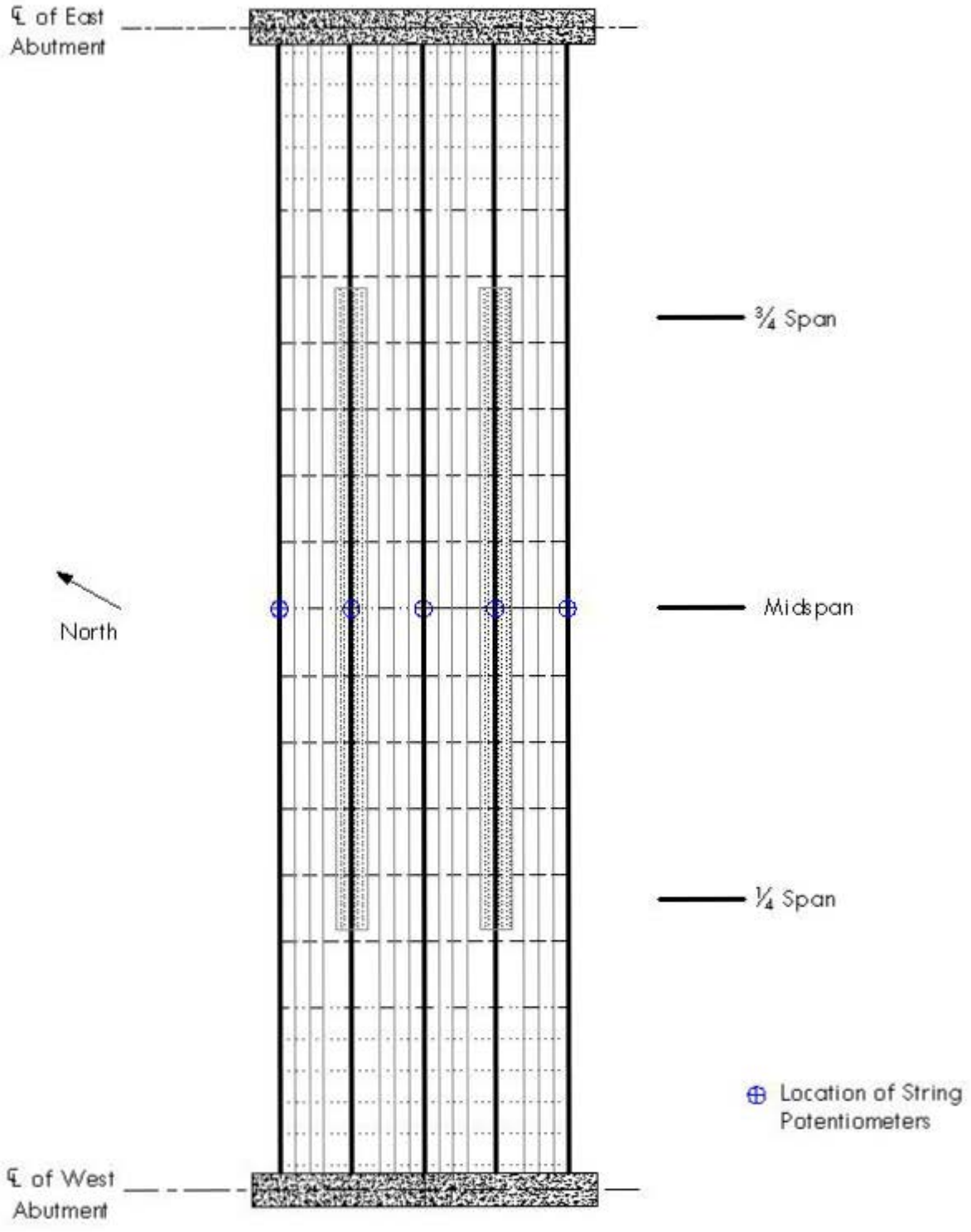

f. Deflection Instrumentation

Figure D.7. Continued

a. Head-on view of load test

a. Side view of load test

Figure D.8. WINNRRFC pseudo-static field load test

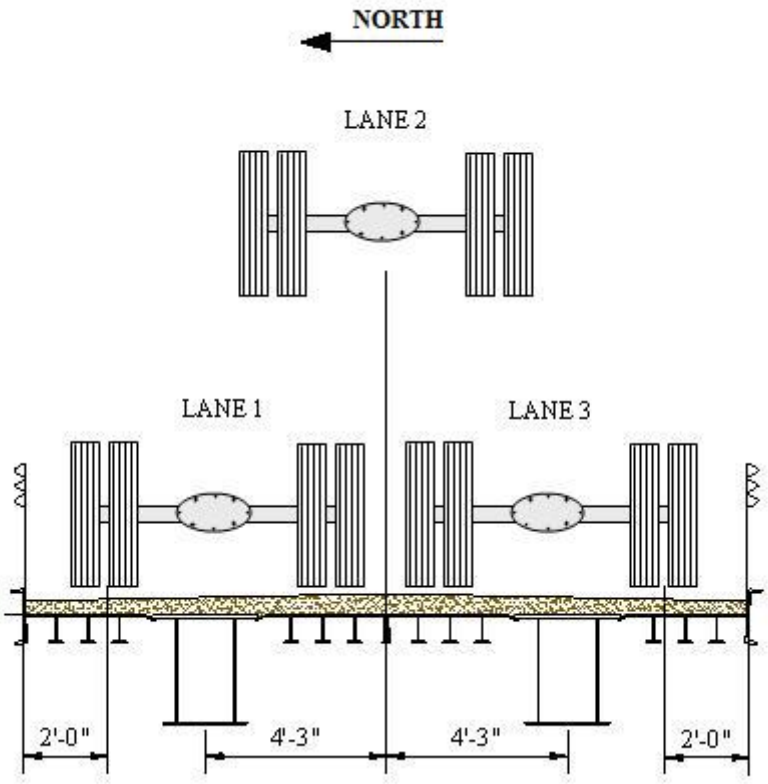

Figure D.9. WINNRRFC lane configuration

D.4 Dead Load Analysis

The total stresses occurring in the WINNRRFC bridge are the resultant of the live load stresses caused by the test vehicle and dead load stresses caused by the weight of the bridge. To determine the total stresses in the bridge, a dead load analysis was completed. As was done with previous RRFC bridges, several assumptions were made to simplify the dead load analysis. Based on the results of a grillage analysis conducted on the 89-ft flatcar as part of TR-444 [3], the entire dead load is conservatively assumed to be resisted by the two interior primary girders. Also, as was done with the previous RRFC bridges that have been analyzed, the connected flatcars were assumed to form a rigid cross section. This allows for any superimposed dead load to be considered uniformly distributed on the bridge.

The dead load for WINNRRFC is comprised of mainly the driving surface and the weight of the flatcars. Based on previous research conducted during the RRFC investigation, the 89 ft flatcars were assumed to weigh 42,000 lbs, or 472 lb/ft if distributing the weight of the RRFC evenly along the flatcar length. For the midspan section, the assumption of an evenly distributed weight is slightly non-conservative since the RRFC is comprised of a deeper section at this location. However, this weight distribution has been used successfully in previous RRFC dead load analyses. The WINNRRFC driving surface is comprised of approximately four inches of gravel with an assumed unit weight of 120 lb/ft^3. The longitudinal connection and the guardrail (assumed to weigh 100 lb/ft) also added to the dead load. The additional plates added approximately 49 lb/ft to the dead load. The total dead load per car for the WINNRRFC bridge was determined to be 912 lb/ft where there no plates and 960 lb/ ft where the plates were added.

To determine the dead load stresses, an idealized model of the bridge was analyzed using a structural analysis program. The dead load (either 912 lb/ft or 960 lb/ft) was applied to the model and an analysis conducted to determine the resulting maximum moment at the critical locations (midspan and adjacent to the end of the added strengthening plates).

After determining the dead load moment at the critical locations, the dead load moments were divided by the section modulus of the interior primary girder of the bridge to determine the corresponding dead load stresses. The section modulus of the main girder was calculated by determining the location of the neutral axis based on the bridge cross section at the locations of interest. The moment of inertia for the main girder was then found with respect to this neutral axis (instead of the neutral axis for the main girder only). This approach was used to better represent the true behavior of the bridge. This method also produced a more conservative section modulus. For the WINNRRFC bridge, the section modulus was determined to be 458 in^3 for main section without the additional plate and 750 in^3 with the additional plate.

Although the WINNRRFC bridge was designed and constructed with integral abutments, there was some rotational restraint uncertainty associated with the WINNRRFC bridge abutments. To account for this uncertainty, the dead load analysis was conducted for a fixed-fixed condition as well as a pinned-pinned condition with the maximum flexural moment at each critical section being used to conservatively calculate the dead load strains and stresses. For both critical sections, the dead load moments from the pinned-pinned analysis controlled, and the corresponding strains (stresses) are presented in Table. D.1 (“+” indicates tension and “-” indicates compressive). Unless noted otherwise, the strains (stresses) reported are bottom flange values. The strains were calculated from the calculated stresses assuming a modulus of elasticity of 29,000 ksi, as discussed in the following chapter.

Table D.1. WINNRRFC dead load strains (stresses) at critical locations

Location	Dead Load Microstrain	Dead Load Stress (ksi)
Midspan	+313	+9.1
End of Additional Plates	+313	+9.1

D.5 Field Load Test Results

The 2003 AASHTO Standard Specification for Highway Bridges specifies an allowable flexural stress for compact steel sections not subjected to lateral-torsional buckling equal to 55 percent of the yield strength [4]. The assumption that the member is not subjected to lateral-torsional buckling requires sufficient lateral bracing of the member compression flange, which is provided by both the

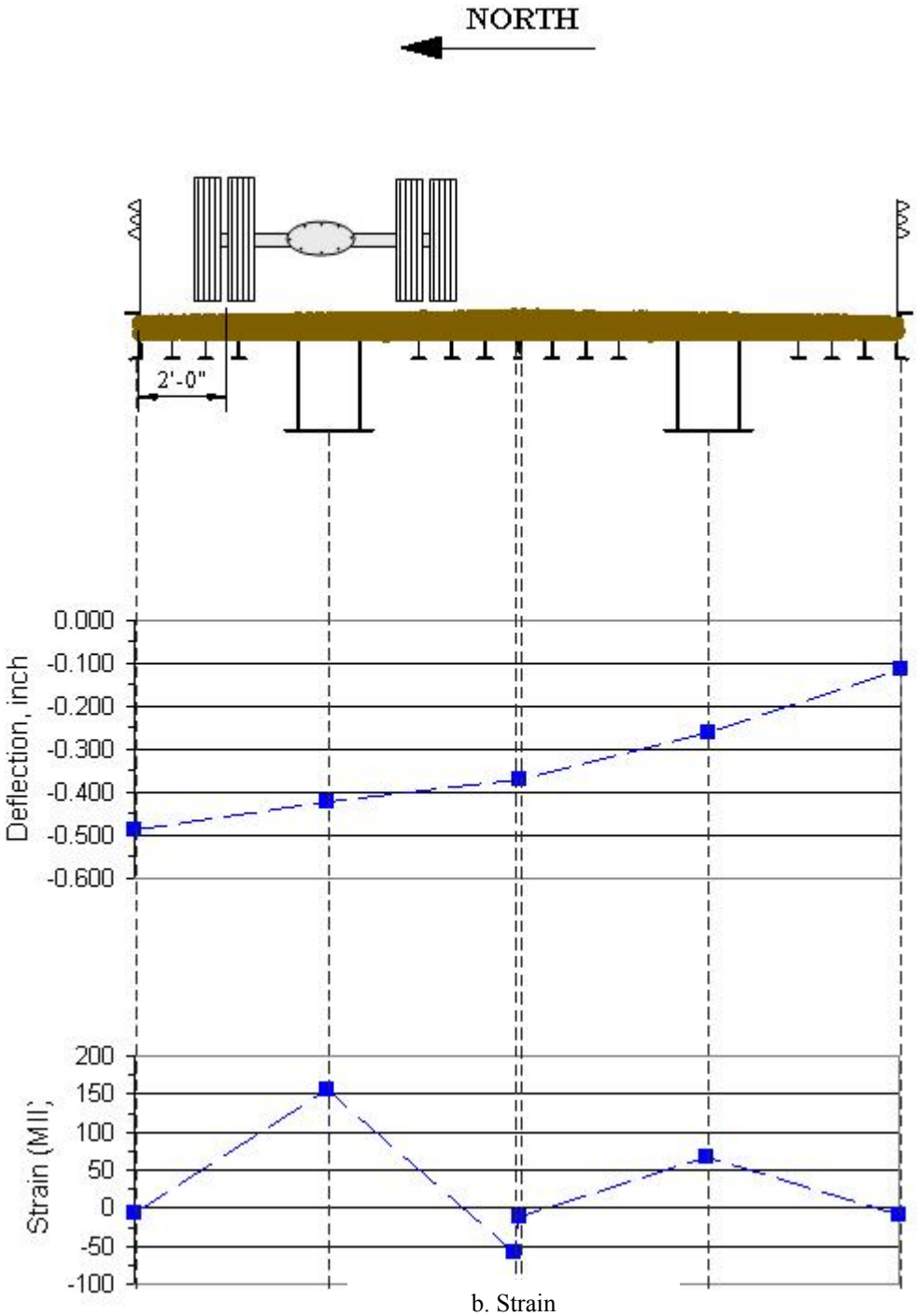

b. Strain

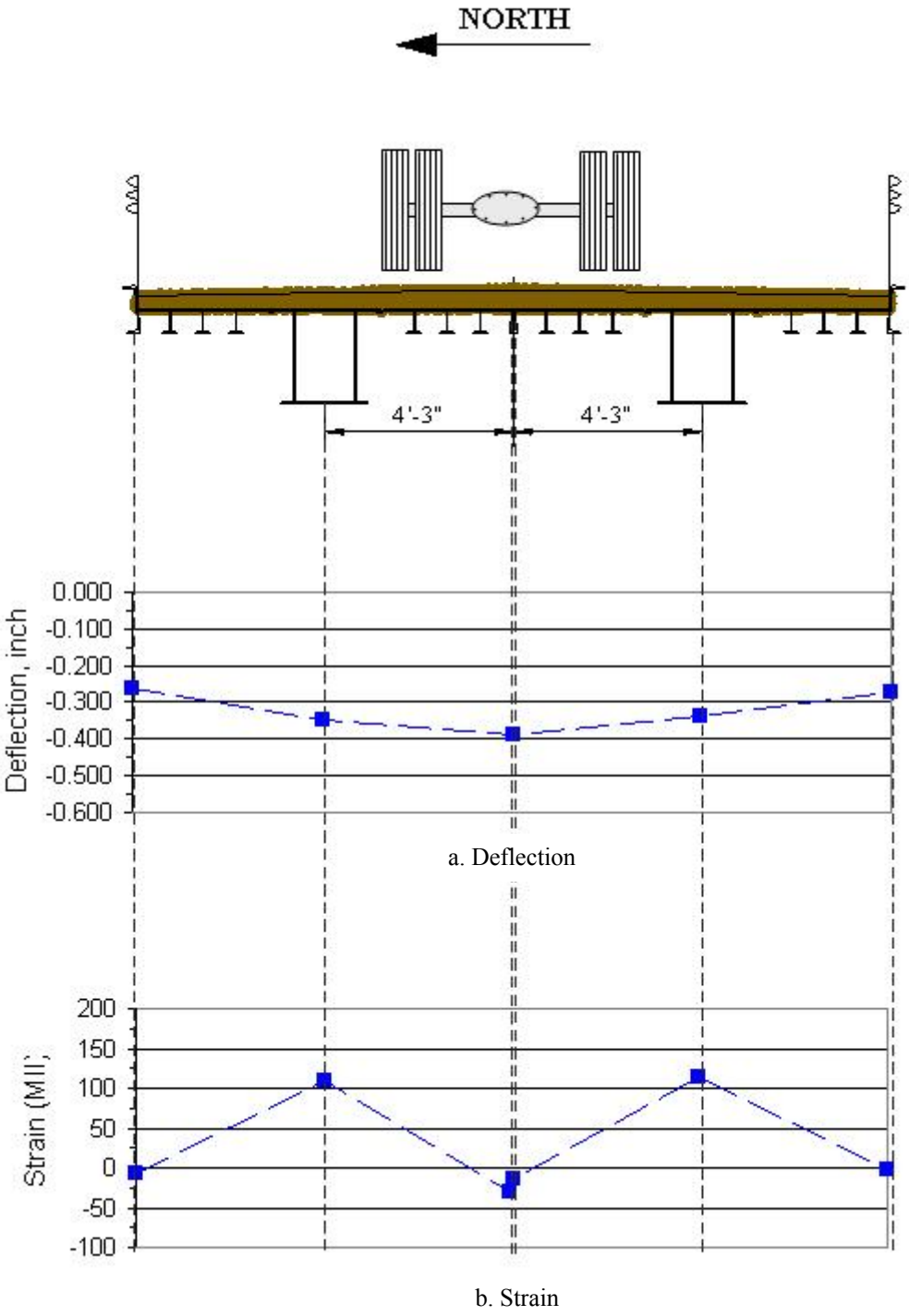

Figure D.11. WINNRRFC Lane 2 midspan live load deflections and strains

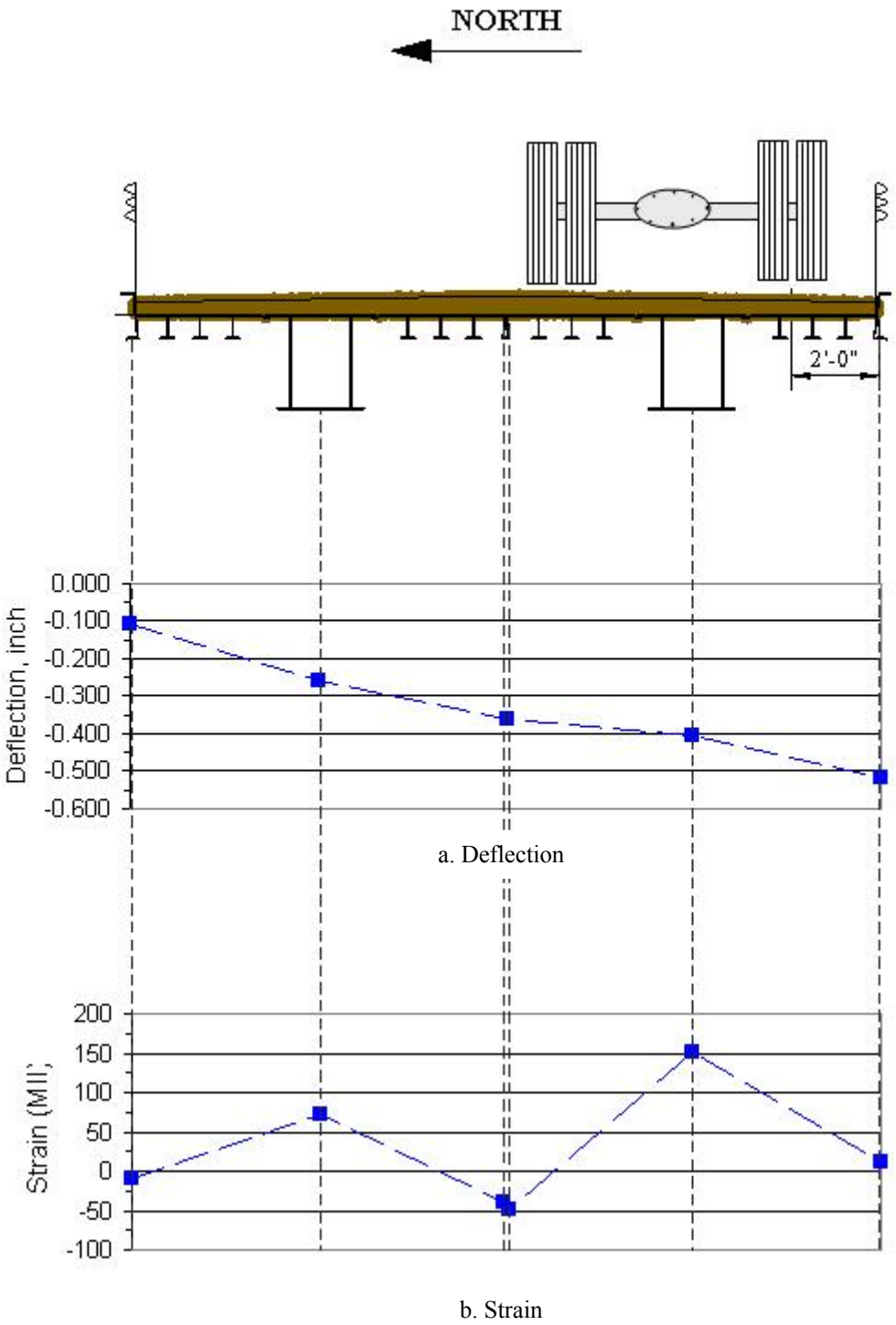

a. Deflection

b. Strain

Figure D.12. WINNRRFC Lane 3 midspan live load deflections and strains

unloaded portion of the bridge cross section. Comparing the results for the three load tests reveals that approximate transverse symmetry exists in the lateral distribution of the load.

The maximum live load tensile strain that occurred at midspan as a result of the load test was +156 microstrain (+4.5 ksi) with the test vehicle positioned in Lane 1. After applying the calculated dead load strain (stress), +313 microstrain (+9.1 ksi), the tensile strain (stress) occurring at the bridge midspan was increased to +469 microstrain (+13.6 ksi), or approximately 69% of the 19.8 ksi (683 microstrain) allowable limit. Midspan compressive strains (both live load and dead load) were significantly less than the tension strains and are therefore not reported.

The AASHTO LRFD Bridge Design Specification recommends a maximum allowable live load deflection of 'span'/800 for legal truck loads [5]. Using this criterion and assuming an abutment face to abutment face span length of 66'-0", the maximum allowable live load deflection for the main span of the WINRRFC bridge is 0.99 inches. The maximum midspan live load deflection for the test vehicle was 0.517 inches, or approximately 52% of the recommended limitation.

As was done in the testing of previous RRFC bridges, an adjustment factor was used to increase the results from the test vehicle to that of an HS-20 truck, the likely design vehicle for the bridge. To determine the adjustment factor, the test vehicle loading and an HS-20 loading were each positioned with the load center of gravity at the midspan location. The respective maximum moment values were then compared (maximum moment for test vehicle loading vs. maximum moment for HS-20 loading) to produce the adjustment factor, which was calculated to be 1.563 for the WINNRRFC bridge. Using this value, the predicted maximum total strain for an HS-20 test vehicle on the WINNRRFC bridge becomes +557 microstrain (+16.1 ksi) at midspan, which is still below the allowable value of 19.8 ksi (683 MS). Using the same approach, the maximum live load deflection is predicted to be 0.808 inches, also still within the AASTHO guidelines.

The maximum strain recorded by BDIs at the ends of the additional plates (Detail A and C in Figure D.7) during the WINNRRFC bridge load test was +208 microstrain (+6.0 ksi), which is slightly larger than the strains recorded at midspan. After applying the calculated dead load strain/stress at the ends of the plates, +313 microstrain (+9.1 ksi), the total tensile strain (stress) occurring in the vicinity of the end of the additional plates increased to +521 microstrain (+15.1 ksi), or approximately 76% of the 19.8 ksi (683 microstrain) allowable limit. After applying the HS-20 adjustment factor, the maximum projected live load strain occurring at the end of the plates is +325 microstrain (+9.4 ksi); hence the projected total maximum tensile strain increases to +638 microstrain (+18.5 ksi), or 93% of the allowable strain/stress of 683 microstrain (19.8 ksi).

D.6 Summary and Conclusions

D.6.1 Summary

In this Appendix, the structural behavior of the Winneshiek County, Iowa RRFC bridge located on Coon Creek Road eight miles east of Decorah has been summarized. To determine the behavior of the bridge, strain and deflection instrumentation was attached to the bridge to measure the response of the bridge during field load testing. To perform the field load test, a Winneshiek County Secondary Road Department tandem axle truck traversed the bridge in three predetermined traffic lanes to produce pseudo-static data records of the behavior of the WINNRRFC bridge. To determine the dead load

stresses, a simplified dead load analysis was conducted using conventional beam theory and techniques developed in the analysis of other RRFC bridges.

The results for the field load test indicated compliance with appropriate AASHTO criteria for allowable stress and live load deflection. The total strain/stress was below the allowable strain of 683 microstrain (19.8 ksi) for both the test vehicle (+521 microstrain or +16.1 ksi) as well for the projected HS-20 loading (+638 microstrain or +18.5 ksi). The live load deflections, 0.517 inches for the test vehicle and a predicted 0.808 inches for HS-20 loading, were also below the recommended maximum of 0.99 inches.

D.6.2 Conclusions

The following conclusions can be drawn from the data collected and the subsequent analysis that was completed as part of this investigation on the behavior of the Winneshiek County, Iowa RRFC bridge (WINNRRFC).

- By adding the strengthening plates to the bottom of the interior primary girders of each RRFC, the moment of inertia of the members (and thus the moment of inertia of the bridge) was sufficiently increased so that the total strain, the sum of the calculated dead load strain and the measured live load strain, was below the allowable limit as defined by AASHTO.
- Live load deflections measured during the field load test were below the AASHTO recommendation for maximum live load deflection.
- The longitudinal flatcar connection provided adequate transverse live load distribution.